

HEATSTORE

Environmental effects of UTES technologies in Europe

Prepared by: Luca Guglielmetti (ed.), University of Geneva
Martin Bloemendal (ed.), KWR
Florian Hahn (ed.), Fraunhofer IEG
Mette Hilleke Mortensen (ed.), GEUS
Joris Koornneef (ed.), TNO

Peter Alt-Epping, University of Bern
Daniel Birdsell, ETHZ
Alexandros Daniilidis, University of Geneva
Isabella Nardini, Fraunhofer IEG
Carole Nawratil de Bono, Services Industriels de Genève
Peter Oerlemans, NIOO-KNAW & IF Technology
Reza Sohrabi, University of Neuchâtel
Benoit Valley, University of Neuchâtel
Daniela van den Heuvel, University of Bern
Thomas G. Vangkilde-Pedersen, GEUS
Christoph Wanner, University of Bern

Checked by: Joris Koornneef (WP6 leader), TNO

Approved by: Holger Cremer (HEATSTORE coordinator), TNO

Please cite this report as: Guglielmetti, L., Bloemendal, M., Hahn, F., Koornneef, J., Hilleke Mortensen, M. 2021: *Environmental effects of UTES technologies in Europe*, GEOTHERMICA – ERA NET Cofund. 120 pp.

This report represents HEATSTORE project deliverable number D6.6

TNO innovation
for life



storengy



KWR



u^b



HEATSTORE (170153-4401) is one of nine projects under the GEO THERMICA – ERA NET Cofund aimed at accelerating the uptake of geothermal energy by 1) advancing and integrating different types of underground thermal energy storage (UTES) in the energy system, 2) providing a means to maximise geothermal heat production and optimise the business case of geothermal heat production doublets, 3) addressing technical, economic, environmental, regulatory and policy aspects that are necessary to support efficient and cost-effective deployment of UTES technologies in Europe.

This project has been subsidized through the ERANET cofund GEO THERMICA (Project n. 731117), from the European Commission, RVO (the Netherlands), DETEC (Switzerland), FZJ-PtJ (Germany), ADEME (France), EUDP (Denmark), Rannis (Iceland), VEA (Belgium), FRCT (Portugal), and MINECO (Spain).



About HEATSTORE

High Temperature Underground Thermal Energy Storage

The heating and cooling sector is vitally important for the transition to a low-carbon and sustainable energy system. Heating and cooling is responsible for half of all consumed final energy in Europe. The vast majority – 85% - of the demand is fulfilled by fossil fuels, most notably natural gas. Low carbon heat sources (e.g. geothermal, biomass, solar and waste-heat) need to be deployed and heat storage plays a pivotal role in this development. Storage provides the flexibility to manage the variations in supply and demand of heat at different scales, but especially the seasonal dips and peaks in heat demand. Underground Thermal Energy Storage (UTES) technologies need to be further developed and need to become an integral component in the future energy system infrastructure to meet variations in both the availability and demand of energy.

The main objectives of the HEATSTORE project are to lower the cost, reduce risks, improve the performance of high temperature (~25°C to ~90°C) underground thermal energy storage (HT-UTES) technologies and to optimize heat network demand side management (DSM). This is primarily achieved by 6 new demonstration pilots and 8 case studies of existing systems with distinct configurations of heat sources, heat storage and heat utilization. This will advance the commercial viability of HT-UTES technologies and, through an optimized balance between supply, transport, storage and demand, enable that geothermal energy production can reach its maximum deployment potential in the European energy transition.

Furthermore, HEATSTORE also learns from existing UTES facilities and geothermal pilot sites from which the design, operating and monitoring information will be made available to the project by consortium partners.

HEATSTORE is one of nine projects under the GEOTHERMICA – ERA NET Cofund and has the objective of accelerating the uptake of geothermal energy by 1) advancing and integrating different types of underground thermal energy storage (UTES) in the energy system, 2) providing a means to maximize geothermal heat production and optimize the business case of geothermal heat production doublets, 3) addressing technical, economic, environmental, regulatory and policy aspects that are necessary to support efficient and cost-effective deployment of UTES technologies in Europe. The three-year project will stimulate a fast-track market uptake in Europe, promoting development from demonstration phase to commercial deployment within 2 to 5 years, and provide an outlook for utilization potential towards 2030 and 2050.

The 23 contributing partners from 9 countries in HEATSTORE have complementary expertise and roles. The consortium is composed of a mix of scientific research institutes and private companies. The industrial participation is considered a very strong and relevant advantage which is instrumental for success. The combination of leading European research institutes together with small, medium and large industrial enterprises, will ensure that the tested technologies can be brought to market and valorised by the relevant stakeholders.

Table of Contents

About HEATSTORE.....	3
1. Introduction.....	6
2. Aquifer Thermal Energy Storage	7
2.1. General effects ATES	7
2.1.1. Hydrogeological effects.....	7
2.1.2. Soil mechanic effects	9
2.1.3. Groundwater quality.....	10
2.1.4. Reservoir thermal effects	10
2.1.5. Physical properties.....	10
2.1.6. Reservoir water geochemistry.....	11
2.1.7. Microbiology	12
2.1.1. Primary energy savings	12
2.2. Case studies in the Netherlands.....	13
2.2.1. Koppert Cress.....	13
2.2.2. NIOO	23
2.3. Case study in Switzerland.....	39
2.3.1. Geneva case study	39
2.3.2. Bern case study	70
2.4. Case study in Denmark	73
2.4.1. ATES test site.....	73
2.4.2. HT-ATES	74
3. Mine Thermal Energy Storage.....	75
3.1. General effects MTES	75
3.1.1. Drinking water protection	75
3.1.2. Construction and decommissioning	75
3.1.3. Approval process	75
3.1. Case study in Germany	75
3.1.1. Groundwater monitoring	77
3.1.2. Seismic monitoring.....	82
3.1.3. Geomechanical monitoring	86
3.1.4. Carbon intensity.....	87
3.1.5. Microbiological monitoring.....	88
3.1.6. Fast-track risk assessment	89
4. Borehole Thermal Energy Storage	90

4.1. General effects BTES	90
4.1.1. Thermal effect.....	90
4.1.2. Seepage along insufficiently sealed BTES boreholes	91
4.1.3. Leakage of brine from BTES boreholes to groundwater	91
4.2. Case study in France	92
4.3. Case study in Denmark	93
4.3.1. Brædstrup BTES.....	93
4.3.2. Thermal heating of groundwater.	95
4.3.3. Risk of leaks	95
5. Pit Thermal Energy Storage	98
5.1. General effects PTES.....	98
5.1.1. Thermal effects	99
5.1.2. Water supply for the PTES.....	99
5.1.3. Leaks	99
5.2. Case study in Denmark	100
5.2.1. Monitoring of the PTES at Marstal	100
6. Assessment framework.....	105
6.1. General observations	105
6.1.1. Structure and framework of assessment of environmental performance and risks differs per country	105
6.1.2. Every UTES project site is unique; environmental impacts are site-specific.	105
6.1.3. Environmental themes and topics are not unique.....	105
It is very important to discern between environmental impacts and risks.....	107
6.1.4. System components	108
6.1.5. Clarity is need on the impacts and risk for the different project phases	108
6.1.6. Data and assessment quality of the environmental impacts assessed is not always clear	109
6.2. Appendix Environmental criterion/topic	115
7. Conclusion	117
8. References	118

1. Introduction

UTES technologies are becoming more attractive amongst industrial operators as they can contribute to improve the efficiency and decarbonize an energy system. Some of the low temperature technologies available such as PTES, BTES and ATES have a quite high level of maturity and they are already established in several countries in Europe (ref HEASTORE Deliverable 1.1). However, high temperature UTES systems, in particular ATES and MTES have a rather low maturity and the effect on the environment of such systems need to be further investigated.

Environmental concerns are highly relevant in the perception, acceptance, and development of HT-UTES technologies. Identification of potential effects of HT-UTES systems is therefore necessary to optimise their design and to ensure the sustainability of the operation.

The most important environmental effects brought about by UTES utilization are 1) surface disturbances, 2) subsurface chemical and 3) physical effects, 4) noise, 5) thermal effects and 6) emissions in both the atmosphere and in the subsurface. However, UTES systems can also have positive effects on the environment, if considering potential of reducing CO₂ intensity of heat supply. Previous studies focused on subsurface effects distinguishing between hydrogeological, thermal, chemical and microbiological (Bonte et al., 2011).

In this report, a set of potential effects related to subsurface, surface and operations has been identified and described and classified in terms of risk and opportunities according to the data resulting from the field operations at the study site based on the activities carried out in WP4 and WP5. Where such data are not available, information from existing experience, literature review and predictions based on the activities carried out in WP2, are considered to define possible scenarios.

Each study site is presented with its own specificities; therefore, the identification of common assessment criteria was not trivial. A set of indicators has been used to define to assess the potential environmental effect with associated risks and opportunities for the different types of UTES technologies.

This framework can be used as a template for real-case UTES systems.

2. Aquifer Thermal Energy Storage

2.1. General effects ATES

2.1.1. Hydrogeological effects

In the application of ATES systems, groundwater is extracted and, after being heated or cooled down, it is returned to the same aquifer. This extraction and infiltration of groundwater causes changes in the hydrologic equilibrium such as in the hydraulic head, which can affect the direction and speed of groundwater flow within the aquifer, and possibly even between aquifers; this means that the hydraulic head (or groundwater level) can also be affected in other aquifers (Figure 1).

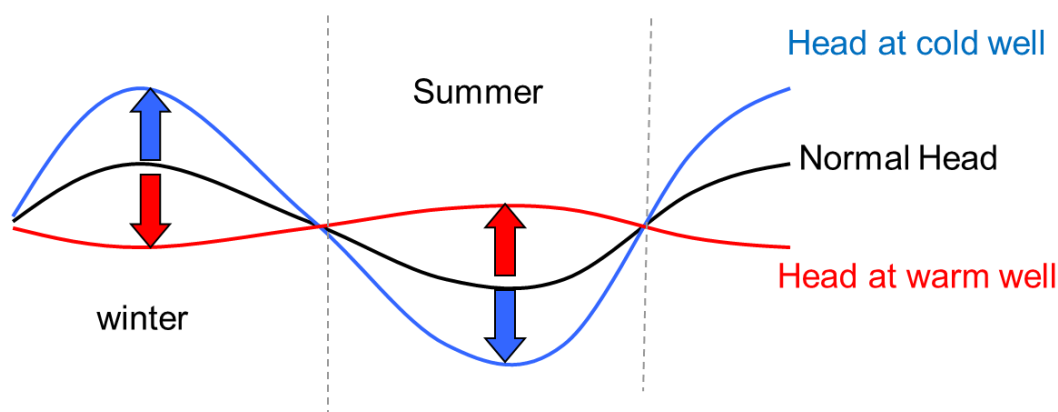


Figure 1. Head changes in ATES wells.

The changes in hydraulic head and groundwater level are the direct hydrological effects of the application of ATES systems, while indirect effects include soil settlements and displacement of water-quality limits. Below it is listed which stakeholders or processes can be influenced by the various effects:

1. Hydraulic head changes:
 - Other groundwater uses in the vicinity (for example drinking water, other ATES systems, industrial extraction or temporarily dewatering/lowering the groundwater level).
 - Underground infrastructural works, which have been designed based on a certain regime of hydraulic head.
2. Groundwater level changes:
 - Construction (flooding or groundwater shortage)
 - Agriculture (water damage or drought damage)
 - Nature/ecology (desiccation/watering)
 - Archaeological values (reducing groundwater level can be harmful)
 - Other groundwater users
 - Underground infrastructure.
3. Soil settlements:
 - Buildings and infrastructure.
4. Mixing of water with different quality:
 - Groundwater contamination
 - Freshwater/saltwater transitions.

Because the extracted groundwater in ATES systems is simultaneously returned to the same soil layer, the volume reduction from extraction is partially compensated by the increase in volume from infiltration. At a greater distance, the hydraulic effect of the extraction is opposite but the same in magnitude as the effect of the infiltration, resulting in a negligible net effect. This means that the area hydraulically influenced is often relatively small for ATES systems (up to a few hundred metres), compared with extractions of comparable magnitude where no return of extracted water takes place (such as for extractions for drinking water, where effects can reach up to several kilometres).

The hydraulic head and groundwater level changes caused by ATES can be easily predicted with existing geohydrology tools, provided that the subsurface conditions and the extraction-infiltration pattern of the system are known. To avoid underestimation of the expected effects, in practice the worst-case assumptions of soil properties and extraction-infiltration pattern are used.

As a result, the hydraulic head changes and groundwater level changes may only be of importance in the vicinity of the ATES wells and when ATES is applied in a shallow aquifer.

Note also that the configuration of the boreholes of the ATES system will have an influence on the potential environmental impact of the system. Indeed, the geometry of the injector and producer boreholes will affect the perturbation of the piezometric level: some configuration will tend to generate a lowering of the piezometric level on the system favouring a convergence of the flow lines toward the ATES. This can promote a hydrodynamic isolation of the ATES and thus limit potential interaction with the environment. Other configurations will promote a piezometric high on the ATES promoting diverging flow lines and implying a ATES which is hydrodynamically open on the environment. In Figure 2, this principle is presented for 3 typical well configurations envisaged for ATES. The doublet configuration (Fig. 2a) generates a configuration that is basically open on the environment with the water injected that can potentially swap a large area of the aquifer. A 5-spot configuration with a central injection well and with 4 peripheral production wells (Fig. 2b) over which the flow is distributed generate an overall piezometric high over the system and thus the flow lines are diverging toward the environment. The last illustrated configuration (Fig. 2c) is a 5-spot with the production well in the centre and 4 peripheral injectors. With this configuration a piezometric low is centred on the system and thus the circulating water is isolated from the environment. The last configuration is thus theoretically the safest in terms of environmental concern. However, this must be also considered in view of the thermal storage performance of the system (cf. Mindel & Driesner, 2020).

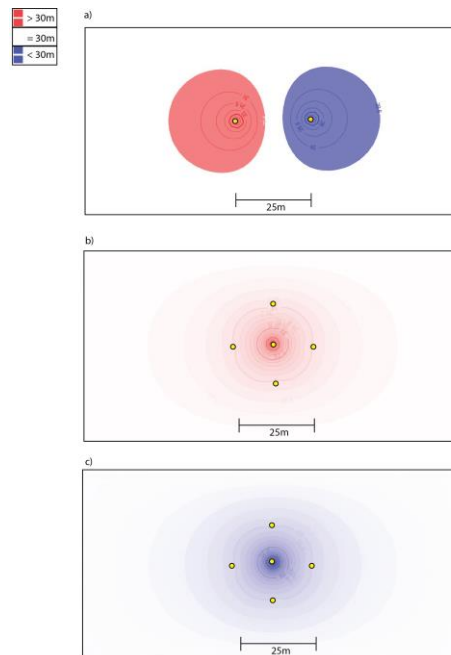


Figure 2. Piezometric perturbation implied by an ATEs with various borehole configuration. a) doublet configuration, b) 5-spot configuration with the injector as central well. c) 5-spot configuration with the producer as the central well. In these models the initial piezometric level is at 30m. Red areas denote elevations and blue areas depressions of the piezometric.

2.1.2. Soil mechanic effects

A decrease in the hydraulic head or groundwater level creates an additional load and may therefore cause subsidence. The extent to which settling occurs depends not only on the head change, but also on the soil's sensitivity to settling and the thickness of the soil layer. For example, clay and peat soils are much more sensitive to settling than sand and gravel soils. The extent to which the soil layer has been weighed down in the past – the so-called pre-load – is also important. The loads from the past have caused a certain amount of compression, and as long as the new load does not exceed the maximum load from the past, the soil layer will not be further compressed.

Soil settling is relevant to ATEs, as they can cause damage to buildings and infrastructure. They are especially harmful when there are large differences in settlement from place to place; if the settlement is even, it does not cause any damage, unless very large. Settlement at greater depths is 'damped' by the overlying layers. Settlement at surface level is thus divided over a larger area and is much smaller and more uniform than settlement at depth. In the case of shallow ATEs systems, the probability of variations at ground level is much higher, because hardly any damping can take place.

As far as is known, no damage has ever occurred in practice because of settlement due to hydraulic head changes by ATEs. However, there are at least 10 ATEs programmes known in the Netherlands where the calculated settlement has been a reason for ground level monitoring to be required.

An open research question is how the settling measured in existing ATEs systems relates to the calculated settling (with specific consideration of the high-temperature heat storage systems in connection with thermal settlement and swelling). Settlements due to hydraulic head changes can be calculated. However, much less is recorded in the scientific literature and observed in practice about settlement that can be expected because of temperature

changes: with large changes in temperature in the soil, thermal settling can occur due to the expansion or shrinkage of soil particles. In laboratory tests, a linear relationship for elastic stress formation has been found in the temperature range from 0 to 80°C, both for clay and for sand. Settlements of up to 0.0014% /°C occurred for sand and 0.03% /°C for clay, while measurements in practice seem to indicate that the actual effects are smaller.

2.1.3. Groundwater quality

ATES systems attract groundwater from around their wells, which may have different water qualities. In the well these different waters are mixed, and any substances diluted and injected into the other well. In shallow aquifers substances can be anthropogenic of origin (e.g. contaminations or nitrates/sulphates due to agriculture). In coastal areas ATES systems may cause mixing of fresh and saline groundwater resulting in salinization.

Salinization is an almost irreversible process: once it has occurred, the groundwater system will not recover quickly (at least not within decades). If the mixing of fresh and saline water takes place in an ATES system, the fresh groundwater availability will decrease. The use of ATES in aquifers with a transition from fresh to saline groundwater is therefore usually not permitted, unless it can be demonstrated that no adverse effects are likely to occur.

2.1.4. Reservoir thermal effects

There is considerable knowledge about heat transfer in the subsurface. Various tools/models can be used to predict changes in temperature resulting from ATES systems (Alt-Epping et al., 2020), when the subsurface characteristics are known. However, uncertainty in predicting temperature effects lies in the pattern of use of the ATES system. In practice, the infiltration temperatures and the displaced water quantities often deviate from the design values. The change in temperature may affect the physical properties, the geochemistry and microbiology of the groundwater/subsurface material.

An inventory of ATES systems in the Netherlands showed that almost none of the investigated systems had a thermal balance, meaning that cold or heat is discharged into the aquifer and long-term cooling or warming of groundwater is occurring (Bonte et al., 2011). A study in Winnipeg, Canada, showed the long-term rising groundwater temperatures using the aquifer solely for cooling purposes making such approach not sustainable (Ferguson and Woodbury, 2006).

2.1.5. Physical properties

Due to temperature change water viscosity and temperature changes, and as a result so does the hydraulic conductivity of the aquifer. For LT-ATES systems this affects the required pumping energy to extract and inject the water, as viscosity change is strong at low temperature range, Figure 3. Whereas density change at higher temperatures, for HT-ATES may these trigger buoyancy flow, Figure 3.

Density and viscosity of water vs temperature

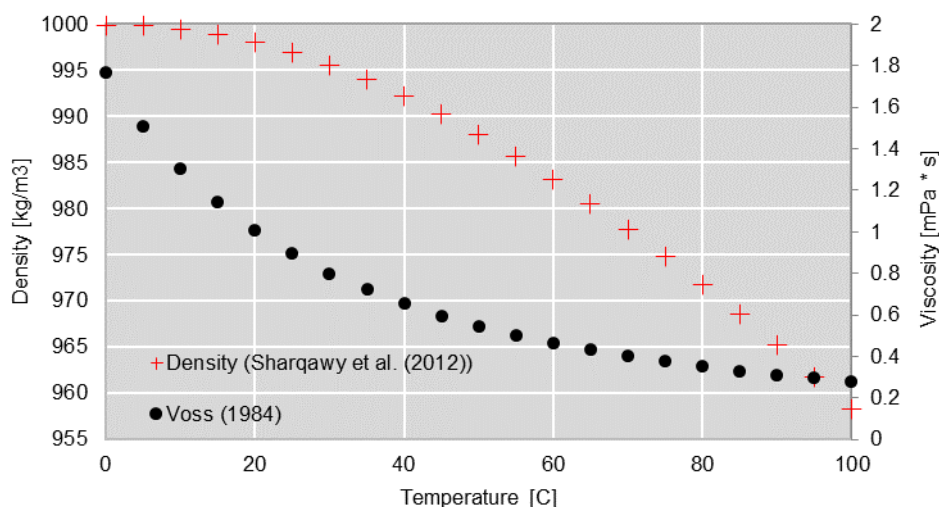


Figure 3. Density and viscosity dependency on temperature.

From the literature it appears that the influence of temperature on the specific heat capacity (C_p) and the thermal conductivity (k_T) of liquids and solids is very small. Since the average value for the heat capacity of sand and clay is the same. As a result, the influence of heterogeneity on the distribution of the heat capacity in the subsurface is limited.

2.1.6. Reservoir water geochemistry

The extent to which geochemical processes can lead to a significant change in groundwater quality depends on the ATES system (e.g. temperature differences) and the geochemical properties of the groundwater system (e.g. redox states, composition of the groundwater). For LT-ATES, research has shown that the effects on geochemistry are limited (Bonte, 2014; MMB, 2012). At low temperatures, it is mainly through mixing that effects can be expected, especially when there is a strong vertical variation in the original groundwater composition. In addition to the mixing of different groundwater qualities inside the extraction well, mixing also takes place along the edges of the injected water volumes. This is caused by the gradients between the mixed groundwater within the ATES system, which has changed composition, and the groundwater outside the ATES system. It is expected that during injections, stronger deviations for mineral equilibriums and larger redox contrasts may occur between mixed groundwater and aquifer sediment.

At higher temperatures ($> 50^\circ\text{C}$), the precipitation of calcium carbonate (CaCO_3) and silica (SiO_2), are important known changes in geochemistry, leading to well clogging. In addition to Calcium (Ca) and Silicon (Si), other macro-chemical parameters are usually also investigated. At higher temperatures also mobilisation of trace elements also occurs, but lab experiments also show re-adsorption when the groundwater is cooled down again (Dooren et al., 2019).

The most important knowledge gaps in geochemistry are the influence of ATES on trace elements has not yet been sufficiently investigated and mixing groundwater at different depths can give rise to reactions between the mixed water and the soil material, especially if there is strong vertical variation of the groundwater quality.

2.1.7. Microbiology

An increase in temperature is generally expected to have a limited effect on the total number of micro-organisms in the ground water. The main reason for this is that in the deep groundwater, under usual prevailing conditions, there is no or very little assimilable organic carbon that micro-organisms need in order to grow. In cases, however, that nutrients are supplied by the groundwater, the number of micro-organisms can increase. Competition arises between the various types of micro-organisms, as those that are adapted to the circumstances will survive better and niches will occur.

The composition of microbial populations in groundwater can therefore be influenced by a change in temperature and groundwater mixing caused by ATES systems. The effect of these changes has yet to be thoroughly investigated. So far, microbiological research of soils and groundwater focuses mainly on indicating the presence of specific groups and species of micro-organisms. In some studies, the focus is also on detection of specific soil functions (nitrate reduction, iron oxidation, etc.).

No significant increase in pathogens has so far been observed in any of the ATES projects that have been monitored. Faecal organisms such as *E. coli* have been found at a single location, but not in excessively increased numbers. In fact, it appears that the pathogens in ATES systems can even decrease. Pathogens that do not occur naturally in the subsurface have little chance of survival, as they are insufficiently adapted to the conditions and are outcompeted by the naturally occurring micro-organisms.

Further research is required to determine the indirect effects of ATES systems on the soil ecology. Currently, the effect of temperature on the release of assimilable organic carbon and nutrients, as well as the effect of groundwater mixing on soil ecology, have been examined in a limited number of field and lab tests.

2.1.1. Primary energy savings

The intrinsic value of storage technologies is that available heat is utilised. How much primary energy use are saved depends strongly on site specific conditions. In the case studies this is illustrated in detail, in this section a general example is provided. Table 1 shows the operational efficiencies of both systems, expressed in coefficient of performance (COP = Heating/cooling delivered divided by primary energy used). Direct cooling from the ATES well is very efficient as it only requires some well and circulation pump to run. The exact COP strongly depends on the achieved temperature difference between the warm and cold well. Compression cooling machines generally have a COP of about 3. For heating the normal low temperature ATES systems COP is lower than cooling because the heat pump is now used. For HT-ATES heat pump operation is less or even prevented, which results in even higher COP for heating. Gas fired boilers usually have an efficiency of about 90%. Assuming balanced heating and cooling load the primary energy use of an ATES system is a factor 8 lower than conventional.

Table 1. Example operational efficiencies for ATES and conventional system.

Item / system	ATES	Conventional
Cooling COP	20-40	3
Heating COP	3-4	0.9
Average COP (balanced heating and cooling demand)	16	2

The exact emission reductions depend on local installation costs, gas and electricity prices and the total amount of heating and cooling that is needed.

2.2. Case studies in the Netherlands

2.2.1. Koppert Cress

2.2.1.1. Site description

Koppert-Cress is a horticulture company situated in the western part of the Netherlands. To provide sustainable heating and cooling, an ATES system was installed with 4 warm and 4 cold wells (Figure 4). As part of a Dutch research project the normal ATES was converted to a HT-ATES pilot (Bloemendal et al., 2019, Bloemendal et al., 2020). To obtain insights in the heat spreading and water quality changes associated to the ATES the site is intensively monitored.

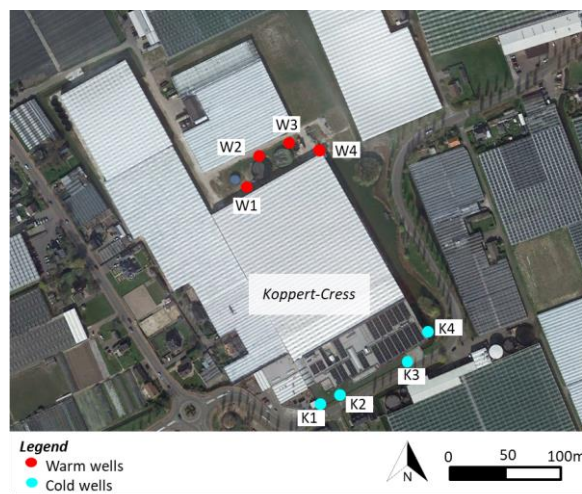


Figure 4. Overview of Koppert-Cress site with well locations.

Local subsurface composition is provided in Figure 6, together with the locations of the ATES well screens. The ATES system utilizes 2 aquifers with screens up to $\pm 170\text{m}$ depth. The ambient groundwater flow is close to 0, there is virtually no head gradient in the area.

The heating loads to/from and temperature of the warm wells is depicted in Figure 5. This illustrates the strong imbalance in heating and cooling demand of the system. The distance of the temperature front is referred to as the thermal radius (R_{th}), and is due to the imbalanced operation not larger than 15 m.

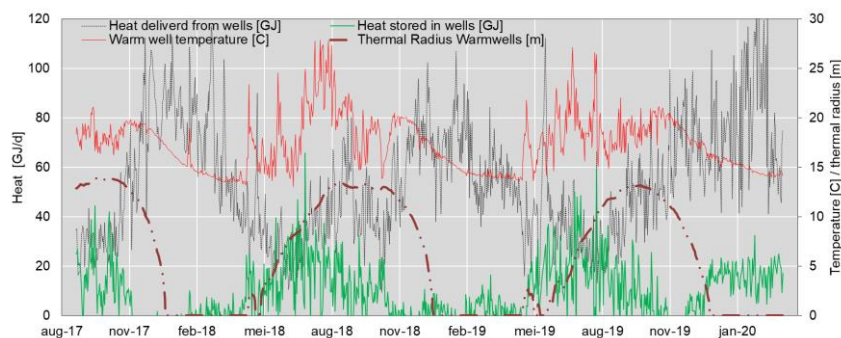


Figure 5. Daily heat to and from the warm ATES wells, well temperature and size of the thermal radius in the 2.5 year period from August 2017 to March 2020.

2.2.1.2. Monitoring

Figure 6 and Figure 7 shows the locations and depth of the DTS temperature monitoring installed. This allows to closely monitor the temperature profile and heat distribution around the warm well. Next to that also 3 monitoring wells are installed, from which periodically water samples are taken to analyse the water quality. Figure 7 also shows the locations of these 3 monitoring wells (PB in the figure), 1: at 20m distance from W3, 2: at 75 m distance from W4 (as a reference, without any influence of the warm well) and 3: at 5m distance from W1. Table 2 shows the dates and status of the warm well when the water samples are taken. The following microbiological parameters are analysed: ATP, DNA/qPCR, CFU22 and following bacteria (groups): (E) coli, Legionella pneumophila, vibrio and sulphate reducing. And the following chemical components: Carbon hydroxide, DOC, Methane, Chloride, Sulphate, nitrate, Ortho phosphate, ammonium and various heavy metals using ICP-MS.

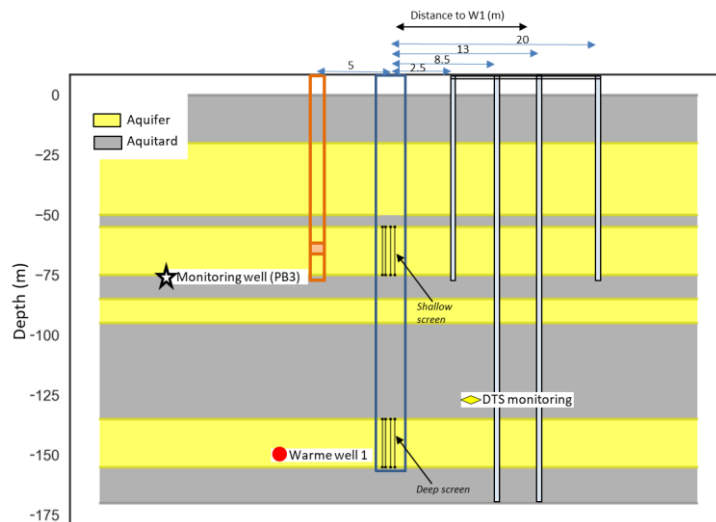


Figure 6. subsurface composition and monitoring infrastructure at warm well 1 – Koppert-Cress.

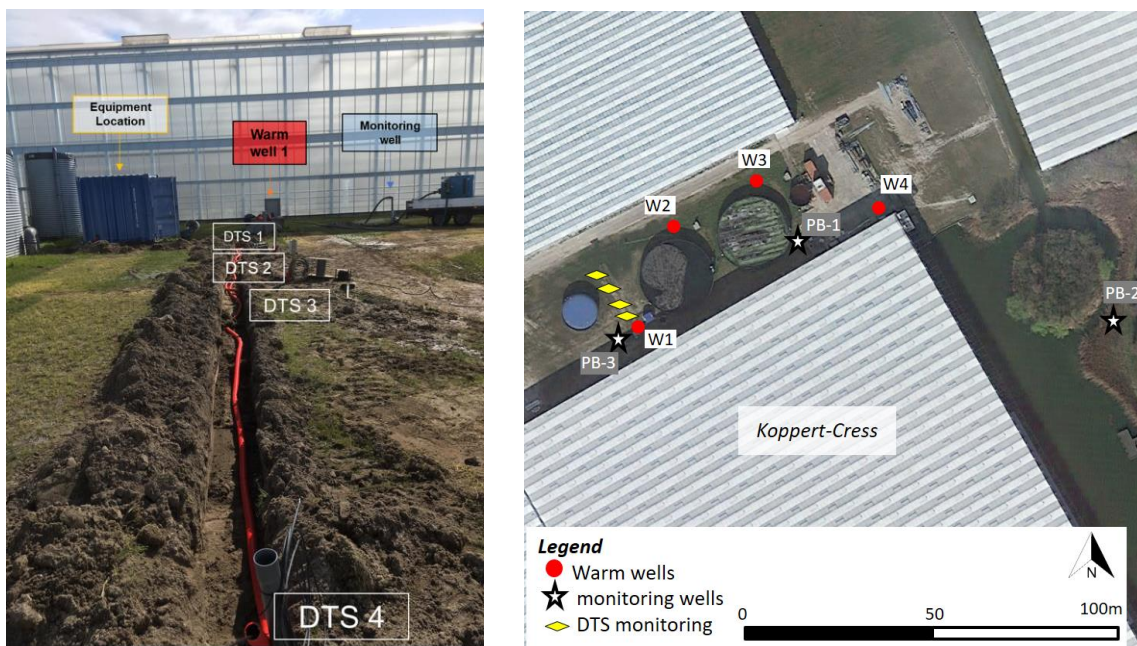


Figure 7. Overview of the monitoring facilities around 'warm well 1'.

Table 2. Overview of groundwater quality samples obtained.

Date sample	Period	Warm well status	T PB3	T PB1	T PB2
17-9-2018	End of charging heat	full			
3-2-2020	50% discharging	25% full	15.9	13.3	13
16-3-2020	End of discharging	empty	13.4	13.2	12.8
10-8-2020	75% of charging	75% full	24.6	16.1	13.6
14-9-2020	End of charging heat	Full	18.5	16.4	16

2.2.1.3. Results

Temperature effects

Figure 8 shows the temperature profiles measured by the DTS from October 2019 until September 2020. The temperature increase is apparent in the two aquifers employed by Koppert-Cress, with the strongest temperature changes near to the well, while at the DTS location at 18m distance a limited change in temperature is observed. This corresponds with the expected reach of the thermal radius of about 15 m (Figure 4). The middle 2 DTS monitoring locations show a difference in spreading of heat between the upper and the lower aquifer. The heat has a larger reach in the shallow aquifer, indicating that this aquifer is more productive and contributes more to the total flow of the well compared to the deeper aquifer. The temperature variations at about 40m depth is caused by a thin sandy layer, from which heat conduction for the well is transported into this layer.

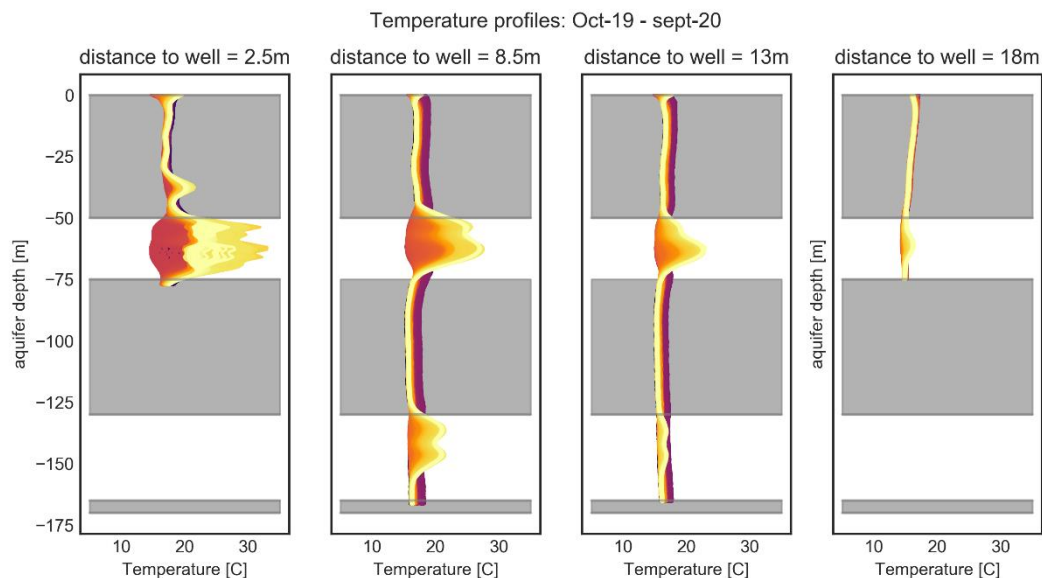


Figure 8. DTS temperature monitoring results at 4 different locations from the warm well. Each line is a moment in time, Purple is in the beginning, yellow half-way and red at the end of the time series.

The DTS measurements do not show considerable heating of the clay layers covering the aquifer employed for heat storage. The measurements at 2.5 and 8.5 m distance show heating at the bottom of the clay layer, but at lower temperatures than measured in the aquifer and almost returning to ambient like is also the case in the aquifer at the end of winter.

Figure 9 shows the temperature increase over time. This confirms the observation that the temperature inside the aquifer as well as in the confining layers returns towards ambient conditions during winter, due to the imbalanced use of the ATEs system. The temperature change contour of 5°C illustrates how the confining layers slowly heat-up during summer and cool down during winter.

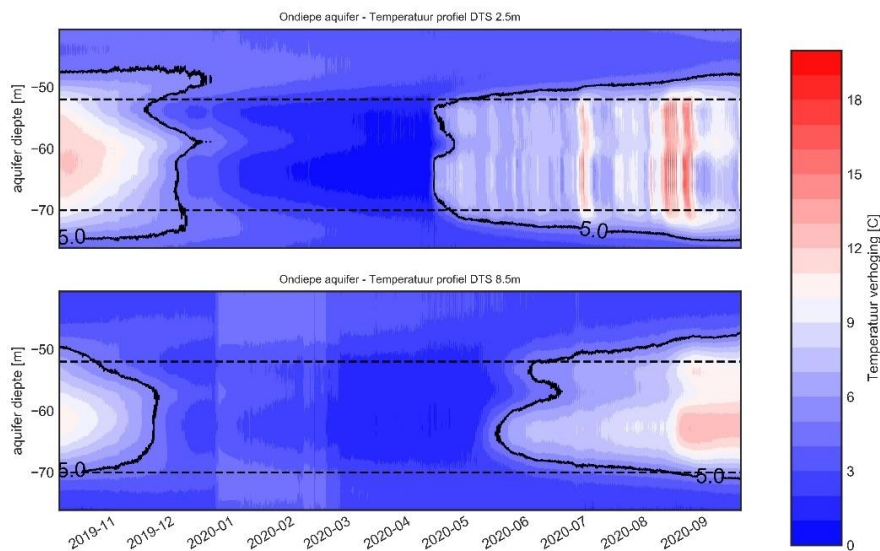


Figure 9. Temperature increase in the shallow aquifer over time, at 2.5 and 8.5 m distance.

Aquifer heterogeneity affects the temperature distribution in the subsurface, Figure 10 shows that some layers show better conductivity as they respond quite well to injection and extraction (e.g. 52-55 m and 62-67 m. While at around 60 m depth the response is much slower and less strong as well, indicating that this layer has a lower hydraulic conductivity and hence contributes less to the total flow of the well.

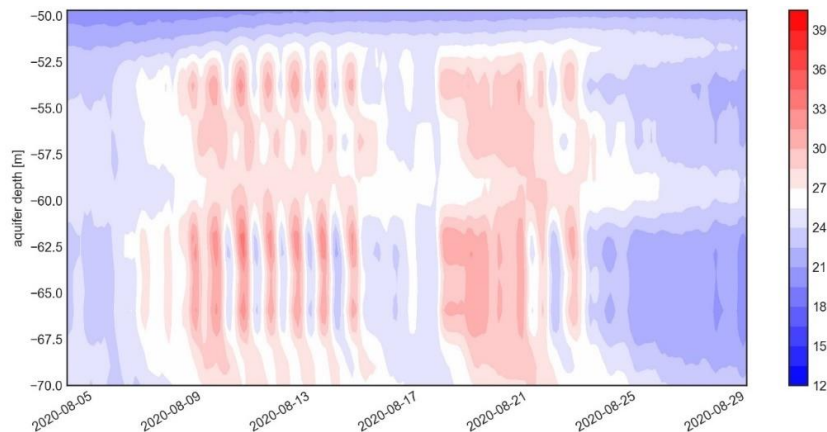


Figure 10. Heterogeneity made visible via the temperature distribution over the full aquifer thickness at 2.5m distance from the warm well.

Reservoir water quality

Temperature change of the groundwater may also affect the composition of the groundwater through interactions ((im)mobilisation, de/ab-sorption) with minerals present in the sediment and/or deposition of dissolved components in the groundwater (or solution of depositions). Temperature affects these processes as temperature change may cause shifting of chemical equilibria and change of reaction kinetics. The resulting effects on the groundwater composition are usually a complex set of interactions of multiple reactions.

Processes known to be important to the matter at hand are: the calcite balance and deposition of carbonates, increased degradation of organic matter, redox potential and the mobilisation of trace elements present in the sediment.

NB. Next to the effects of temperature change on groundwater composition, ATEs systems may also affect the groundwater composition in different way, of which one dominating is mixture and spreading of groundwater of different composition. The mixing and lack of reference samples from the deeper aquifer complicated the analysis of the groundwater quality due to temperature change, as well as the limited temperature changes.

Temperature change of the groundwater may also affect the composition of the groundwater through interactions ((im)mobilisation, de/ab-sorption) with minerals present in the sediment and/or deposition of dissolved components in the groundwater (or solution of depositions). Temperature affects these processes as temperature change may cause shifting of chemical equilibria and change of reaction kinetics. The resulting effects on the groundwater composition are usually a complex set of interactions of multiple reactions.

Processes known to be important to the matter at hand are: the calcite balance and deposition of carbonates, increased degradation of organic matter, redox potential and the mobilisation of trace elements present in the sediment.

NB. Next to the effects of temperature change on groundwater composition, ATEs systems may also affect the groundwater composition in different way, of which one dominating is mixture and spreading of groundwater of different composition. The mixing and lack of reference samples from the deeper aquifer complicated the analysis of the groundwater quality due to temperature change, as well as the limited temperature changes.

Mixing

The ATES wells of Koppert-Cress extract and inject in 2 different aquifer, of which the deeper aquifer as a higher salinity. Figure 11 shows the increase in chloride concentration in the monitoring wells in the shallow aquifer. The steady increase is the result of the mixing of the water from 2 different salinity aquifers. Monitoring well 2 (PB2) also shows an increase, this was supposed to be a reference well, but is already affected by the cold well hydraulic influence, due the large imbalance of the system.

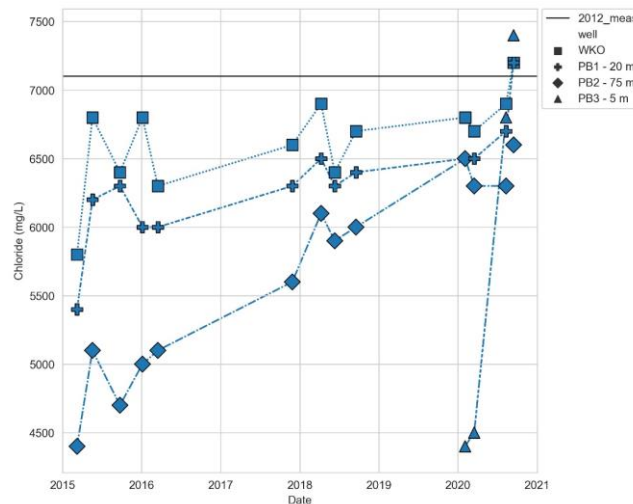


Figure 11. Chloride concentration in the monitoring wells in the shallow aquifer over time, the solid black line indicates the concentration of the groundwater extracted from the well (mixture of shallow and deep aquifer).

Temperature effects

As a result of dominating mixing effects as well as the limited temperature change, water composition changes due to temperature (Figure 12) were not clearly identified. It is known from literature that sulphate reduction occurs at higher temperatures (Bonte et al., 2013). However, in Figure 13 an increasing trend in sulphate is visible, due to mixing, not temperature. The same is true for Arsenic, instead of the possible increase it decreases due to mixing, Figure 14. Also, deposition of calcium carbonates is not occurring, as well as no relation between temperature and changes in iron, DOC, phosphate or ammonium.

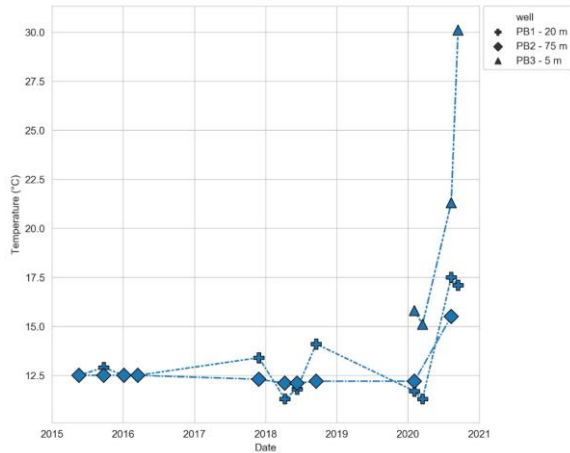


Figure 12. temperature in the monitoring wells during sampling actions.

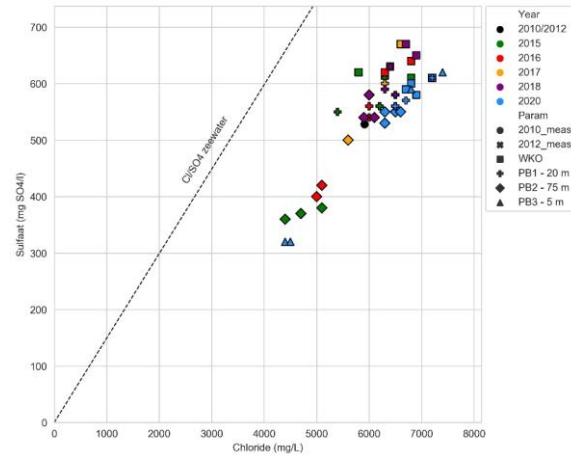


Figure 13. Chloride concentration relative to Sulphate concentration. The dashed line represents the seawater sulphate equilibrium.

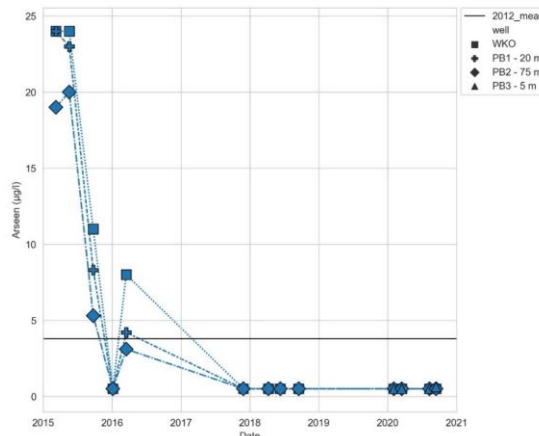


Figure 14. Arsenic concentration over time. After 2017 all samples are lower than the detection limit.

Microbiology

Micro-bacterial activity may also change due to changes in temperature, this may cause risks for the public health of the people working with the system which may get exposed to the groundwater if this concerns harming pathogens, or for the function of the system due to clogging as a result of bio-fouling. Also the microbial population may change due to changes in temperature. The presence and growth of opportunistic and entero pathogens are monitored at Koppert-Cress (Table 3). Geochemical conditions and temperature determine if a microorganism can survive and reproduce or not. The reference sampling of the water quality shows that the groundwater at Koppert-Cress is anaerobic and without denitrification (Lieten et al., 2010).

Table 3. List of the monitored micro biological parameters.

Microbiological parameters
ATP
<i>Vibrio</i> spp.
<i>Escherichia coli</i>
Bacteriën van de coligroep
SSRC (sporen van sulfiet reducerende <i>clostridia</i>)
<i>Legionella pneumophila</i>
<i>Stenotrophomonas maltophilia</i>
<i>Acanthamoeba</i> spp.
Nontuberculeuse Mycobacteriën

During the monitoring campaign ATP has been analysed for each sampling moment, Figure 15. The measured ATP concentrations vary, but not in correlation/correspondence to temperature changes. The results give a mild indication to little higher biomass presence in summer compared to winter, which may be caused by the higher temperatures.

Figure 16, shows the results of the Clostridium bacteria (SSRC). The concentrations vary across the years and across the monitoring wells. The increase in SSRC in monitoring well 2, where no increase in temperature was measured, indicates that the observed variations are not caused by temperature changes (Bloemendal et al., 2020).

Similar results apply to the other monitored pathogens: either not detected, or some variation are observed, but non relate-able to the temperature change of the groundwater. All in all, the increased groundwater temperature does not lead to growth of the investigated opportunistic pathogens. The concentration of pathogens monitored do not lead to risks for public health.

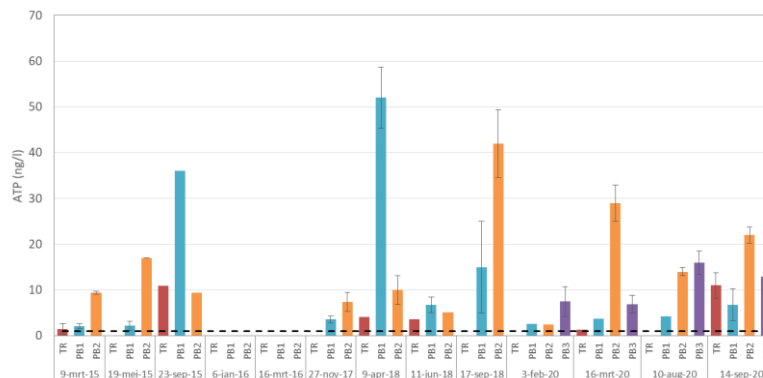


Figure 15. ATP concentrations during monitoring campaign at Koppert-Cress ATEs system. Dashed line indicates the detection limit. TR = Technical Room / Plant Room. PB= Monitoring well.

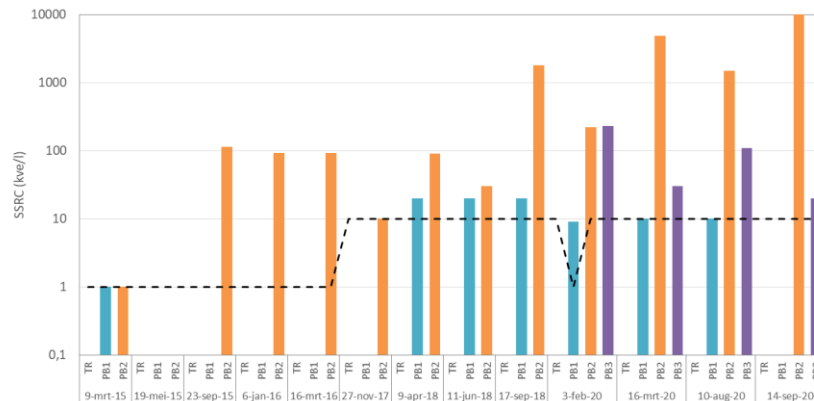


Figure 16. SSRC concentrations during monitoring campaign at Koppert-Cress ATES system. Dashed line indicates the detection limit. TR = Technical Room / Plant Room. PB= Monitoring well.

Energy savings and CO₂ Intensity

The energy monitoring of the components and heat flows in the system of KC are used to calculate the costs and emission associated with the ATES system. these same energy flows are used to asses costs and emission for different alternative heating and cooling supply systems:

- 1) Gas fired boiler and compression chiller
delivered heating and cooling is delivered with a boiler with an efficiency of 95% and a chiller with a COP of 3.
- 2) LT-ATESà normal warm well temperature
The following operations are carried out to identify energy use of a normal ATES system:
 - a. Heat pump capacity scales with the available heat from the wells and the flow rates between the wells stay the same
 - b. The heat available from the well scales down by a factor 2 as the yearly average ΔT between wells is a factor 2 lower for all ATES systems in NL (6°C, (Willemsen, 2016)), compared to current practice for KC (12°C).
 - c. Due to lower warm well temperature, the heat pump has a lower COP, proportional to the change in Carnot efficiency.
 - d. Cooling by wells is also smaller, due to lower ΔT between the wells.
 - e. Power use of the circulation pumps is the same as in current practice (due to lower temperature levels COP's are smaller)
- 3) ATES as applied at KC
Electricity use of the different components is monitored (circulation pumps, well pump and heat pump. Also, gas use of the peak boiler. These data is used to assess the performance of the system, given the amount of heating and cooling delivered.
- 4) Higher temperature of the warm well for the existing ATES at KC.
the following operations are carried out to assess the performance as if KC would have an even warmer warm well temperature.
 - a. Heat pump capacity scales according to the heat available from the wells.
 - b. Heat available scales up with a factor 1.5 as we assume a yearly average ΔT increase of 6°C, so 18°C instead of the 12°C under current operation.
 - c. Heat pump COP scales according to the Carnot efficiency associated to the increased warm well temperature.
 - d. Cooling by wells is also more, due to higher ΔT between the wells.

- e. Power use of the circulation pumps is the same as in current practice (due to higher temperature levels COP's are larger)

Koppert-Cress buys sustainable electricity at a €0.093/kWh rate and gas €0.19/m³. The gas emission factor is 1.77 kg CO₂/m³. For the electricity use two electricity emission factors are used, A) one for the total chain emission for the sustainable power bought by KC: 0.05 kg CO₂/kWh and B) the mix at the power grid of the Netherlands: 0.32 kg CO₂/kWh (Bloemendal et al., 2020; Vreede and Groot, 2010). Figure 17 shows the results of the comparison. The higher the temperature of the warm well the better the system performs. Electricity use increased due to more heat pump electricity use. Gas use decreases considerably, resulting in lower overall GHG emissions, despite more heat is delivered.

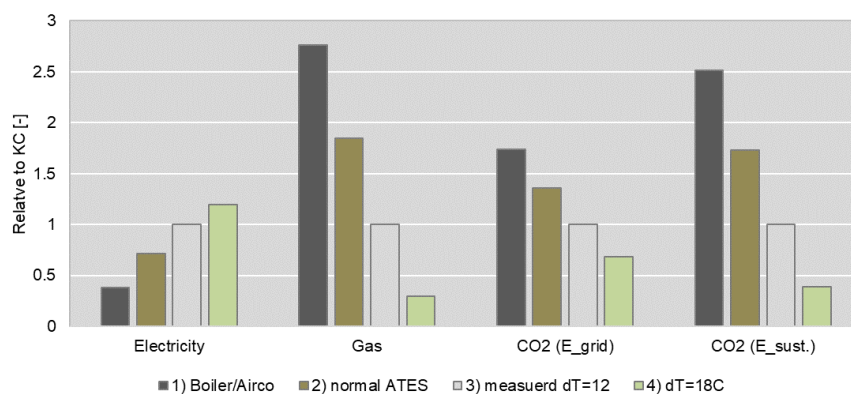


Figure 17. Relative change in energy use and associated CO₂-emissions and operational costs relative to the current Koppert-Cress system (gray bar = 1 everywhere).

2.2.1.4. Discussions

- Upgrade ATES to HT-ATES: maximum infiltration temperatures from 25°C up to 45 °C, average ΔT between wells from 6°C to 12°C .
- Installation of 2 shallow and 2 deep Distributed Temperature Sensor (DTS) monitoring locations and sampling of groundwater quality.
- Thermal effects are negligible. All heat is extracted, hence no continuous heating of aquifers or confining layers occurs.
- Temporal high infiltration temperatures of >30°C flatten to <30°C in the subsurface and subsequent extraction.
- Water quality effects are dominated by mixing effects, important changes in salinity, arsenic and sulphate are all contributed to the mixing of water from 2 different aquifers. No change in water composition is caused by changes in temperature, due to the fact that temperature changes are limited and only locally around the wells.
- The limited increase in groundwater temperature does not lead to growth of the investigated opportunistic pathogens.
- Higher storage temperatures results in larger amounts of heat to be stored and hence lower GHG emissions.

2.2.1.5. Fast-track Risk assessment

A fast-track risk assessment is carried out for the KC operational phase (Table 4).

Table 4. Fast-track risk assessment for the Koppert-Cress site.

Koppert-Cres							
Effect	Phase	Operations (predicted)					
		P	A	M	Probability	Consequences	Risk
Air quality					L	L	L
Noise and vibration					L	L	L
Formation water quality					M	M	M
Formation water temperature					M	M	M
Surface clear water					L	L	L
Soil occupation					L	L	L
Wastes and dangerous substances					L	L	L
Environment					L	L	L
Nature					L	L	L
Soil mechanics					L	L	L
Seismicity					L	L	L
CO2 intensity redyction					H	M	H

2.2.2. NIOO

NIOO is the Netherlands Institute of Ecology. The research institute has performed ecological research for over 60 years and is renowned for its long-term and consistently high quality research across all ecological disciplines. Following the ‘Cradle-to-Cradle’ philosophy, NIOO has the ambition to close as many cycles as possible, including the energy cycle of its own building. NIOO, opening itself up as an experimental garden for innovation, has realized a HT-ATES system in 2010 that is used to store heat from solar collectors. Temperatures and groundwater composition have been monitored ever since, offering a unique 10-year field data series. In the framework of the HEATSTORE project this dataset was used to investigate the effects of HT-ATES on the subsurface. An individual and more elaborate case study of the NIOO HT-ATES system is currently in preparation and will be delivered within the HEATSTORE program. It is referred to this report for further details.

2.2.2.1. Well locations and monitoring setup

At NIOO, both a regular ATES system (injection temperatures < 25 °C) and a High Temperature (HT) ATES system (storage of heat with temperatures up to 45 °C) was realized. This report focusses on the HT-ATES system and its monitoring results. The HT-ATES system consists of three wells: the hot well, the cold well and the monitoring well (see Figure 18). The hot and cold well pump groundwater from 220-295 mbgs for storage and recovery of heat. At each of these three locations, four small sampling wells were installed at different depths (see Table 5).

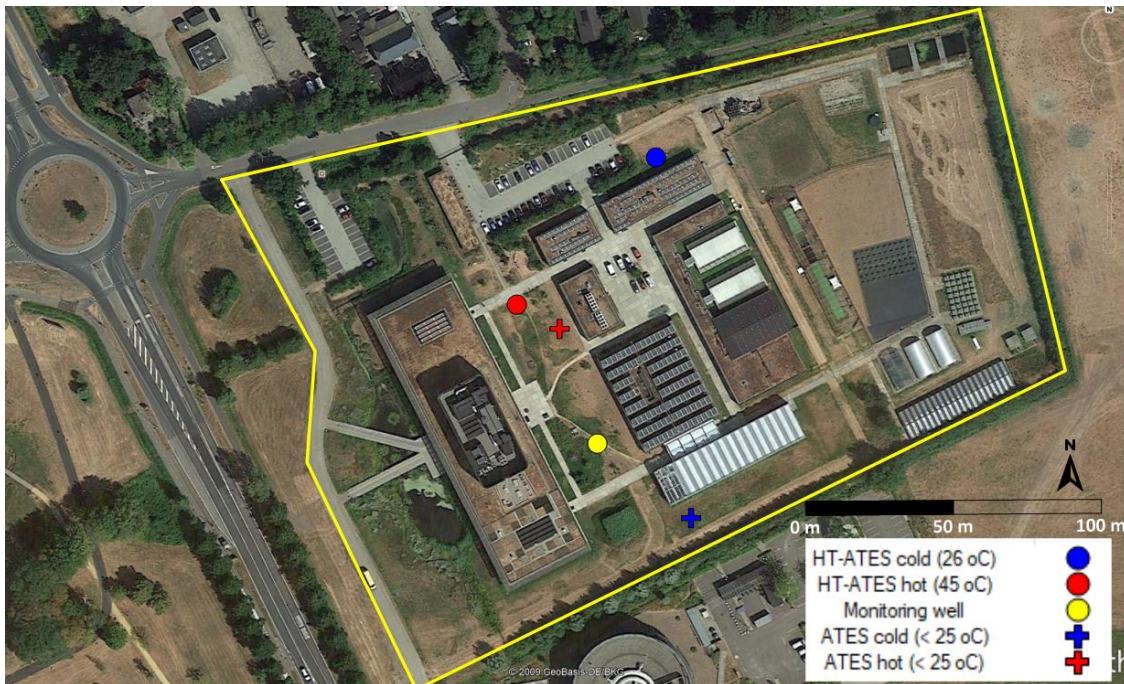


Figure 18. A bird’s-eye view of the NIOO terrain with the hot, cold and monitoring well of the HT-ATES system shown as a red, blue and yellow dot respectively. The locations of the regular ATEs wells (< 25 °C) are indicated with crosses.

Table 5. Specifications of the piezometers that were installed in annulus of the hot well (prefix ‘W’) and cold well (prefix ‘K’) and in the monitoring well (prefix ‘MP’). F1 to F4 refer to the piezometer screen numbers, with increasing numbers referring to larger depths of the screened interval.

Hot well code	Perforation depth (mbgs)	Cold well code	Perforation depth (mbgs)	Monitoring well code	Perforation depth (mbgs)
W-F1	170-172	K-F1	170-172	MP-F1	170-172
W-F2	193-195	K-F2	193-195	MP-F2	193-195
W-F3	220-222	K-F3	220-222	MP-F3	220-222
W-F4	280-282	K-F4	293-295	MP-F4	285-287

A visualization of the subsurface properties and the depths of the wells and piezometers are schematically shown in Figure 19. The well casing and the piezometers are installed in the same borehole.

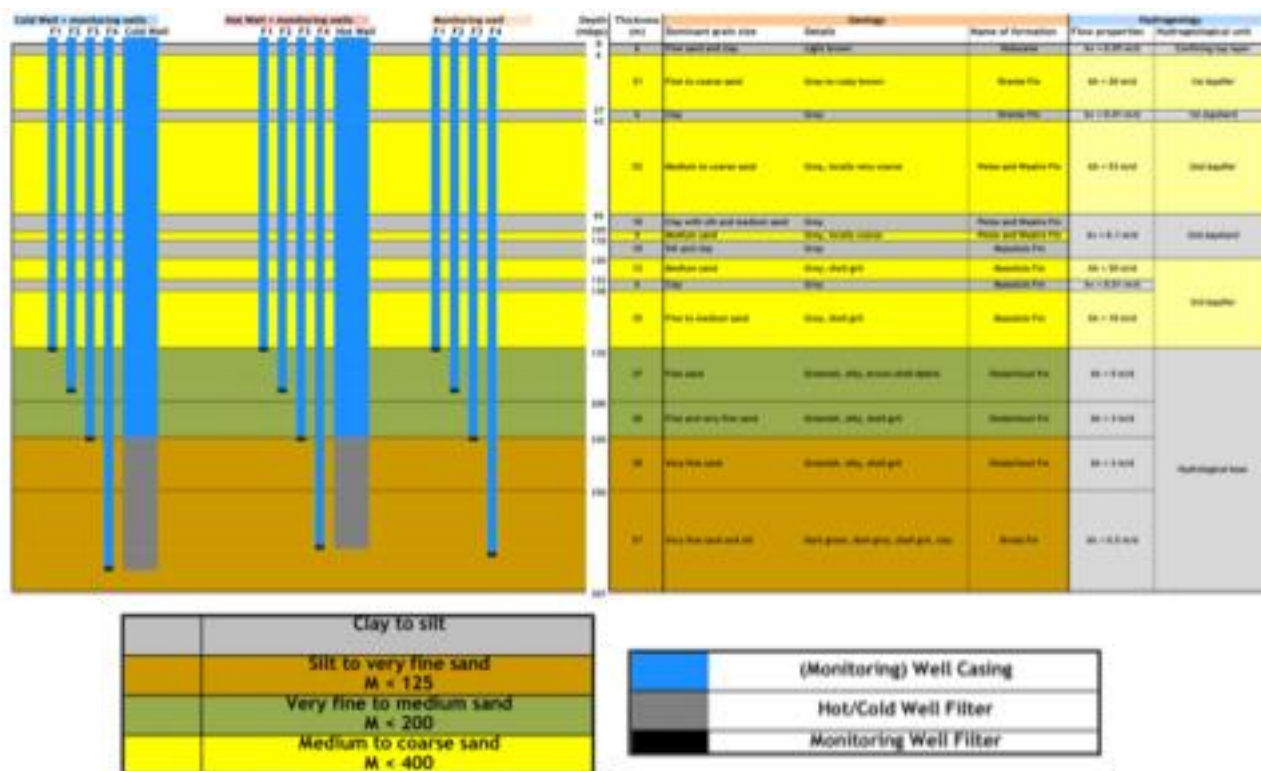


Figure 19. Schematic cross-section of the subsurface, as based on the borehole logs. The piezometer configuration is shown on the left hand side, the (hydro)geological properties of the subsurface on the right hand side.

The monitoring setup at NIOO focusses on tracking the effects of the heat storage (at 220 – 285 mbgs) on the shallower 3rd aquifer (138 – 170 mbgs) which holds pristine fresh groundwater. To enable sampling of the groundwater from different depths, piezometers were installed with screens at four depths:

- Directly next to the top and bottom of the well filters (220 and ~285 mbgs)
- At the bottom of the 3rd aquifer (170 mbgs)
- Between the top of the well screen and the bottom of the 3rd aquifer (around 195 mbgs)

2.2.2.2. System operation

The monthly water volumes that were pumped by the system between 2010 and 2019 (Figure 20) show that heat is stored during the summer months and recovered in the first colder months (autumn and winter). In Figure 21, the monthly average injection temperatures are presented. The designed injection temperature at the hot well is 45 °C and at the cold well 26 °C.

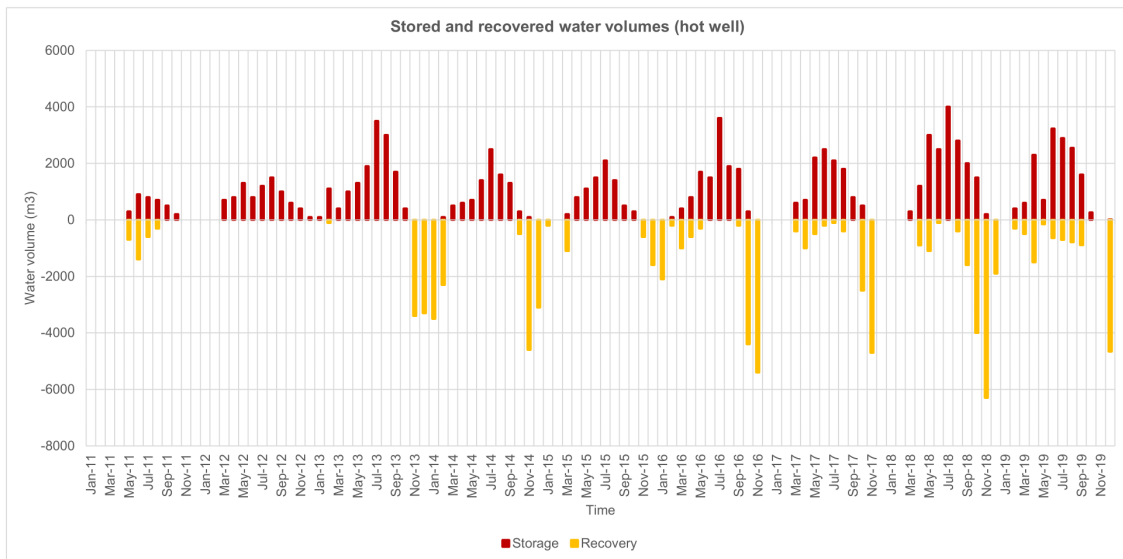


Figure 20. Monthly volumes of water pumped from the cold to the hot well ('Storage') or vice versa ('Recovery') for the HT-ATES system of NIOO.

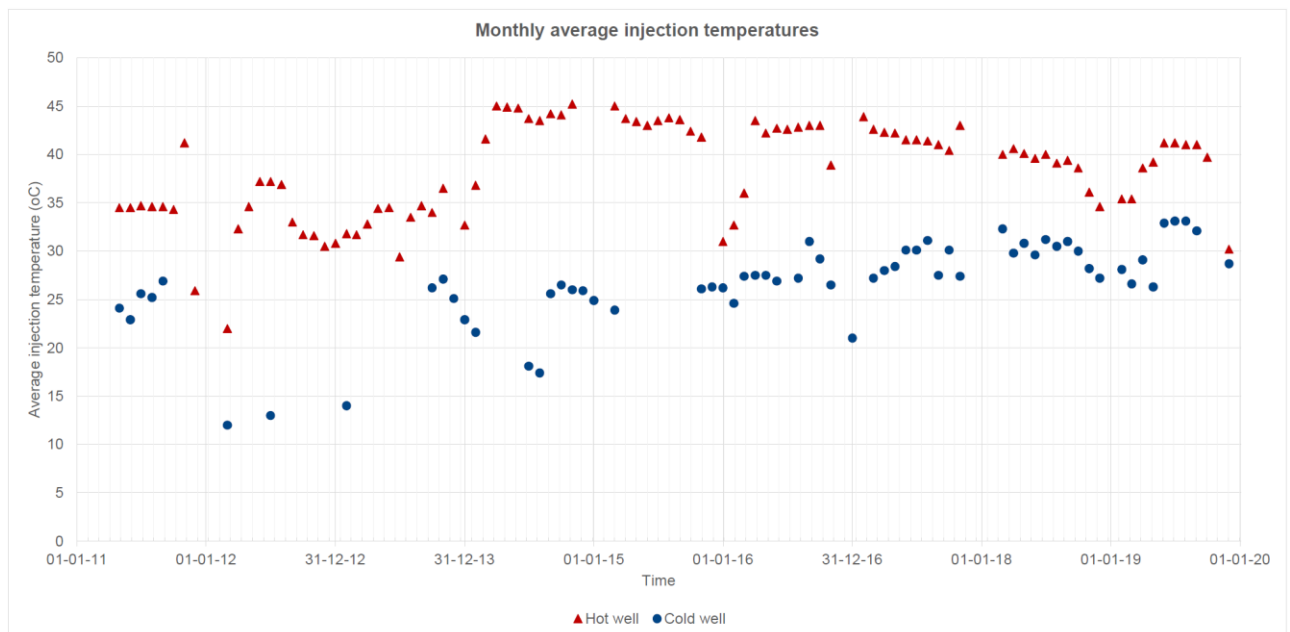


Figure 21. Monthly average injection temperatures at the hot and cold well of the HT-ATES system.

2.2.2.3. Monitoring results and discussion

Temperature

At the end of each summer and the end of each winter, a temperature log was taken at the hot, cold well and the monitoring well. A 5m-interval temperature log was obtained by descending a temperature probe into the deepest piezometers of the hot well, cold well and monitoring well. Results for these locations are shown in Figure 23 and Figure 24.

The piezometers at the hot and cold wells are located adjacent to the well casings, through which the stored/recovered water flows (distance of ~ 10 cm, see Figure 22). The

temperature in these piezometers are strongly influenced by the temperature of the water that has flowed through the well, in the period before the temperature measurement took place. This means that the results are partly determined by the timing of the measurement.



Figure 22. Top view of the well head of the hot well of the HT-ATES system. Next to the well, four piezometers pipes are present (blue), which all reach to different depths and are used for sampling of the groundwater and periodic temperature logging.

The temperature logs of the hot and cold wells show a similar thermal gradient (with depth) as the reference measurement. Temperature peaks and dips along the profile can be explained by differences in regional groundwater flow velocity at different depths. In layers with a high groundwater flow velocity, heat that is lost through the well casing is transported away from the well by the regional groundwater flow. Therefore, the temperature in these layers tends to approach the initial groundwater temperature much more rapidly than in layers with a low groundwater flow velocity (convective heat transport is minimal and because conductive heat transport is a slow process, temperatures around the well casing remain higher in these zones). Since groundwater flow velocity is closely related to hydraulic conductivity, the temperature peaks and dips are an indication for the variation of hydraulic conductivity with depth. For example, the relatively low temperatures in aquifer 2 are explained by a relatively high regional groundwater flow velocity (> 75 m/y) in this aquifer and the higher temperatures directly above aquifer 2 are the result of the low hydraulic conductivity (and thus the low groundwater flow velocity) in the 1st aquitard.

At the monitoring well, no water is produced or recovered (except for sampling). Figure 24 shows that, at this location, temperatures in the 2nd aquifer show a strong variation with time. These variations are caused by the influence of both the hot and cold wells of the ATES system (low temperature storage of heat and cold, < 25 °C, in the 2nd aquifer). Since 2010, no temperature increase at HT-ATES storage depth was observed, indicating that the heat from the HT-ATES system has not yet reached the monitoring well. This is caused by the fact that considerably less heat (and water) was stored in the HT-ATES system than was expected during the well design phase.

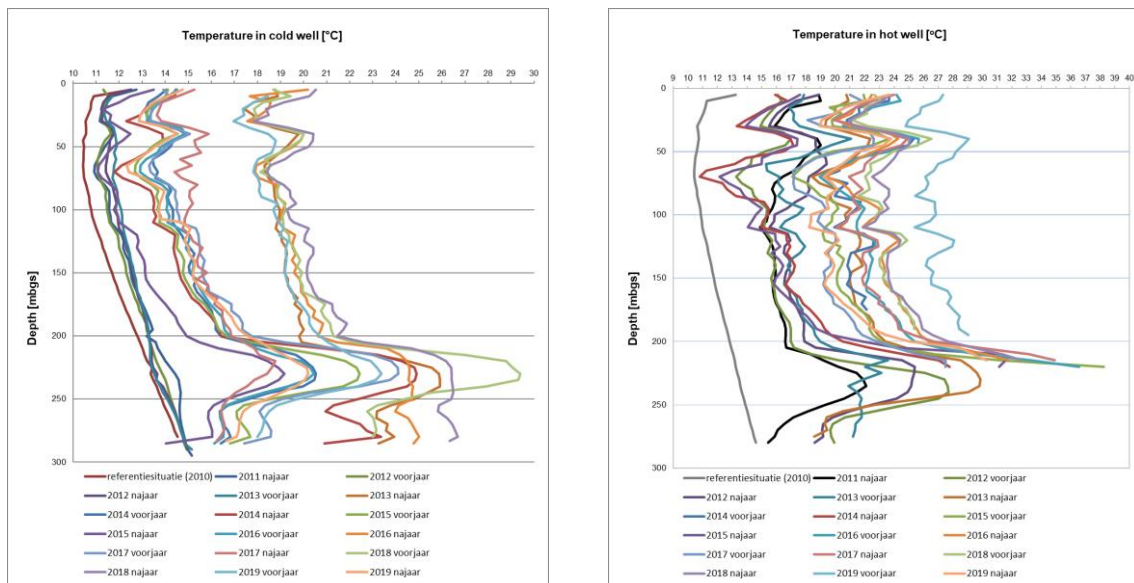


Figure 23. Temperature profiles at the cold well (left) and hot well (right), taken twice a year in spring ('voorjaar') and autumn ('najaar'). The reference measurement of 2010 ('referentiesituatie (2010)') is shown in dark red (cold well) and grey (hot well).

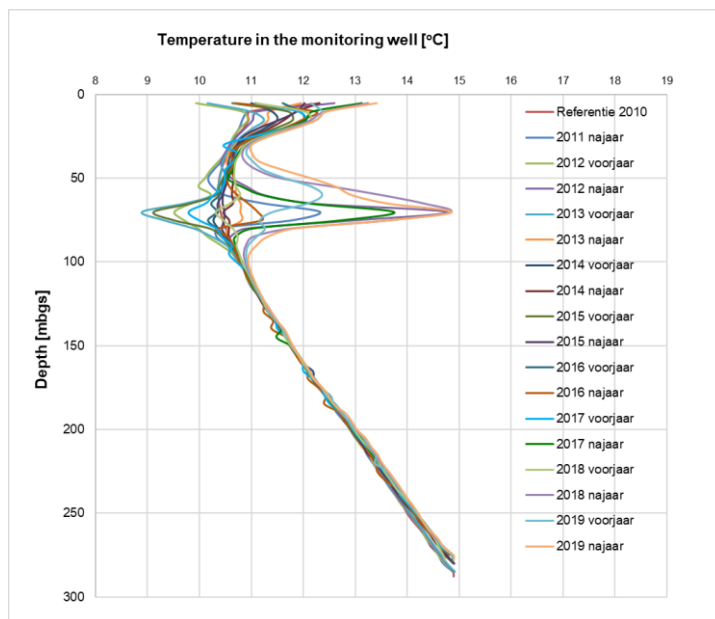


Figure 24: Temperature profiles at the monitoring well, taken twice a year in spring ('voorjaar') and autumn ('najaar'). The reference measurement of 2010 ('referentiesituatie 2010') is shown in red.

Chloride

Before the system was taken into operation, reference groundwater samples were taken from the installed piezometers and its chemical composition was analysed. During operation, at the end of each summer and at the end of each winter, chloride concentrations were measured at the hot and cold wells. This has resulted in a data series on chloride concentration development around the HT-ATES system. Figure 25 shows that the original

groundwater (indicated as dashed lines) at the top of the well screens ('Ref2-MP-F3') is fresh, whereas the groundwater at the bottom of the well screens (Ref2-MP-F4') is saline. Mixing of saline water that is extracted at the bottom of the well screen with fresher water that is extracted from the top of the well screen has resulted in an increase of chloride concentration in the upper part of the well screen (at W-F3 and K-F3) over time. Although the concentration range seems to stabilize between 700 – 900 mg/l, a slight increasing trend can still be observed, suggesting that deep saline water is attracted into the heat storage, potentially by the cold well that reaches deeper (295 mbgs) than the hot well (283 mbgs). The production of relatively saline water at the cold well is supported by the monitoring data, incidentally showing chloride concentration peaks at K-F4 (see also the HEATSTORE NIOO case study report (currently in preparation)). Temperature-related density driven flow of groundwater in upward direction may also contribute to the increasing concentration trend. The concentration range at W-F3 and K-F3 is in line with the expected chloride concentration as based on the flow distribution along the well screen, as derived from flowmeter logs, and the initial variation of chloride concentration with depth.

In the NIOO case study report, a numerical model was constructed to simulate the chloride concentration distribution over time, based on the real pumped water volumes at NIOO. The results are in line with the chloride concentrations observed in the piezometers.

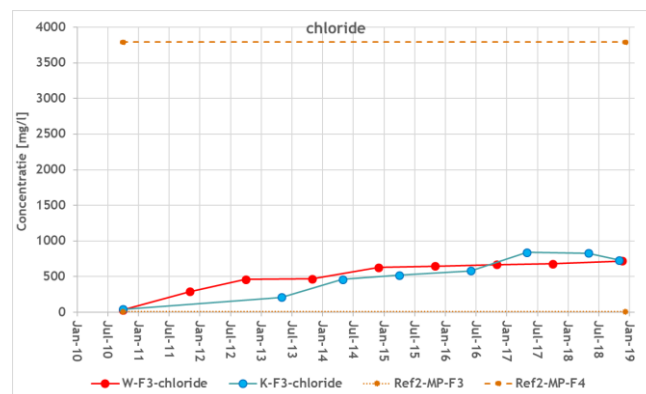


Figure 25. Reference concentrations are shown in brown, for the top of the storage depth (220 mbgs, 'Ref2-MP-F3') and the bottom of the storage depth (285 mbgs, 'Ref2-MP-F4'). The chloride concentrations at the top of the hot well ('W-F3') and at the top of the cold well ('K-F3') are shown in red and blue respectively.

Chemical parameters

At NIOO, concentrations of the following chemical species were measured twice a year: chloride, calcium, DOC, boron, bromide, iron, magnesium, manganese, methane, sodium, ortho-phosphate, silicon, sulfate, sulfide and tin.

In Figure 26, the results are shown for Electroconductivity (EC), magnesium, calcium and bromide. These trends support that mixing is the primary process determining the concentrations of several species near the well. Most of the other measured groundwater parameters show a similar trend, supporting that mixing is a primary process controlling the groundwater concentration around the HT-ATES. Below, some chemical parameters that may be influenced by temperature-related processes are discussed. In the NIOO case study report, results are explained more elaborately.

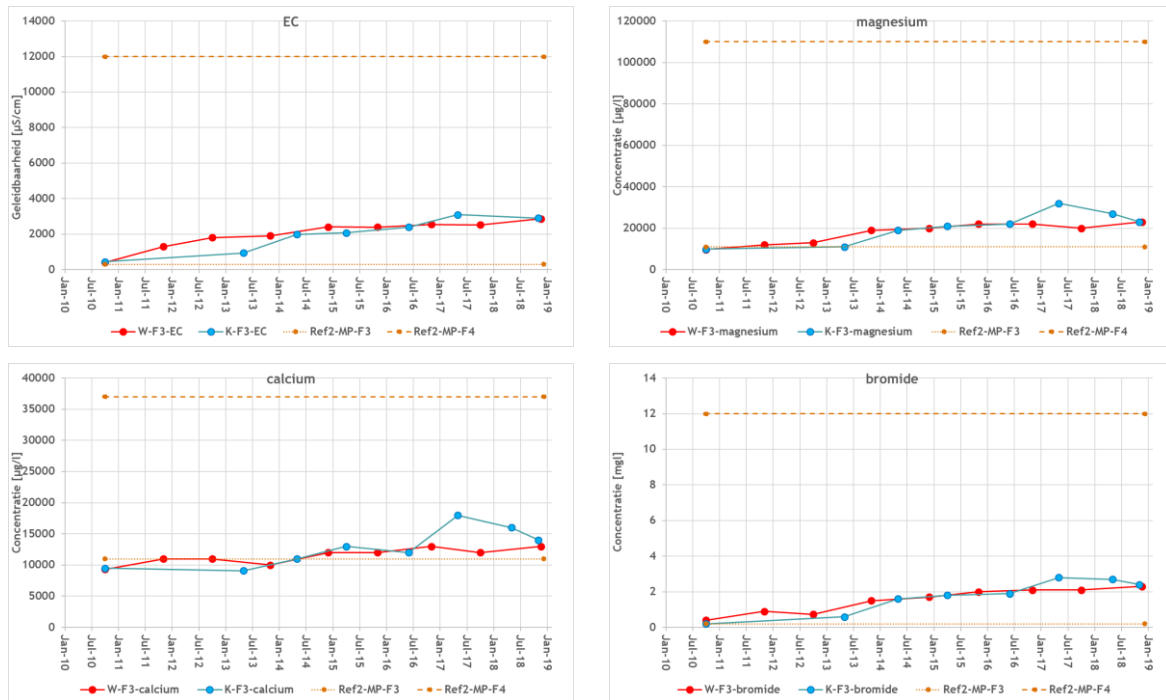


Figure 26. Trends of EC, magnesium, boron and bromide concentrations with time.

Calcite precipitation

Since storage temperatures are up to 45 °C, no significant precipitation of carbonate minerals like calcite was expected and hence no water treatment has been applied at NIOO. Figure 26 shows that calcium and magnesium, two parameters involved in carbonate precipitation, show a similar mixing-related trend as chloride, suggesting that mixing processes dominantly control its concentration, and that precipitation of calcite minerals do not have a dominant control over groundwater composition. Moreover, in January 2020, the well screens of the HT-ATES system were inspected by descending a camera into the well, but no calcite precipitation was observed on the well screens. These findings are in line with the literature and with earlier research that showed that no observable calcite precipitation occurs at these temperatures (Bakema et al., 2019 and the references therein). The presence of natural inhibitors like phosphate and Dissolved Organic Carbon (DOC) may contribute to inhibiting calcite precipitation in the wells and the aquifer.

Mobilization of organic carbon

The DOC (dissolved organic carbon) concentrations are plotted in time in Figure 27. In 2010-2013, DOC concentrations < 5 mg/l have been measured, but in the figure the concentration is plotted at 5mg/l since this was the detection limit in that period. This detection limit was lowered since 2013, providing more accurate data ever since. Literature sources state that DOC concentrations increase when temperatures rise due to mobilization of organic carbon from the solid phase (Brons, 1992; Bonte, 2013). However, no distinct increase of DOC concentrations was observed at the wells. Concentrations remain close to the concentration range that is expected from the mixing process. This suggests that mixing is a more dominant process controlling DOC concentrations than mobilization. Another theory that may explain the absence of an increase in DOC, may be that DOC could be directly consumed by microbes after it was mobilized. Such microbial respiration processes also requires an electron acceptor like sulphate. Although subtle, sulphate decrease seems larger than could

be expected from the mixing process (Figure 27). This can be explained either by the presence of microbial processes, breaking down organic matter with sulphate as electron acceptor directly, or by the additional mixing of deeper, sulphate-poor groundwater into the heat storage. Bonte (2013) referred to enhanced sulphate reduction at this temperature range. However, Brons (1992) investigated DOC mobilization and found that only a fraction of the mobilized DOC was suitable for metabolization in microbes.

The camera inspection of the wells in 2020 showed some brown-yellowish flocculent material, expectedly of organic nature. This suggests that microbes are active in and around the wells. Based on the measurements, DOC and sulphate concentrations can be explained by the mixing process. However, microbially facilitated sulphate reduction may occur to some extent, although its influence on DOC and sulphate concentrations seems subordinate to the effects of mixing. Since the concentration of microbes in deep groundwater bodies is typically very low and growth rates are also low, it may take several years before the microbial population of a certain species is large enough to have a significant impact on the groundwater composition. Therefore, future changes in the groundwater composition due to microbial processes cannot be excluded.

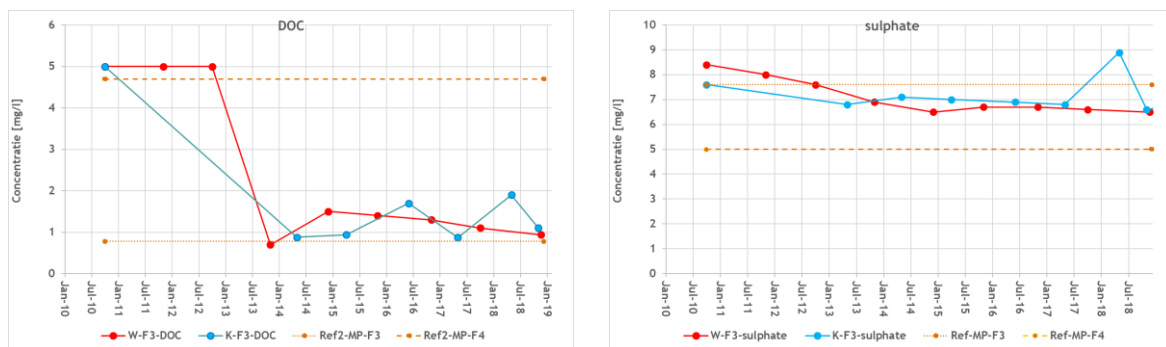


Figure 27. Concentrations of Dissolved Organic Carbon (DOC, left) and Sulphate (right) over time. For DOC, the measurements between 2010 – 2012 are set to 5 mg/l, corresponding to the detection limit applicable to these first years. Since 2013, the detection limit was improved and results were more accurate.

Arsenic mobilization

In the literature, arsenic is repeatedly reported to be mobilized when temperatures of the sediment and the groundwater rises (Bonte, 2013). In 2010, before the system was taken into operation, arsenic concentrations were measured at F2, F3 and F4 of the hot, cold and monitoring well, to obtain an idea of the natural concentrations at several depths. An additional extensive arsenic measurement was performed in November 2018. To investigate whether arsenic concentrations have increased at NIOO, arsenic was measured on a regular basis in 2018 – 2020, at F2, F3 and F4 of the hot and cold well. The results are summarized in Table 6

Table 6. Arsenic concentrations ($\mu\text{g/l}$) as measured at the HT-ATES system of NIOO between 2010 – 2020.

Sampling well	Depth (mbgs)	Concentration ($\mu\text{g/l}$)					Nov 2020
		Oct 2010 (REF)	Oct 2017	May 2018	Nov 2018	Jun 2019	
W-F1	170 - 172						20
W-F2	193 - 195	5.7			28	31	31
W-F3	220 - 222	<5	<5		<5	<5	<1
W-F4	280 - 282	0.2			<5	<5	<1
K-F1	170 - 172						14
K-F2	193 - 195	8.8			<5	<5	3.6
K-F3	220 - 222	<5		<5	<5	<5	1.1
K-F4	293 - 295	50			<5	<5	1.4
MP-F1	170 - 172	<5					
MP-F2	193 - 195	<5			6.3		
MP-F3	220 - 222	<5			<5		
MP-F4	285 - 287	<13			21		

The reference measurement of W-F2, K-F2 and MP-F2 in 2010 and the measurement at MP-F2 in 2018 suggests that the natural arsenic concentration at the F2 well filters are about 0 – 10 $\mu\text{g/l}$. The depth of the F2 piezometers are 25 m above the heat storage depth. In 2018 – 2020, increased arsenic concentrations of 28 – 31 $\mu\text{g/l}$ are found at W-F2. This observation may be explained by the mobilization of arsenic at high temperatures at the hot well of the HT-ATES system, where it is subsequently transported upwards by advective/convective transport. Bonte (2013) performed a chemical modelling study on arsenic mobilization around HT-ATES wells. He found that arsenic is mobilized near the heat storage and subsequently transported towards the outer parts of the storage, where it is cooler and the arsenic can be sorbed again. Although sorption is not investigated at NIOO, the monitoring results may support Bonte's theory. However, the arsenic concentrations measured at W-F3, at the hottest part of the heat storage, have remained low (< 5 $\mu\text{g/l}$). It is suggested to continue the monitoring of arsenic concentrations at various depths, to obtain a clearer view of the arsenic concentrations around the HT-ATES system with time.

Microbiology – standard monitoring program

Microbial groundwater composition was measured twice a year. The results of the general colony counts at 25 and 37 °C show a similar pattern (see Figure 28). An initial peak in general microbial activity can be observed due to the disturbing effect of the drilling activities, after which the concentrations of CFU sharply drop and remain low. This is in line with earlier observations reported in the literature (Meer met Bodemenergie, 2012).

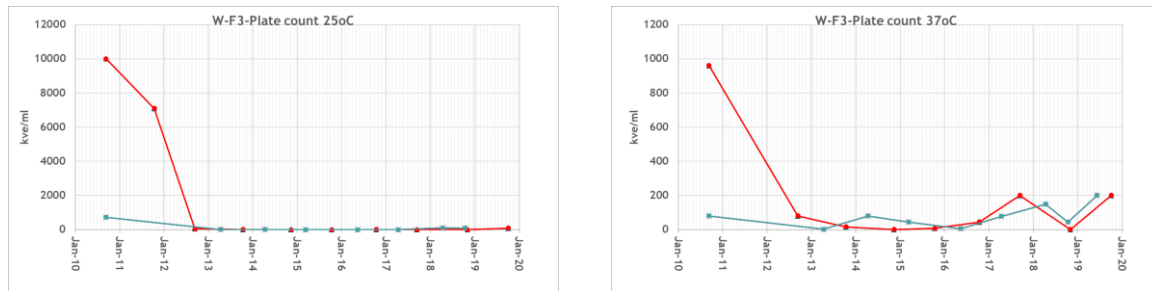


Figure 28. Results of the general colony counts performed on the groundwater samples at NIOO. Groundwater sampled from K-F3 and W-F3 were plated and subsequently contained under aerobic conditions, at a temperature of 25 °C (left) and 37 °C (right). The number of colony-forming units (CFU) per ml are indicated on the vertical axes ('kve/ml').

At NIOO, also the concentration of spores of sulfite-reducing clostridia was analysed. However, the results have shown that concentrations in the samples have not surpassed the detection limit of 10 CFU/100ml. Although sulphate reducing bacteria may survive in anoxic conditions when sulphate is present, these were not found in measurable numbers and these do not seem to assert a dominant control on the groundwater composition at NIOO.

Additionally, the groundwater was tested on four pathogenic microbial species: Aeromonas, Coliforms (37 °C), E. Coli (at 44 °C) and Enterococci. The results are consistently showing that <1 colony-forming unit was found per 100 ml sample, for all these species. Only for Aeromonas, the very first measurement (reference) shows a peak, expectedly caused by the drilling activities. The data suggest that none of the analysed pathogen microbes can survive in the HT-ATES system, in which groundwater is anaerobic, saline and nutrient-poor. This is also known from the literature. For example, drinking water companies make sure that the groundwater produced for drinking water production has a certain residence time in the subsurface before reaching the wells, because pathogens die off under subsurface conditions (Meer met Bodemenergie, 2012). The monitoring results at NIOO with respect to pathogens are in line with previous studies of Hartog et al. (2013) KWR (2013) which suggested that most pathogens cannot develop to measurable population sizes when oxygen is (near) absent. Relevant exceptions to this are pathogens like Acanthamoeba and Vibrio spp., which were researched at NIOO using DNA-based methods, as described in the next section.

Microbiology – additional measurements in 2019

The standard technique used at NIOO for the microbiological measurements involved plating techniques. Replica plating (or: plate counting) is a way to quantify the relative abundance of a microbial species in a sample. Part of the sample is mixed with a nutrient-rich medium, and poured on a Petri plate so that it can grow. The number of colonies formed are representative for the original number of cells that were present in the sample. However, this standard technique comes with a low sensitivity, as typically <10% of the microbes present are detected and the variability is relatively high (Deltares, 2010; OnCyt, 2020). Therefore, alternative microbial analysis methods were used at NIOO, additional to the regular microbial monitoring: NGS, qPCR and ATP analysis.

Two DNA-based microbiological analysis techniques have been developed over the past decade:

- Next Generation Sequencing (NGS) can be used to identify (nearly) all organisms present in a water sample, by looking for their characteristic DNA-sequence. Using existing genomic libraries on numerous (microbiological) species, the microbiological

population of the sample can be characterized on a Genus level with this powerful analysis tool. The result of such an analysis offers a 'fingerprint' of the microbiological population in the sample.

- Quantitative Polymerase Chain Reaction (qPCR) is another DNA-based analysis method which is used to identify a specific microbial species, by checking whether its characteristic DNA-sequence is found in a sample. This analysis is suitable when looking for a specific species of which the unique genomic sequence is known.

These DNA-analysis methods cannot distinguish between DNA from dead and living organisms, meaning that intact DNA-strings from dead microbes will also influence the results.

Another general way of researching the activity of microbes present in a sample, is by measuring the concentration of AdenosineTriPhosphate (ATP). ATP is an energy-rich chemical substance that plays an important role in the metabolism of each living organism. The concentration of ATP in a sample is hence representative for the (relative) activity of the biomass present.

The possible inaccuracy of the standard plating technique used at NIOO since 2010, as well as the potential discovery power of the more recently developed (DNA-based) microbial analysis techniques, brought NIOO to perform additional measurements on microbiology using these newer methods. The objectives of the extra measurements were...

- to compare the results of new DNA-based analysis techniques (NGS, qPCR) with the results of standard plating techniques;
- to investigate whether specific pathogenic microbes (like Acanthamoeba and Vibrio), which may survive the subsurface conditions, are actually found in the subsurface;
- to measure the general microbial activity of the groundwater by measuring the ATP concentration.

In September 2019, groundwater was sampled from the heat storage depth, at the hot well (W-F3) and the monitoring well (MP-F3). NGS was applied to both samples to obtain a general picture of the microbial population at these two locations. Additionally, several analyses were performed on the W-F3 sample:

A number of species were looked for in the W-F3 sample, using qPCR:

- Aeromonas spp., Enterococcus EPA, E.coli HSP: three species that have been measured since 2010, following the permit instructions and using plating techniques. In this way, the results of the qPCR method could be compared with the long-term trend from the "regular monitoring data".
- Acanthamoeba: this is a pathogen that is potentially capable of surviving in deep, anoxic, saline groundwater, as identified in a report on microbiological risks at a HT-ATES in Brielle (KWR, 2011).

Another pathogen that may survive in the harsh environment around a HT-ATES was the Vibrio spp.. Since no qPCR analysis was available for this species, its presence in the W-F3 sample was analyzed using a plate count technique, performed by the RIVM institute (National Institute for Public Health and Environment) in the Netherlands. Also, the ATP concentration at W-F3 was measured to obtain a general insight in the activity of the biomass near the hot well. The results of the measurements are shown in Measurement results for pathogenic microbes, as identified by the NGS, qPCR, plating and other microbiological analysis techniques. Sampling was performed in September-October 2019 at sampling wells W-F3 and MP-F3.

NGS-analysis				qPCR-analysis				Plating (oct 2019)			
Samples taken 24-9-2019				Samples taken 24-9-2019				Samples taken 23-10-2019			
Pathogen name	Method	MP-F3	W-F3	Pathogen name	Method	W-F3	unit	Parameter name	Method	W-F3	unit
total Krona reads	NGS	59662	10154								
% of total DNA counts											
Burkholderia (Genus)	NGS	0.70%	2.00%								
Campylobacter (Genus)	NGS	0.10%	0.10%								
Pseudomonas (Genus)	NGS	1.00%	2.00%								
Enterobacterales (Order-level)	NGS	0.80%	0.20%								
Enterococcus (Genus)	NGS	0.06%	not found	Enterococcus (EPA)	qPCR	<240	gene copies/l	Coliformen	filtration + plating	<1	cfu/100ml
Legionella (Genus)	NGS	0.20%	not found					Enterococcen	filtration + plating	<1	cfu/100ml
Aeromonas (Genus)	NGS	0.10%	0.10%	Aeromonas spp.	qPCR	<1200	gene copies/l				
Vibrio (Genus)	NGS	0.08%	not found					Aeromonas spp.		<1	cfu/100ml
Salmonella (Genus)	NGS	0.04%	not found								
Escherichia (Genus)	NGS	0.02%	not found	E. Coli (HSP)	qPCR	<240	gene copies/l	Escherichia coli (44C)	filtration + plating	<1	cfu/100ml
Stenotrophomonas (Genus)	NGS	0.10%	0.10%								
Total concentration of DNA found	µg/ml	0.252	0.281	Acanthamoeba	qPCR	3580	gene copies/l	sulfite-reducing clostridia traces	filtration + plating	<1	cfu/100ml
								Colony count (22C)	plating	88	cfu/ml
								Colony count (25C)	plating	92	cfu/ml
								Colony count (37C)	filtration + plating	>200	cfu/100ml

Other measurements			
taken from sampling well W-F3, at 24-9-2019)			
Parameter name	Method	result	unit
Vibrio species (37C)	Plating	<1	MPN/l
ATP	n.a.	<1	pg/ml

Figure 29. Measurement results for pathogenic microbes, as identified by the NGS, qPCR, plating and other microbiological analysis techniques. Sampling was performed in September-October 2019 at sampling wells W-F3 and MP-F3.

Looking at the results of the additional measurements, the fact that both aerobic and (semi)anaerobic genera are found in the NGS-analyses suggests that both microbes from the subsurface and microbes living in the sampling well (under semi-aerobic conditions) are sampled. Still, when looking at the low representation of pathogenic microbes in all of the NGS, qPCR and plating analyses, it seems that the conditions in and around HT-ATES are not favorable for growth of pathogens. Acanthamoeba was detected at W-F3, but since no reference measurement was performed at MP-F3, it is unknown whether this represents an increase or decrease with respect to more natural groundwater at that depth. Additional measurements on Acanthamoeba at both MP-F3 and W-F3 is recommended. To the best of the author's knowledge, no Dutch target values are present for Acanthamoeba concentrations in groundwater or drinking water. Moreover, the ATP-analyses show that the activity of the biomass present is very low, indicating that microbes will not grow easily, let alone flourish, in the harsh subsurface environment around the HT-ATES system. Since this additional measurement represents only one specific moment in time, the base for these interpretations is relatively small, hence more measurements, as well as more research on this topic in general, is recommended. Additional measurements using DNA and non-DNA techniques were performed at NIOO in Q3 2021 to further research the composition of the microbial community, as described below.

Microbiology – additional measurements in 2021

In 2021, a more extensive microbiological measurement was performed with the aim (1) to find how the analyses results are influenced by the sampling methodology, (2) to see how the microbial conditions differed between the hot and monitoring well and (3) to investigate the changes compared to 2019:

(1) Groundwater samples were gathered from the piezometers at storage depth at the hot and monitoring well, using two different methods. Applying the regular method, at least 3 piezometer volumes are discharged before sampling and the sample is gathered from the top 5 m of the groundwater in the piezometer. The new method was similar, but samples were gathered at greater depths in the piezometer (~20 m below the water level). Hypothetically, the water collected using the new, deep sampling method would provide a sample which is more representative for the groundwater in the aquifer, compared to the sample gathered using the regular method. The hypothesis was confirmed by the analyses

results, as the concentrations of DNA, ATP and genes (as identified by qPCR) were consistently considerably lower with the new method (with one exception for *Aeromonas*). In addition, applying the new method, the variation between measurements in duplo was smaller. Assuming anoxic conditions and considering the chemical groundwater composition at NIOO, a low biomass and activity of microbes was expected. This means that groundwater originating from a more oxic location (like the top of the piezometer) may have a large influence on the total microbial composition of water samples. Because the groundwater in the piezometer originates from an anoxic aquifer, the introduction of oxygen at the depth of the water level in the piezometer creates relatively favorable conditions for microbes. Oxidizing components (oxygen) and reduced species (dissolved iron, ammonium, etc.) come together and result in (bio)chemical processes and associated microbial activity. Only a small percentage of water from the top of the piezometer may have a large impact on the microbial composition and concentration in the samples. Thus, in researching the microbial effects of HT-ATES using sensitive microbial analyses methods with a large discovery potential like NGS and qPCR, one must assess whether the sampling methodology will deliver a groundwater sample that is representative for the storage aquifer. This aspect was also found to be important at the other HEATSTORE Case Study of Koppert-Cress in Monster, the Netherlands. There, KWR used an adapted procedure for groundwater sampling in order to minimize these disturbing effects.

(2) The microbial compositions of water samples taken from the piezometers at the hot well (i.e. within the HT-ATES zone of influence) were compared to samples from the monitoring well (i.e. outside of this zone). The results consistently showed higher DNA-concentrations (NGS, qPCR) and activity (ATP) at the hot well. This suggests that more microbes can survive and live around the HT-ATES system. However, based on the data, it cannot be stated with certainty that the main cause for this difference with the monitoring well is the elevated temperature at the hot well: as described earlier, the water samples are probably influenced by groundwater originating from the top of the piezometers. At the hot well, the water level in the piezometer fluctuates frequently because of the variations in the pumping activities, so that the top of the piezometer is more intensively exposed to air, which may facilitate the growth of microbes. At the piezometer in the monitoring well, the fluctuations are considerably smaller (or may be absent), constraining microbial growth at the top of the piezometer. This explanation is supported by the NGS data, which showed that the majority of the identified microbes from the monitoring well were strictly anaerobic, while those at the hot well were mainly aerobic or nitrate-reducing. This may explain the difference in microbial results between the hot and monitoring well. Still, the piezometer at the hot well will be heated by the hot well casing, as the temperature data showed, and this may have stimulated microbial growth in the piezometer of the hot well. So, the data merely shows the differences in microbiological composition and activity in the piezometers, but the question remains to what extent this is representative for the situation in the storage aquifer.

(3) Comparing the results from 2021 with 2019, it becomes clear that the DNA-concentrations and the activity have increased significantly both at the monitoring well and the hot well piezometers with screens at storage depth. The NGS-analyses of the samples taken with the new method showed a relatively larger portion of aerobic species in 2021 compared to 2019. Using the old sampling method, this relative portion was still larger. This suggests that the increase of the DNA in 2021 compared to 2019 for both the piezometers at the monitoring and hot well may be explained by an increased size and activity at the top of the piezometer, rather than at storage depth. Moreover, at the piezometer with screens at storage depth in the monitoring well, no thermal and chemical changes have been observed yet, so the increase in microbial activity at this location is probably not caused by the HT-ATES effects but rather by improved conditions in the piezometer. At the hot well, the increased temperatures in the piezometer (due to heat losses) may have contributed to the

increase, while the role of the heat storage itself on this finding remains subject to debate. Regarding pathogenicity, the qPCR analyses on samples taken with the new sampling methods (that are expected to be more reliable) showed that gene concentrations of *E. Coli* and *Enterococcus* were still close to the detection limit (similar to 2019), while the concentrations of *Aeromonas* and *Acanthamoeba* were both considerably higher. Still, the NGS results showed a limited relative presence of *Aeromonas*, as the relative number of counts are < 0.06% of the total. This suggests that, although the absolute number of *Aeromonas* gene found in the qPCR analysis of 2021 was higher compared to 2019, the relative presence of this species remains low. Also, in DNA-based analysis methods, there is no distinction between DNA of living and dead organisms. This may explain why these pathogens were not found with the plating techniques, from which only living species are derived that are able to grow under the plating conditions.

2.2.2.4. Conclusions and recommendations

Based on the monitoring results and research activities performed at the NIOO HT-ATES case study, the following conclusions and recommendations arise for other HT-ATES systems in a similar temperature range:

- At NIOO, the subsurface temperatures were measured by descending a temperature probe in a piezometer. At the hot and cold wells, these piezometers are located directly next to the well casings through which the groundwater is pumped, so that the temperature results are influenced by the temperature of the water flowing through the well casing. Therefore, for future HT-ATES systems, it is recommended to measure temperatures at some distance from the well casing. Fibre optic Distributed Temperature Sensing (fibre optic DTS) is a relatively new application by which temperatures can be continuously monitored along the fibre optic string.
- At the HT-ATES system of NIOO, mixing of groundwater of different compositions by the HT-ATES system has been the dominant process controlling the chemical groundwater composition around the well.
- Having a maximum infiltration temperature of 45°C, no clear temperature-related effects on the chemical groundwater composition were observed. However, as also reported in the literature (Bonte, 2013), arsenic may be mobilized in this temperature range. At NIOO, irregular arsenic measurements showed that arsenic concentrations have increased at W-F2, 25 m above the heat storage. This may be caused by mobilization of arsenic near the heat storage and subsequent upward advective transport towards the shallower W-F2 piezometer. This finding at NIOO is in line with an earlier chemical study by Bonte (2013), which showed that arsenic is mobilized from the hot zones and subsequently concentrated towards the boundaries of the heat storage. At NIOO, arsenic will be measured on a regular basis during the coming years to provide more insights.
- No indications for calcite precipitation were found at NIOO, supporting earlier research that this process will be naturally inhibited when temperatures remain moderate (<45 °C).
- Based on the literature, no pathogenic microbes were expected to flourish at the NIOO HT-ATES system, assuming that groundwater remains anoxic. The dataset of 2010-2019 consistently shows pathogen concentrations below the detection limit using plating techniques.
- Additional DNA-based microbiological analyses at NIOO in 2019 supported that pathogenic microbes were either absent, or present in very low concentrations with very low activity. qPCR analysis showed the presence of *Acanthamoeba*.
- Still more extensive DNA-based microbiological analyses were performed in 2021, which showed that microbial analysis results are highly sensitive to the method of sampling and

that water from the top of piezometers may contaminate the sample. Hence, it is recommended to develop reliable and practical sampling protocols, and to be aware of possible contamination processes during the assessment of microbial analysis results.

- DNA-concentrations were higher in 2021 compared to 2019 but the increase in relative abundance of aerobic species indicated sample contamination from the top of the piezometer. Although gene-concentrations of the pathogenic species (*Acanthamoeba* and *Aeromonas*) increased significantly from 2019 to 2021, their relative abundance has remained limited. More research to these parameters in HT-ATES context is recommended.
- It was concluded from the NIOO case study measurements that increased temperatures do not lead to significant growth of pathogenic microbes in the heat storage aquifer. However, microbes, including pathogens, may grow at the top of the piezometer where conditions are (semi-)oxic due to atmospheric influences and this may influence analyses results.
- It is recommended to perform a test drilling before designing the HT-ATES system, and to place well screens below a confining layer as to limit environmental effects to shallower layers and to limit heat losses.
- It is recommended to perform extensive reference measurements at newly planned HT-ATES systems before operation starts, to obtain a reliable image of the natural chemical and microbiological groundwater composition around HT-ATES wells. In any case, the influence of the drilling of the wells on the reference measurements should be kept in mind when interpreting the data. To get an image on the natural microbial population in the groundwater, the DNA-based method of Next Generation Sequencing (NGS) is advised because of its large discovery power.

2.2.2.5. Fast-track Risk assessment

A Fast-track risk assessment was applied with regard to the operational phase of NIOO, based on the calculations performed during the permitting procedure, and the measurements during operation of the system (Table 7).

Table 7. Fast-track risk assessment for the NIOO site.

NIOO						
Effect \ Phase	Operations (calculated or measured)					
	P	A	M	Probability	Consequences	Risk
Air quality				L	L	L
Noise and vibration				L	L	L
Formation water quality				H	L	M
Formation water temperature				H	L	M
Surface clear water				L	L	L
Soil occupation				M	L	M
Wastes and dangerous substances				L	L	L
Environment				L	L	L
Nature				L	L	L
Soil mechanics				L	L	L
Seismicity				L	L	L
CO2 intensity reduction						

2.3. Case study in Switzerland

The case study in Switzerland for ATES systems focuses on the identification of the environmental effects at the surface and in the subsurface on two main stages of the projects: drilling (and associated logging and reservoir testing) and operations.

For the Geneva areas the focus is directed to the environmental effects identified by SIG as associated with the drilling operations, on the prediction of the water-rock interactions, hence on the effects on the reservoir water chemistry based on Thermo-Hydraulic-Chemical modelling and laboratory experiments performed by UniBe in WP2 and of the ground deformation effects associated with production/injection cycles predicted via Thermo-Hydraulic-Mechanic modelling performed by ETHZ in WP2. Additionally, ground deformations and micro-seismicity have been monitored by SIG in the framework of WP5 and the results have been summarized in this report.

For the Bern site, information available provided by EWB include the prediction of the water-rock interaction at the Forsthaus site performed by UniBe in WP2, therefore the focus will be limited on the potential effects on the reservoir water chemistry.

2.3.1. Geneva case study

The identification of the environmental effects associated with the drilling operations at the G_{EO}-01 and G_{EO}-02 well sites result from the environmental impact assessment performed by SIG prior drilling. These two wells drilled into the fractured Mesozoic Carbonate units also represent the study cases for the HEATSTORE project. The main geologic sub-units representing the potential targets are the so-called “Siderolithic” which represents the weathered and karstified erosional surface at the top of the Lower Cretaceous and the fractured Lower Cretaceous and Upper Jurassic carbonates. These units have shown different performances in terms of fluid circulation and geometry; therefore, they have been considered to define the potential operational scenarios for TH, HM and THC models to assess the effects on subsurface thermal perturbation, ground deformation and reservoir water chemical variations. The main data used for the different simulations are listed in Table 8.

Table 8. Exploration well data for the Geneva case study

Geologic Unit	G _{EO} -01	G _{EO} -02
Top Siderolithic (m bg.l.l)*	404 (Uncertain)	630
Top Lower Cretaceous (m bg.l.l)*	407	770
Top Upper Jurassic (m bg.l.l)*	648	996
Bottom hole (m bg.l.l)*	744	1456
Flow Rate (l/s)	55	0.6
Wellhead pressure (bars)	8	12
Wellhead temperature (°C)	34	18
Reservoir temperature (°C)	34	55

*Depth below ground level (b.g.l.) are reported as Measured Depth (MD)

To get the drilling authorizations from the local authorities, Services Industriels de Geneve (SIG) carried out environmental impact assessments for the two wells (SIG, 2017, 2018) which are summarized in the present report. The approach adopted is based on a classification of the site-specific environmental constraints. Four levels of constraints are defined and are described below:

- **Major environmental constrains** regions whose environmental constraints do not legally allow the development of any geothermal project.
- **Significant environmental constraints:** sector characterized by the presence of environmental constraints requiring the implementation of significant technical and/or administrative measures. GEO-02 well falls into such category.
- **Moderate environmental constraints:** the environmental components identified in the area impacted by the drilling operations do not a priori imply redhibitory constraints to obtaining a drilling permit from an environmental point of view. GEO-01 well falls into such category.
- **No particular environmental constraints identified:** sector without identification of any particular environmental issue. However, the implementation of a geothermal project in this sector will include all the usual legal requirements in terms of the environment at the time of execution. A priori, no additional technical or administrative measures should accompany the construction project developing under the law of this area.

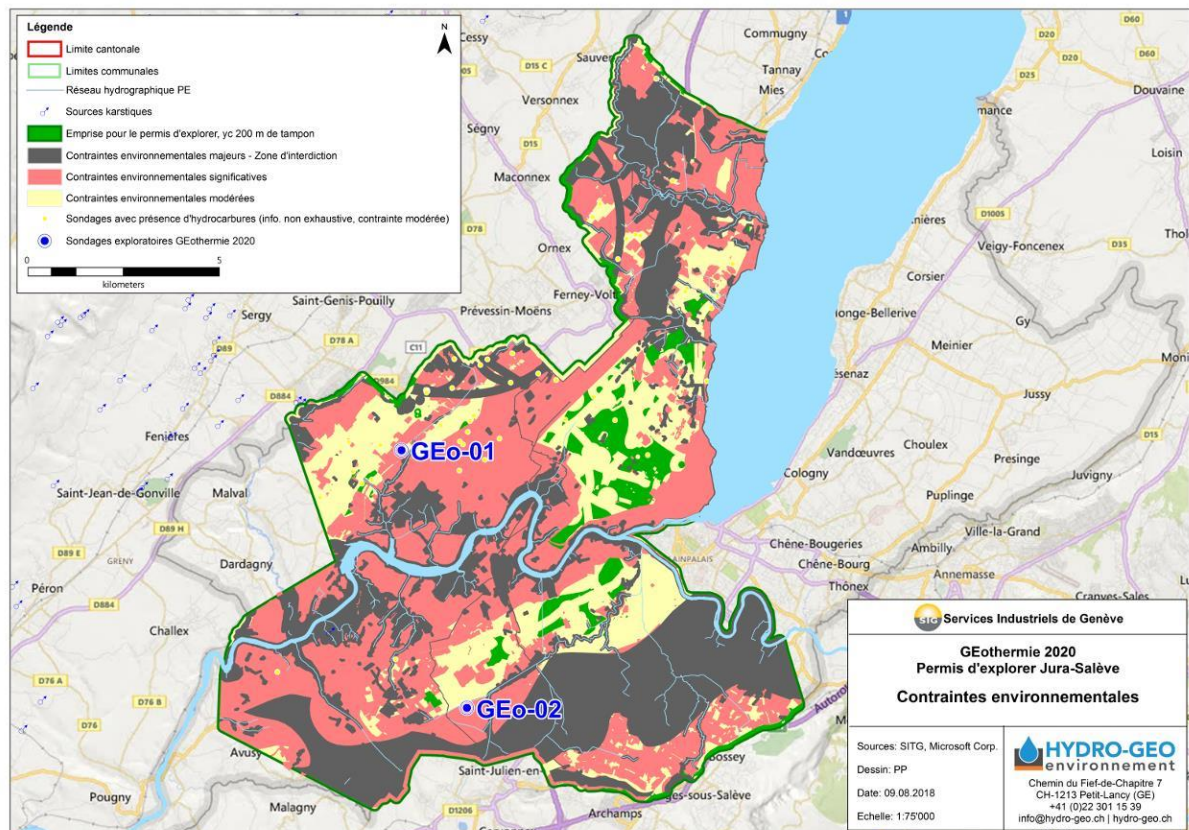


Figure 30. Environmental constraints within the exploration perimeter authorised in 2017 and implementation of drill holes GEO-01 and GEO-02.

The selection of the drilling techniques employed for both wells was also driven to ensure the mitigation and management the environmental effects and the main elements are:

- **Mud drilling:** The choice of mud drilling was driven by the desire to reduce as far as possible the geological and technical risks incurred during such medium-depth drilling. Compared to conventional drilling with clear water and/or air, drilling with mud ensured higher borehole stability in the upper section (Molasse) and prevention of

potential undesired flow of fluids such as hydrocarbons known to be often present in the Molasse sediments.

- **Installation of a Blow-Out Preventer (BOP):** The two wells are located in sectors of the Geneva Basin where the risk of liquid and gaseous hydrocarbon occurrences within the fractured units and Molasse reservoirs is highly probable. In order to technically control these potential hydrocarbon occurrences without creating safety and environmental problems on the surface (uncontrolled eruptions), a BOP system was installed.
- **Borehole casing:** A drilling protocol with continuous casing and cementing was implemented to ensure the safety of the hole and the surrounding environment including protection against the connection of deep aquifers. The installation of a casing is a response to the need to securely form the drilled hole in order to 1) isolate the borehole from the natural environment; 2) withstand the pressures likely to be encountered during the drilling of the next phase; 3) provide mechanical support for the wellhead components. Cementing allows to 1) anchor the column to the ground; 2) channel the fluids towards the surface; 3) avoid pollution of the shallow groundwater; 4) separate the different producing layers that may contain different fluids at different pressures.

2.3.1.1. Identified impacts during drilling operations

Air Quality		
Air quality conditions before drilling focused on the assessment on nitrogen oxides and fine dust, in order to provide a baseline for monitoring the emissions induced by the drilling pas construction and drilling operations phases.		
	GEo-01	GEo-02
Pre-Drilling	<ul style="list-style-type: none"> • Normal traffic load in the vicinities of the drilling site: 6300 vehicles/day • Annual average NO₂ concentration: <26 µg/m³ (below the 30 µg/m³ defined by the OPair) • Annual average PM₁₀ concentration: 15 µg/m³, (below the 20 µg/m³ defined by the OPair) • Annual NO_x emissions: 3100 kg/km² (source: SABRA-DETA-State of Geneva). 	<ul style="list-style-type: none"> • Normal traffic load in the vicinities of the drilling site: 9'000 vehicles/day • Annual average NO₂ concentration: 18 µg/m³ (below the 30 µg/m³ defined by the OPair) • Annual average PM₁₀ concentration: 14 µg/m³, (below the 20 µg/m³ defined by the OPair) • Annual NO_x emissions: 4030 kg/km² (source: SABRA-DETA-State of Geneva).
Potential Impacts	<p>The main sources of emissions identified for the drilling operations are:</p> <ul style="list-style-type: none"> • Induced traffic • On-site machinery • Presence of natural gas pockets (methane) as observed in various geothermal wells drilled in the past in the Quaternary/Molasse 	<p>The sources of emissions linked to the project are :</p> <ul style="list-style-type: none"> • Induced traffic: 10 movements per day; • The site machinery • The presence of pockets of natural gas having pressures of between 1 and 5 bars at the surface, as observed on various shallow boreholes in the sector.

	sequence with pressures of around 5 bars.	<ul style="list-style-type: none"> • The occurrence of hydrogen sulphide (H₂S) degassing as demonstrated at G_{Eo}-01 associated to the gas dissolved in the geothermal water. • Fine PM₁₀ dust as well as other fine dusts particles was predicted be produced due to the circulation of vehicles
Mitigation Measures	<p>For the G_{Eo}-01 drilling site, level A of the <i>Directive Air Chantiers</i> issued by the Federal Office for the Environment (FOEN, 2016) was complied with given the size of the site area (approx. 2,000 m²) and a duration of less than 1 year.</p> <ul style="list-style-type: none"> • Dust production and propagation was limited by carefully sprinkling/misting of the soil as well as on the wheels of the vehicles which maximal speed on site was limited to 10km/h. • Gas emissions The drilling methodology used in addition of the installation of the BOP allowed to manage gas occurrences that were encountered during drilling. The gas that was encountered during drilling was evacuated to the deaerator and flare. 	<p>For the G_{Eo}-01 drilling site, level A of the <i>Directive Air Chantiers</i> issued by the Federal Office for the Environment (FOEN, 2016) was complied with given the size of the site area (approx. 2500 m²) and a duration of less than 1.5 years.</p> <ul style="list-style-type: none"> • Dust production and propagation was limited by carefully sprinkling/misting of the soil as well as on the wheels of the vehicles which maximal speed on site was limited to 10km/h. • Gas emissions: The drilling methodology using mud in addition of the installation of the BOP able to withstand pressure up to 3000 PSI allowed to manage gas occurrences that were encountered during drilling. The production wellhead assembly (x-mas tree) capable of withstanding surface pressures of 100 bar was installed at the end and was dimensioned on the basis of the known pressure-depth subsurface conditions.
Observed Impacts	<p>The impact of the project on air quality in general and on nitrogen oxides in particular was very low, especially considering the limited duration of the project. PM₁₀ and other dusts emission resulted to be relatively limited due to the low-level circulation on site. Degassing of hydrogen sulphide H₂S was observed but the recorded values were below the admissible legal limits. After drilling no impacts affecting air quality was observed.</p>	<p>Most of the machinery used was not equipped with particle filters, therefore it was not possible to precisely quantify the emissions related to the drilling operations. However, the impact of the construction site was estimated to be relatively limited due to the limited number of machineries involved and vehicles circulating. At the end of drilling operations, the conditions were established to prior-drilling state.</p>

		The gas that was encountered during drilling was evacuated to the deaerator and flare. After drilling no impacts affecting air quality was observed
--	--	--

Noise and Vibrations		
The cantonal authority has drawn up a plan for allocating noise sensitivity levels in accordance with Art. 37 of the Federal Noise Protection Ordinance.		
	GEO-01	GEO-02
Pre-Drilling	The project is located in sensitivity level III* zones (zones where moderately disturbing businesses are permitted). The neighbouring area to the north-east is in an industrial zone where the OPB daytime emission limit value (VLI) for sensitivity levels III* and IV are 65 dB and 70 dB respectively.	The project is located in sensitivity level III* zones (zones where moderately disturbing businesses are permitted). The neighbouring areas 125 meters to the north-west and 225 meters to the east are home with a degree II sensitivity level assigned, not allowing any disturbing activity. The neighbouring zone located 245 meters to the north-east is classified as sensitivity level III (zones accepting moderately disturbing activities). The daytime emission limit value for sensitivity levels II and III are 60 dB(A) and 65 dB(A) respectively. The expected value for the drilling operations in these zones was set to 55 dB(A) and 60 dB(A) respectively.
Potential Impacts	The main sources of emissions identified for the drilling operations are: <ul style="list-style-type: none"> • Induced traffic • On-site machinery • Drilling, logging and production tests 	The impacts attributable to the project are : <ul style="list-style-type: none"> • Daily vehicle movements • Construction equipment activity • Drilling/logging and production tests During the drilling operations at GEO-01 measurements were carried out at the center of all sources of noise on site, revealing the following maximal noise level values at source: <ul style="list-style-type: none"> • Background noise (water pump, mud tank propellers, vibrating sieve, generators): 69.5 dB(A) • Drilling rig: 73.8 dB(A)

		<ul style="list-style-type: none"> • Mud pump (measurement carried out with all the installations in operation): 82.7 dB(A) • Recirculation pump: 80 dB(A) • Sand traps: 72.4 dB(A) <p>The closer receivers are located at 125m from the drilling site where a road with intense daily traffic already generated 60 dB(A) and the drilling operation were not supposed to generate vibrations</p>
Mitigation Measures	<p>In terms of organisation, the construction site will have to comply with the 7:00-12:00 and 13:00-17:00 working hours. The drilling phase was accompanied by vibration monitoring by means of two mobile stations located in the immediate vicinity of the site to document wave propagation in the subsoil, in terms of intensity and frequency. These measurements were also coordinated with CERN, which is carrying out sensitive underground work at a distance of almost 2 km from borehole GGeo-01</p>	<p>Based on the characteristics of the project the construction site operated at a rate of 11 hours per day and complied with the 7:00-12:00 and 13:00-19:00 schedules. Noise barriers were installed to reduce the noise propagation towards the closest receivers. Regarding vibrations, a natural seismicity monitoring network is operating in the Geneva area since 2016 and data were used to monitor the seismicity related to the drilling operations.</p>
Observed Impacts	<p>These impacts were considered as moderate during drilling, in particular due to the drilling method employed. Taking into account the various elements, the project's contribution in terms of emissions is considered negligible. After drilling no impact related to noise and vibrations was observed</p>	<p>No impacts different that forecast was observed during drilling and any impact was recorded after the end drilling operation</p>

Groundwater Quality		
	GGeo-01	GGeo-02
Pre-Drilling	<p>The drilling site is located outside any water protection sector. On the basis of geological knowledge and the drilling results, shallow subsurface is composed by a low-permeable quaternary silt-clay cover. It develops over a</p>	<p>The cantonal hydrogeological data report the presence of the main Aire freshwater aquifer which is currently used for agricultural needs in the proximities of the GGeo-02 well. To verify the hydrogeological setting in the</p>

	<p>thickness of 27 m and overlaps the Molassic sequence which has revealed to be an impermeable sequence at the GGeo-01 location. The cantonal hydrogeological map does not mention the presence of any groundwater body in the Quaternary sediments at GGeo-01.</p> <p>The GGeo-01 exploration borehole drilled into the main geothermal target being the Mesozoic carbonates between 450 and 744 meters, where productive fractures associated to both karstified levels and fractures have been encountered along the entire section. The general hydrogeological setting of deep groundwater flows can be described as a general infiltration of meteoric water in the Jura mountains, about 7-8km North from the drilling site. Such waters percolate through the Mesozoic carbonates and are partially discharged by karstic springs at the Jura foothills (e.g. Allondon, Allemogne, Mathieu, Doua, Annaz, Bouna, Divonne). The remaining part of the infiltrated water circulates at depth in the Upper Mesozoic carbonates and was intersected by the GGeo-01 well (Guglielmetti et al., 2020).</p>	<p>study, a reconnaissance borehole was drilled 80 m from the GGeo-02 borehole revealing a thickness of Quaternary cover of about 46 metres, confirmed by the flowing drilling operation of GGeo-02. The water table was encountered approximately 2.2 m b.g.l.</p> <p>The GGeo-02 exploration borehole targets Lower Cretaceous and Upper Jurassic aquifer formations. Above these units, located between 770m and 1456m metres in depth, the Molasse (Tertiary) formation consisting of alternating marl and sandstone banks then limestone have been drilled. The hydrogeological conditions in this Tertiary horizon is little known and poorly documented in the canton of Geneva. Nevertheless, drilling experiments through this unit in the Bernex region have punctually revealed the presence of water inflows whose sulphate content may be significant. These occurrences are essentially based on the presence of a fracturing network allowing the circulation of fluids. The Mesozoic units showed a low natural flow rate of 0.5l/s with bottomhole temperature of ~55°C. Wellhead temperature recorded after a few weeks from the end of drilling operation was 18°C and wellhead pressure of 10-12bars.</p>
<p>Potential Impacts</p>	<p>The potential impacts of the drilling activities carried out at GGeo-01 can be identified on groundwater quality in the surroundings of the borehole mostly by contamination by drilling fluids and hydrocarbon spills from the machineries, and linked to the risk of connecting deep saline waters geothermal reservoir with the shallow freshwater aquifers possibly present despite not being mapped.</p>	<p>The GGeo-02 exploration borehole reached the same karstic aquifers that supply the various main springs at the foot of the Jura (Allondon, Allemogne, Mathieu, Doua, Annaz, Bouna, Divonne) about 12km towards North. The contamination of such springs by drilling fluids during drilling or by overexploitation during future reservoir testing and production operations is unlikely. Impacts were foreseen regarding the contamination of the freshwater</p>

		Aire aquifer by deep fluids during drilling but considered as limited thanks to the precautions taken during operations.
Mitigation Measures	<p>Because of the risk of connecting the aquifers mentioned above, during drilling particular attention was directed in isolating the non-productive levels in the borehole by:</p> <ul style="list-style-type: none"> • installing casings and cementing the entire Cenozoic sequence (Quaternary and Molasse). • Mud drilling to regulate wellbore pressure and stability with continuous control on the drilling mud and its parameters: Density Viscosity Filtrate The concentration of sand and suspended matter pH • Level of the storage tanks • Installation of a BOP in order to avoid any leaks (water, mud, gas, etc.) at the surface 	<p>In order to control any possible impact on the Aire aquifer water table, existing piezometers in the proximities of the drilling site and located downstream of the ambient flow were continuously monitored (water level, turbidity, physico-chemistry). Due to the risk of the different layers being connected, as mentioned above, particular attention was paid to the isolating the upper section of the well from the lower, open hole section in the Mesozoic units by installing a set of casings and cementing the Quaternary/Tertiary Molasse section. CBL logging was carried out in order to ensure its correctness and a casing integrity test was also be carried out before continuing drilling in the Mesozoic target aquifers. When drilling with mud in the Tertiary section, continuous monitoring was carried out on the drilling mud controlling the following parameters:</p> <ul style="list-style-type: none"> • Density • Viscosity • Filtrate • The concentration of sand and suspended matter • pH • Level of the storage tanks <p>During the drilling of the reservoir sections (Lower Cretaceous and Upper Jurassic) with clear water, monitoring of the physico-chemistry of the water was performed. A BOP was installed to avoid any uncontrolled leaks (water, mud, gas, etc.).</p>
Observed Impacts	The drilling results proved that any water flow was observed in	No impact was observed after drilling

	the Quaternary and no impact was observed after drilling	
--	--	--

Surface clear water		
	GEO-01	GEO-02
Pre-Drilling	The site is located on the Nant-d'Avril creek catchment area, with the installation of an agricultural drainage network joining the watercourse at a distance of around 250m. Apart from this drainage network, the drill site area is currently connected to clear water. Nevertheless, a network of rainwater collectors was implemented along the rue de Satigny road	An agricultural drainage network joining the watercourse at a distance of around 650 m and was connected to clear water network.
Potential Impacts	The distance from the drilling site with respect to the Nant-d'Avril creek of 250m is large enough to allow considering as zero the potential impacts on surface waters,	<ul style="list-style-type: none"> • Presence and use of fuel (diesel) machines. • Mud drilling involving the use and storage of products and substances; and which can alter the water (bentonite, additives); • Artesianism and pumping test phase discharging water whose physico-chemical characteristics are incompatible with the requirements of the OEau for discharge to surface water.
Mitigation Measures	<ul style="list-style-type: none"> • All the meteoric waters were evacuated, after decanting and control, to the clear water network via the existing collector. • All the water from the well were collected, treated and evacuated as wastewater 	<ul style="list-style-type: none"> • That only meteoric water was evacuated, to the clear water network via the agricultural drain collector network; • That all the water from the well during the tests were collected, treated and evacuated as waste water • Definition of the optimal water and hydrocarbon management protocol during production tests
Observed Impacts	In view of the works completed by the drilling operations, no impact was generated on the clear waters	In view of the works carried out by the project, no impact was generated on the clear waters.

Soil occupation		
	GEO-01	GEO-02
Pre-Drilling	The project was developed over a surface area of around 2,000 m ² allocated to the agricultural zone and object of a pedologic study which main outcomes can be summarized as follows: <ul style="list-style-type: none"> • The vegetated topsoil is about 25-35cm thick and the subsoil is about 10-20cm thick 	The project includes a surface area of around 2,000 m ² allocated to the agricultural zone and object of a pedologic study which main outcomes can be summarized as follows

	<ul style="list-style-type: none"> • The subsoil is considered to be medium sandy soil. • The content of gravel and small pebbles is also very important. • The pH is alkaline. • The organic matter (OM) content is low at 1.4%. • The contents of major elements show deficiencies in phosphorus and potassium, but still a good magnesium content. 	<ul style="list-style-type: none"> • The vegetated topsoil is about 30-35cm thick and the subsoil is about 10-20cm thick • The subsoil is considered to be heavy sandy soil. • The content of gravel and small pebbles is zero. • The pH is alkaline. • The organic matter (OM) content is 1.8% in the subsoil. • The contents of major elements in the topsoil is satisfying and shows deficiencies in phosphorus and potassium, but still a good magnesium content
Potential Impacts	The impacts associated with the drilling phase mostly involved the stripping of the soil to a thickness of around 40 cm and its storage in the proximities of the site which expected impacts could have impacted the overall quality of the soil as well as potential deterioration of the drainage system.	The impacts associated with the drilling phase mostly involved the stripping of the soil to a thickness of around 50 cm and its storage in the proximities of the site which expected impacts could have impacted the overall quality of the soil as well as potential deterioration of the drainage system.
Mitigation Measures	<ul style="list-style-type: none"> • Stripping topsoil and subsoil underlay separately; • Storage on the topsoil in the vicinity of the worksite. A monitoring of the heap was carried out during the construction site in order to control the development of invasive alien plants • After the work was completed, the two layers of soil were put back in place; • Seeding of the surface with grass. 	
Observed Impacts	The drilling operations did not affect the quality of the soil as well as any deterioration of the drainage system.	



Figure 31. Geo-01 drilling site during operations in 2018 (top) and in 2020 (bottom)



Figure 32. Geo-02 drilling site during (top) and after (bottom) operations

Wastes and dangerous substances		
	GEo-01	GEo-02
Pre-Drilling	Not applicable	
Potential Impacts	construction materials the production of mud required for drilling Diesel fuels and hydraulic oils	
Mitigation Measures	The organization of the drilling site allowed limiting as much as possible the generation of waste by the application of the following measures: <ul style="list-style-type: none"> • The mud drilling technique made possible to limit the production of waste • Sorting the mud in differentiated bins in the event of hydrocarbon arrivals and transporting it to suitable disposal sites. • Define the optimal waste disposal protocol • A refuelling area was defined on a waterproof surface to prevent the spread of gasoline 	
Observed Impacts	No impacts were observed after the end drilling operation	

Environment		
	GEo-01	GEo-02
Pre-Drilling	<i>Erigeron annuus</i> , <i>Solidago gigantea</i> , <i>Solidago canadensis</i> present in the proximities of the drilling sites.	

Potential Impacts	Potential spreading of neophyte species
Mitigation Measures	A short-term monitoring plan on the vegetation was implemented during the drilling operations. In the medium term the presence of the neophyte is not to be feared, because even if it were present in the temporary meadow, it would be eliminated by ploughing and monitoring is therefore not necessary.
Observed Impacts	No impacts were observed after the end drilling operation

Nature		
	GEo-01	GEo-02
Pre-Drilling	The semi-natural surroundings on the immediate proximity of the drilling site are an extensive strip of meadowland (approx. 250m long by 4m wide) and a native hedgerow between the strip of meadowland and the cycle path.	The semi-natural surroundings on the immediate proximity of the drilling site shows a vegetation mix composed by maple trees and native native shrub plantations.
Potential Impacts	The main impacts identified for the nature focused on the strip of meadow and hedge integrity.	The drilling operation were not expected to impact biological functions of the extensive areas within the immediate project area. Dust raised by traffic could have had a negative effect on the vegetation
Mitigation Measures	The meadow and hedge were preserved during drilling operations and the drilling site was installed keeping a distance of 5m to avoid damages to the roots and	In order to limit dust deposits, a mat will be laid along the fence ("curtain" on the side).
Observed Impacts	The hedge was preserved and no other impacts on the nature was observed after drilling	No other impacts on the nature was observed during and after drilling

2.3.1.2. Potential impacts during production operations

Thermal effects on the reservoir natural state temperature

Thermo-Hydraulic (TH) models have been performed to optimise the design of a preliminary HT-ATES system based on a under different configurations of subsurface conditions (Mindel & Drienser, 2020). The goal for the Thermal-Hydraulic (TH) modeling of Geo-01 and Geo-02 wells is to understand the performance of the considered aquifers for heat storage and to assess the extent of the thermal radius after 15 years of operation. This assessment makes us of simple layer-cake models following the insights and overall design as presented by Mindel et.al. (2020).

Methodology

The Delft Advanced Research Terra Simulator (DARTS) (DARTS, 2021) is used to perform the simulations, using the Operator Based Linearization approach (Khait et al., 2018) that has been shown to be accurate and fast against other simulators (Wang et al, 2020). Water properties are based on IAPWS97 (Huber et al., 2009) as implemented in the python package IAPWS (Romera et al., 2020).

Model Setup

The simulation domain is comprised of the respective reservoir, confined by two 50 m thick bounding layers at the top and the bottom. Spatial discretization is kept constant throughout, with a horizontal resolution of 10 m and a vertical resolution of 2 m. Boundary conditions are implemented with the use of large volume cells at the top and bottom layers, as well as the north and south vertical layers of the modelling domain. The well spacing is kept constant at 150 m for all simulations. The wells are rate-controlled and the systems are operated for 15 years. The hot well uses an injection temperature of 90 °C while the cold well has an injection temperature of 50 °C. Common input parameters are summarized in (Table 10). The scenarios considered in the models are listed in Table 9.

Table 9. Input parameters shared between all models.

Parameter	Value
Well spacing	150 m
Charge – Store – Discharge - Rest	120 – 60 – 120 – 65.25 days
Simulation time	15 years
Porosity	10 %
Pressure gradient	10 MPa / km
Temperature gradient	30 °C / km
Reservoir permeability kv / kh	0.1
Hot / Cold well injection temp	90 / 50 °C
Confining layers permeability / porosity	0.5 mD / 0.1 %

Table 10. Modelling scenarios.

Well and Scenario	Targeted Reservoir	Reservoir Permeability (m ²)	Reservoir Thickness (m)	Injection Rate (kg/s)
GEO-01	LC + Siderolitic	$3 \cdot 10^{-13}$	350	60
GEO-02 SC1	LC-UJ	$7 \cdot 10^{-16}$	700	3.9
GEO-02 SC2	Siderolitic	$7 \cdot 10^{-16}$	150	0.7
GEO-02 SC3	Siderolitic	$3 \cdot 10^{-13}$	150	60

Geo-01

Figure 33 and Figure 34 show the temperature distribution in the production interval after 15 years of production, using the inputs from Table 3. The large reservoir thickness combined with a relatively high permeability results in the hot plume being more prominent in the upper part of the aquifer. Additionally, due to the interaction between the hot and the cold well, the hot plume is asymmetrical, having a reduced extent between the wells and a larger extent away from the wells. The thermal radius is therefore slightly larger at shallower depths and exceeds the 3°C at 100m radius distance from the well as defined by the Swiss water protection law (OEaux, annexe 2 chapitre 21 alinéa 3) at the end of the 15 years operation period simulated.

Table 11. Input parameters Geo-01 model.

Parameter	Value
Domain x, y, z	500 m, 500 m, 454 m
Discretization dx, dy, dz	10 m, 10 m, 2 m
Cell count	567,500
Well rates	60 l/s - 5184 m ³ /day
Permeability	$3 \cdot 10^{-13}$ m ² - 304 mD

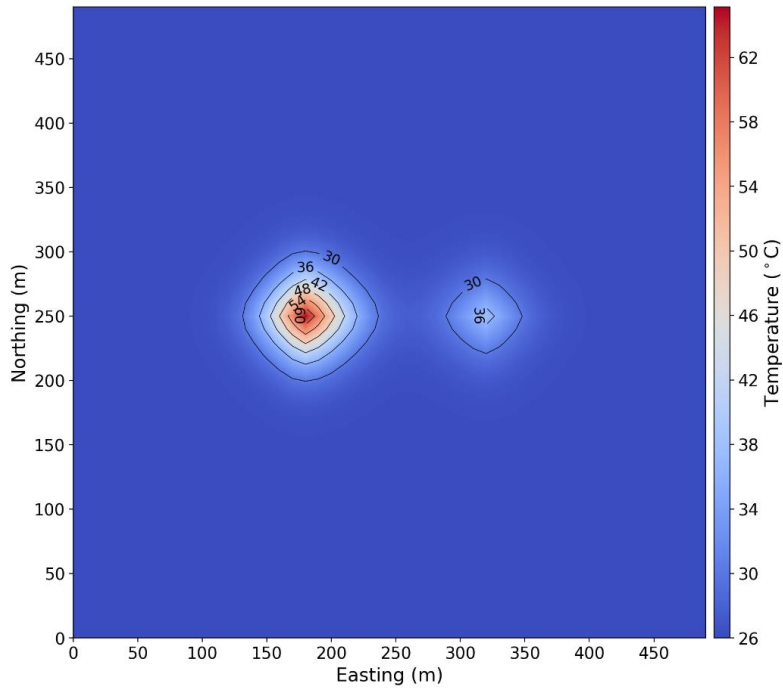


Figure 33. Geo-01 map view at a depth of 575 m after 15 years of operation. The vertical dashed white lines represent a distance of 100m on each side of the hot and cold well respectively.

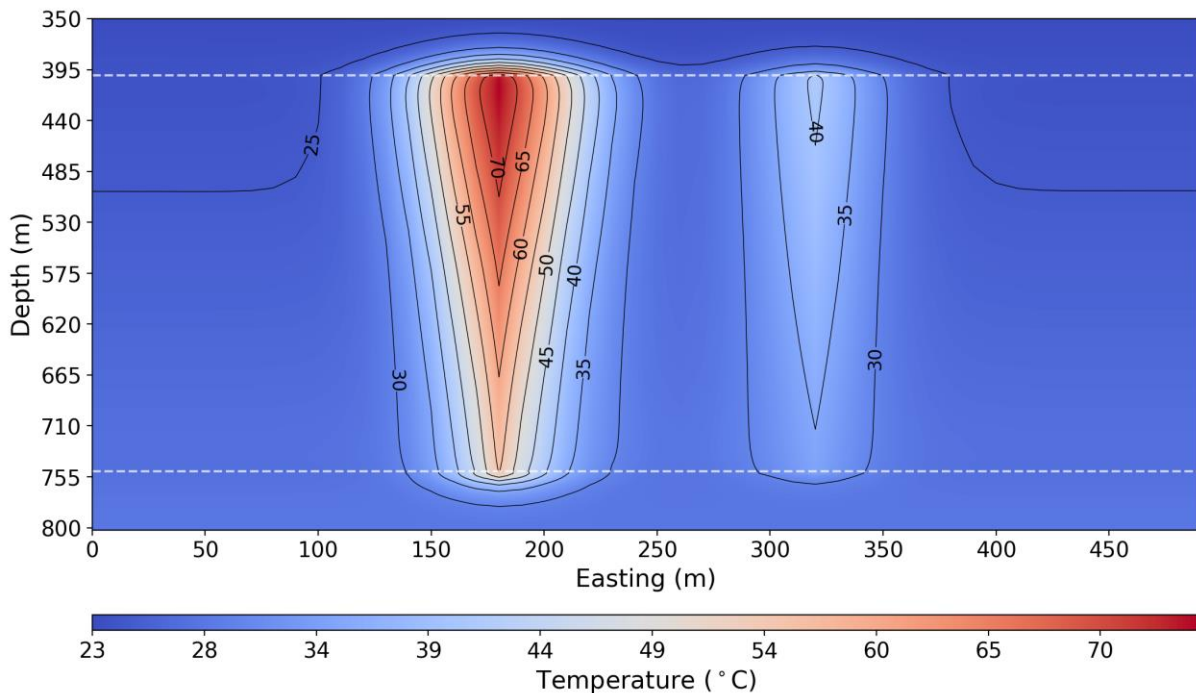


Figure 34. Geo-01 vertical section across the wells (northing = 500 m) after 15 years of operation. The horizontal dashed white lines mark the production interval, while the vertical dashed white lines represent a distance of 100m on each side of the hot and cold well respectively.

Geo-02 SC1

Figure 35 and Figure 36 show the temperature distribution in the production interval after 15 years of production, using the inputs from Table 12. The low permeability and low rates result in a very small thermal radius. Differences between the bottom and the top of the hot plume are attributed mostly to conduction, which is laterally favorable at shallower depths due to the increased temperature gradient with the undisturbed temperature field. Reservoir temperature does not exceed the 3°C at 100m radius distance from the well as defined by the Swiss water protection law at the end of the 15 years operation period simulated.

Table 12. Input parameters Geo-02 SC1 model.

Parameter	Value
Domain x, y, z	500 m, 500 m, 704 m
Discretization dx, dy, dz	10 m, 10 m, 2 m
Cell count	1,005,000
Well rates	0.7 l/s – 60.5 m ³ /day
Permeability	7·10 ⁻¹⁶ m ² – 0.7 mD

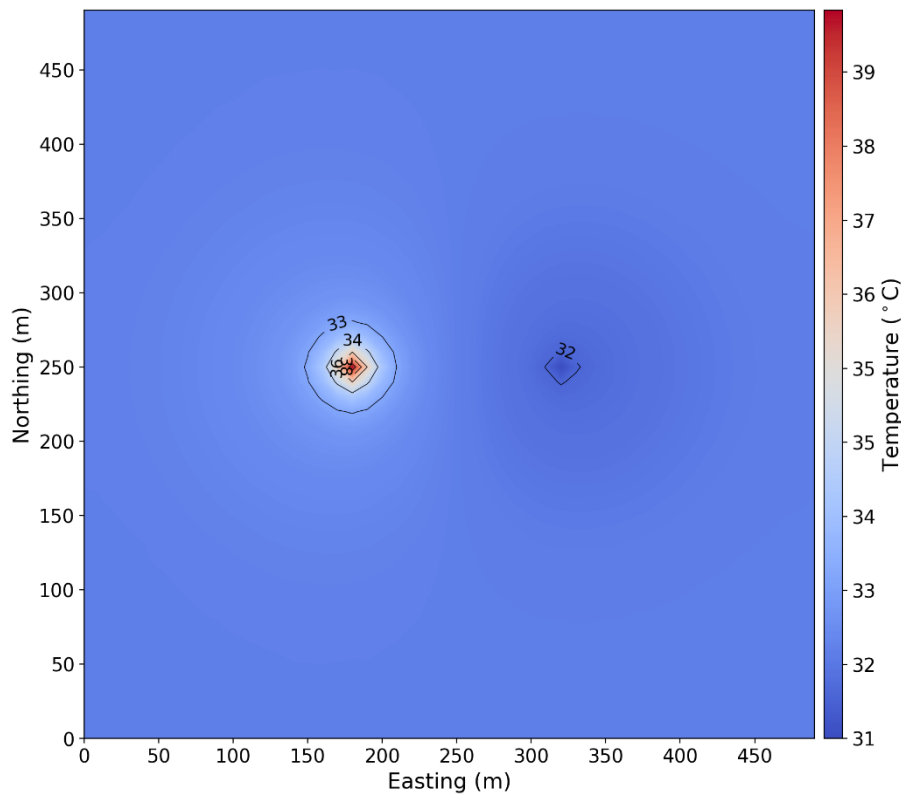


Figure 35. Geo-02 SC1 map view at a depth of 1100 m after 15 years of operation. The vertical dashed white lines represent a distance of 100m on each side of the hot and cold well respectively.

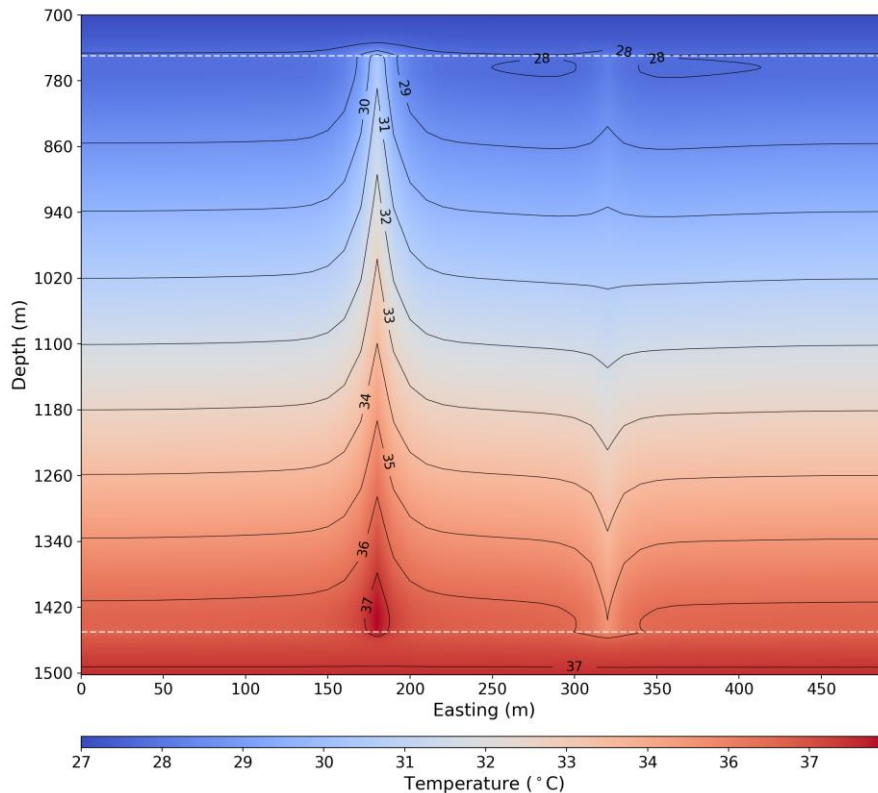


Figure 36. Geo-02 SC1 vertical section across the wells (northing = 500 m) after 15 years of operation. The dashed white lines mark the production interval. The horizontal dashed white lines mark the production interval, while the vertical dashed white lines represent a distance of 100m on each side of the hot and cold well respectively.

Geo-02 SC2

Figure 37 and Figure 38 show the temperature distribution in the production interval after 15 years of production, using the inputs from Table 13. Compared to SC1 using the same rates with a significantly reduced reservoir thickness results in a slightly larger extent of the hot plume. Additionally, the smaller temperature difference at the top and bottom of the domain (due to the lower thickness) results in a more homogeneous lateral extent of the cold plume. The shallower parts of the domain remain slightly less extensive compared to the deeper ones but differences are minor. Reservoir temperature does not exceed the 3°C at 100m radius distance from the well as defined by the Swiss water protection law at the end of the 15 years operation period simulated.

Table 13. Input parameters Geo-02 SC2 model.

Parameter	Value
Domain x, y, z	500 m, 500 m, 154 m
Discretization dx, dy, dz	10 m, 10 m, 2 m
Cell count	317,500
Well rates	0.7 l/s – 60.5 m ³ /day
Permeability	7·10 ⁻¹⁶ m ² – 0.7 mD

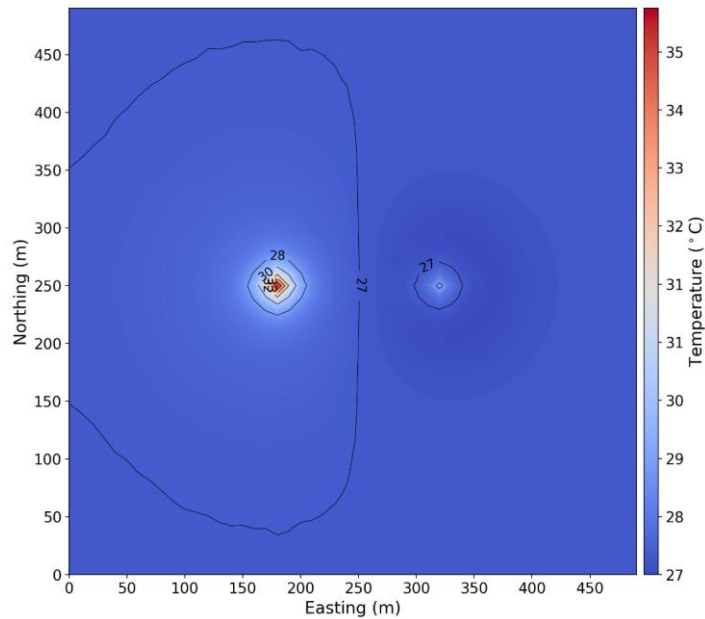


Figure 37. Geo-02 SC2 map view at a depth of 675 m after 15 years of operation. The vertical dashed white lines represent a distance of 100m on each side of the hot and cold well respectively.

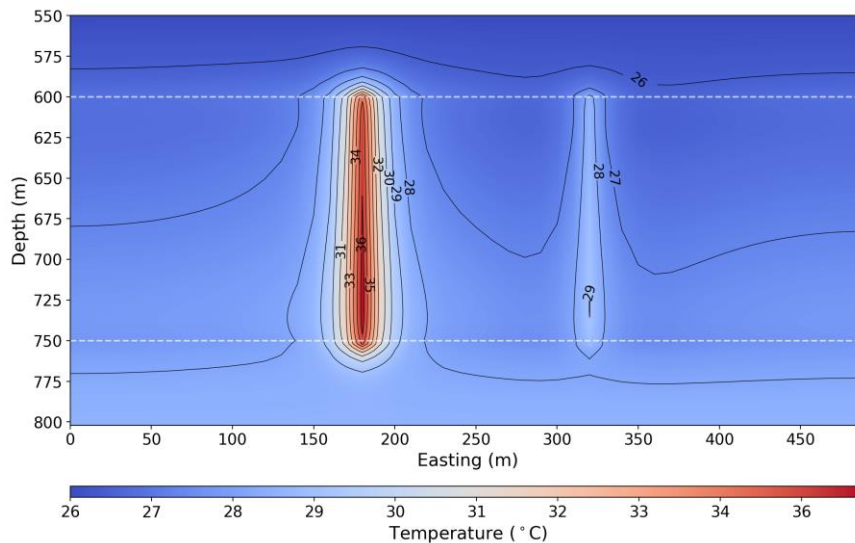


Figure 38. Geo-02 SC2 vertical section across the wells (northing = 500 m) after 15 years of operation. The horizontal dashed white lines mark the production interval, while the vertical dashed white lines represent a distance of 100m on each side of the hot and cold well respectively.

Geo-02 SC3

Figure 39 and Figure 40 show the temperature distribution in the production interval after 15 years of production, using the inputs from Table 14. Increasing both the rate and permeability with the same reservoir thickness as SC2 results in a noticeably larger hot plume laterally and a larger thermal radius. Moreover, the vertical shape of the hot plum is now more pronounced in the shallower part. This is attributed to the large contribution of convection in the temperature field and resembles qualitatively the Geo-01 model. Similarly to the Geo01 model, the hot plume is asymmetric and extends farther away from the wells compared to the space

between the two wells. Reservoir temperature exceeds the 3°C at 100m radius distance from the well as defined by the Swiss water protection law at the end of the 15 years operation period simulated.

Table 14. Input parameters Geo-02 SC3 model.

Parameter	Value
Domain x, y, z	1000 m, 1000 m, 154 m
Discretization dx, dy, dz	10 m, 10 m, 2 m
Cell count	317,500
Well rates	60 l/s – 5184 m ³ /day
Permeability	3·10 ⁻¹⁶ m ² – 304 mD

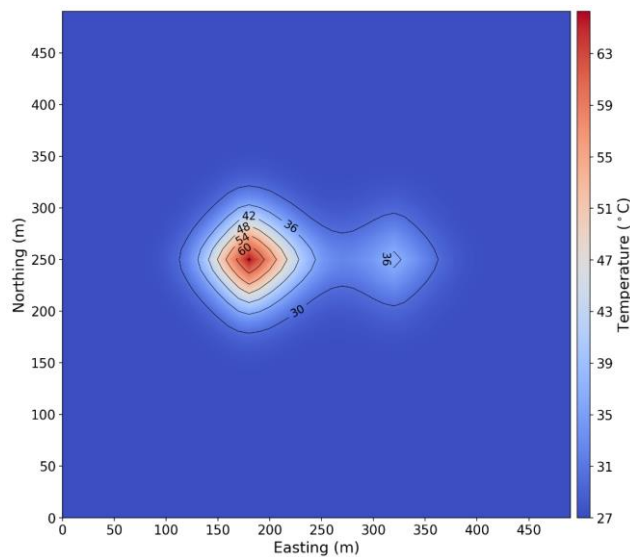


Figure 39. Geo-02 SC3 map view at a depth of 675 m after 15 years of operation. The vertical dashed white lines represent a distance of 100m on each side of the hot and cold well respectively.

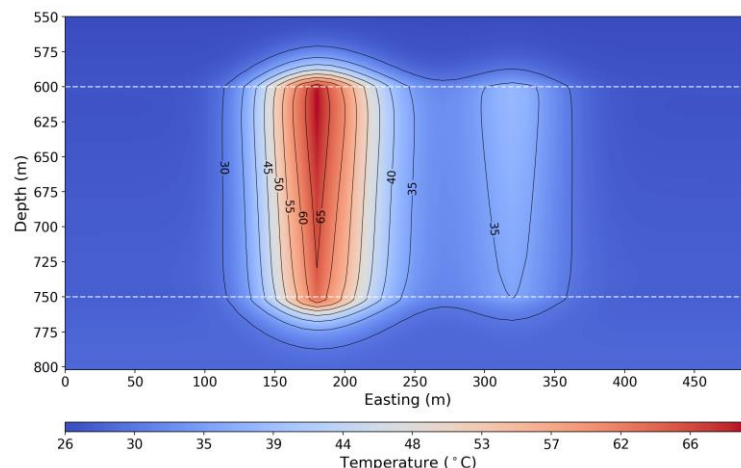


Figure 40. Geo-02 SC3 vertical section across the wells (northing = 500 m) after 15 years of operation. The dashed white lines mark the production interval. The horizontal dashed white lines mark the production interval, while the vertical dashed white lines represent a distance of 100m on each side of the hot and cold well respectively.

2.3.1.3. Soil mechanics effects

We explore two aspects of ground surface deformation at the Geneva wells using a hydro-mechanical (HM) model. Firstly, we model ground deformation during the pumping test at GEO-01 and compare to deformation measurements from Work Package 5. Secondly, we perform predictive simulations of the potential ground deformation resulting from HT-ATES to explore the question: what HM ground deformation could we expect if GEO-01 or GEO-02 were used as one well in an HT-ATES doublet? This report is a summary of work performed to understand ground deformation, but more detailed methodology and results are available in the Month 35 version of Deliverable 2.1 (Driesner, 2021).

Parameters and methodology

Our simulations honor the hydrological, mechanical, geometrical, and design parameters near GEO-01 and GEO-02. In the GEO-01 pumping test simulations, the Lower Cretaceous-Upper Jurassic (LC-UJ) is targeted, permeability and reservoir thickness are informed by well logs and pumping test data, and the flow rates approximate those used at the site. In the predictive modeling simulations, we use permeability and thickness data where it is available, and perform sensitivity studies to honor the range of parameter uncertainty. For example, we vary the Young's modulus, reservoir permeability, and targeted formation (i.e., the LC-UJ or the Siderolitic). Each year contains four stages: Injection, Falloff, Drawdown, and Buildup, which last 120 days, 60 days, 120 days, and 62.25 days, respectively. During the Injection stage, fluid is injected into the hot well and produced from the cold well, and during the Drawdown stage the direction of flow is reversed. The flow rate is set to the smaller of 60 kg/s and the flow rate that would lead to hydraulic fracturing, minus a safety factor (e.g., see Birdsell et al., (2021). No flow occurs in the wells during the Falloff and Buildup stages.

The field-scale Young's modulus is an important and uncertain input parameter to our model. There are two aspects of estimating Young's modulus that need to be considered. First, the Young's modulus needs to represent the quasi-static physics of poroelasticity, rather than the dynamic aspects of seismic waves. Second, the Young's modulus needs to reflect the field-scale rock deformation. It is computationally difficult to account for mechanical heterogeneity at this scale, and it is useful to upscale mechanical properties that account for the stronger, in-tact rock. We use a range of Young's modulus in this work. One estimate (i.e., 35 GPa) comes from seismic data (Koumrouyan, 2019) that is adjusted to a static value of Young's modulus using a heuristic approach (Eissa and Kazi, 1988). A second, lower-bound estimate (0.35 GPa) is found by comparing HM simulations to field observations of deformation at the GEO-01 pumping test.

We use the Multiphysics Object Oriented Simulation Environment (MOOSE) to simulate the hydro-mechanical (specifically the poroelastic (Wang 2000)) response to pumping (<https://www.mooseframework.org/>).

Ground deformation results

The following two sub-sections focus on results for the GEO-01 pumping test and the predictive HT-ATES modelling.

GEO-01 pumping test

Figure 41 shows ground surface deformation during the GEO-01 pumping test. Deformation data comes from two sources: (a) GPS monitoring near GEO-01 and (b) the HM numerical

model. There is not a clear trend of subsidence (or uplift) in the GPS data. The GPS data was provided by Nicolas Houlié Geologie GmbH and Services industriels de Genève (SIG) and was collected as part of Work Package 5. The ground deformation was both positive (upwards) and negative (downwards), depending on the time and the GPS station. For the most part, the magnitude of deformation was less than the size of the error bars, so we cannot interpret any significant deformation from the GPS data. In contrast, the numerical model shows a clear trend of subsidence that increases with time. We perform a sensitivity analysis on the Young's modulus, and find that smaller Young's modulus corresponds to a larger magnitude of subsidence. This makes intuitive sense because Young's modulus is a measure of the strength of the rock, and a weaker rock will deform more under the same pressure change. Subsidence would be clearly seen in the GPS data if the field-scale Young's modulus were below 0.35 GPa, and therefore we infer 0.35 GPa as the lower bound of Young's modulus for the HT-ATES predictive modeling.

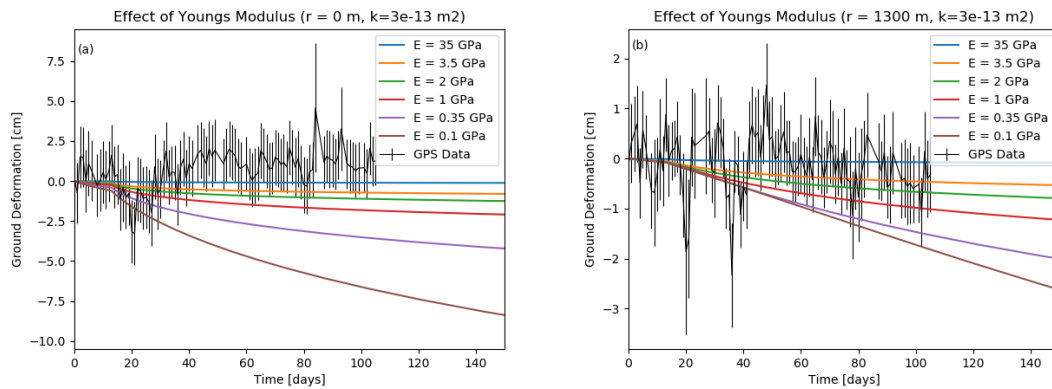


Figure 41. Ground deformation versus time (a) at the well, representing the first GPS station, and (b) 1300 m from the well, representing the second GPS station. Black lines represent GPS data with error bars, and colorful lines represent HM model results for a sensitivity analysis on Young's modulus.

HT-ATES predictive modelling

Table 15. Predictive Simulation Scenarios and Results summarizes the predictive modeling results for a number of scenarios and parameter values. The GEO-01 scenario targets the LC-UJ and uses the permeability inferred from the GEO-01 pumping test (i.e., $3 \cdot 10^{-13} \text{ m}^2$). GEO-02 Scenario 1 targets the LC-UJ, which is deeper at GEO-02, and uses a smaller permeability (i.e., $7 \cdot 10^{-16} \text{ m}^2$), which is in-line with values observed from a pumping test at GEO-02 and observed at the Thônex well. GEO-02 Scenarios 2 and 3 target the shallower Siderolitic rock, and use the permeabilities matching GEO-02 Scenario 1 and the GEO-01 scenario, respectively. When the lower value of permeability is used, the flow rate is curtailed below 60 kg/s, due to the HF constraint.

Table 15. Predictive Simulation Scenarios and Results.

Well and Scenario	Targeted Reservoir and Depth [m]	Reservoir Permeability [m^2]	Reservoir Thickness [m]	Flow Rate [kg/s]	Young modulus [GPa]	Years simulated	Maximum ground deformation [cm]
GEO-01	LC-UJ (400 – 750)	$3 \cdot 10^{-13}$	350	60	35	15	<0.01
					2	1	0.10
					0.35	15	0.49
GEO-02 Scen. 1	LC-UJ (750-1450)	$7 \cdot 10^{-16}$	700	3.9	35	15	0.015
					2	1	0.053
					0.35	1	0.055

GEO-02 Scen. 2	Siderolitic (600-750)	$7 \cdot 10^{-16}$	150	0.7	35	1	<0.01
					2	1	0.015
					0.35	1	0.016
GEO-02 Scen. 3	Siderolitic (600-750)	$3 \cdot 10^{-13}$	150	60	35	1	<0.01
					2	1	0.097
					0.35	1	0.40

Figure 42 shows the aquifer pore pressure and ground surface deformation at the end of the injection stage. We find that pore pressure does not change dramatically from year to year, and the magnitude of the ground surface deformation tends to be largest in the first year. Therefore, we only present the first year of each scenario in the figure. Pore pressure is elevated near the injection well and depleted near the production well. The largest change in aquifer pressure is reached in GEO-02 Scenario 1, followed by GEO-02 Scenario 2. This makes sense because these are the scenarios where the flow rate is limited by the hydraulic fracturing constraint. Surface deformation is positive (upward) for the right portion of the plot (i.e., $x > 2000$ m), whereas it is negative (downward) for the left portion of the plot (i.e., $x < 2000$ m). The ground surface deformation is sensitive to the Young's modulus. The largest modeled ground surface deformations are 0.49 and 0.40 cm, which occur when Young's modulus is 0.35 GPa for GEO-01 and GEO-02 Scenario 2, respectively. For these scenarios, there may be some boundary effects, and it is possible that the predicted uplift would be smaller if a larger mesh were used. All other scenarios have deformation ≤ 0.1 cm.

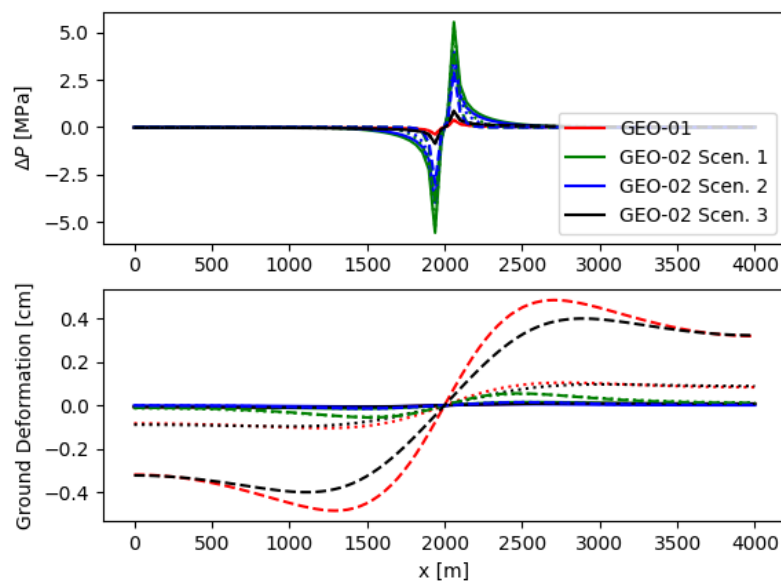


Figure 42. (Top) Difference in aquifer pressure from the initial condition versus spatial coordinate x along a line that intersects the two wells and (Bottom) ground surface deformation versus x at the end of Year 1 injection for each scenario. Solid lines use Young's modulus equals 35 GPa, dotted lines use 2 GPa, and dashed lines use 0.35 GPa. The cold/production well and hot/injection well are located at $x = 1925$ m, and $x = 2075$ m, respectively.

2.3.1.4. Discussion and Conclusions

In this section, we used a poroelastic model to examine potential for ground surface deformation at the ongoing GEO-01 pumping test and in predictive modeling of a hypothetical HT-ATES doublet at GEO-01 or GEO-02.

We acknowledge certain limitations to this work. For example, the deformation is sensitive to the field-scale, static Young's modulus. Indeed, modulus are determined from sonic logging which provide borehole-scale dynamic properties that have to be converted to static properties (4, 5). Upscaling to reservoir scale static properties involves large uncertainties. While we inferred lower bounds on the Young's modulus (0.35 GPa) by comparing modeled subsidence to observed subsidence at GEO-01, the modulus remains uncertain. Reducing this uncertainty in the field-scale Young's modulus parameter would reduce uncertainty in ground deformation. Furthermore, we specifically consider poroelastic deformation, which does not account for the potential for thermal contraction/expansion or clay swelling.

Nevertheless, for most scenarios we considered, the deformation remains small, suggesting that poroelastic deformation is manageable. For the GEO-01 pumping test, the GPS data shows no significant deformation. Modeling suggests that, given no deformation has occurred thus far, it is unlikely that large deformation will occur for the full duration of the pumping test. In the predictive HT-ATES simulations, the two scenarios with largest deformation both utilize the lower-bound value for the field-scale Young's modulus. One scenario targets a relatively shallow reservoir (GEO-01) and the other targets a relatively shallow and relatively thin reservoir (GEO-02 Scenario 3). All other scenarios resulted in ≤ 0.10 cm of ground surface deformation. It seems that poroelastic deformation can be managed by choosing operating pressures and flow rates based on the target reservoir in conjunction with monitoring. For example, flow rate may need to be curtailed if: (a) reservoir permeability, thickness, or depth are not sufficient, especially if the pressures would approach the hydraulic fracturing threshold or (b) observed deformation becomes large.

2.3.1.5. Seismicity

The Geneva area is located in a rather seismically quiet region, despite the proximity to the tectonically-active western Alpine front. However, the knowledge of the occurrence and distribution of micro-seismic events is poorly constrained. Historical records show that the area was affected by seldom seismic events such as the one possibly responsible for the tsunami along the shores of the Lake Geneva in 563 AD (Kremer et al. 2014). The largest seismic events occurred along the Vuache fault, in 1996 (Baize et al. 2011, Fig. 1) but apart from this unique large event, the seismicity in the Geneva area is rather diffuse and located in the upper 15km in the crust.

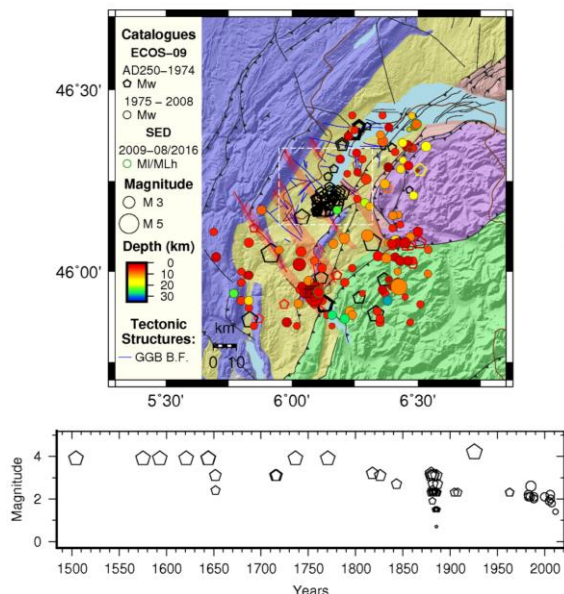


Figure 43. Seismicity map for the GGB area with information about the background seismicity according to literature data (Antunes et al. 2020).

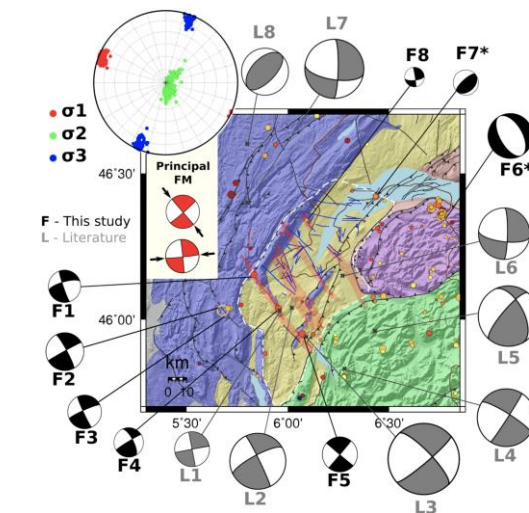


Figure 44. Geological and tectonic map with the relocated events, their magnitudes ML, and retrieved focal mechanisms (Antunes et al. 2020).

The University of Geneva has implemented (from September 216 to January 2018) a temporary seismic network to densify the existing seismic monitoring network and to improve the identification on micro-events (Antunes et al. 2020). The 17 months of seismic data show a low seismic rate for the GGB, with 17 detected events counting a total of 12 earthquakes per year. No events were located in the canton of Geneva, where the geothermal activities will take place.

As part of the GEOBEST-CH research project, the Swiss Seismological Service (SED) at ETH Zurich is using seven additional measuring stations to monitor the Geneva Basin, the area on which the GEOthermie 2020 project is focusing. One aim of this monitoring is to improve knowledge about natural, local seismicity. But it should also help to detect earthquakes quickly and accurately, and also to clarify whether they are associated with the geothermal project or are instead of natural origin.

The monitoring network consists of seven measuring stations. Five surface stations (COLLE, PERON, SAVIG, SALEV, CERNIS) and two borehole stations (CHALL and FORET) have been set up in the Geneva Basin area (in both Switzerland and France), adding to the Swiss National Seismic Network's SGEV station and the French National Seismic Network's OGS2 station in the area being monitored. Most of the surface stations listed are equipped with broadband seismometers, but SGEV and CERNIS are strong motion measuring stations fitted with accelerometers. Another accelerometer has been installed at the CHALL well site.

Since 2019 no earthquake has been recorded.

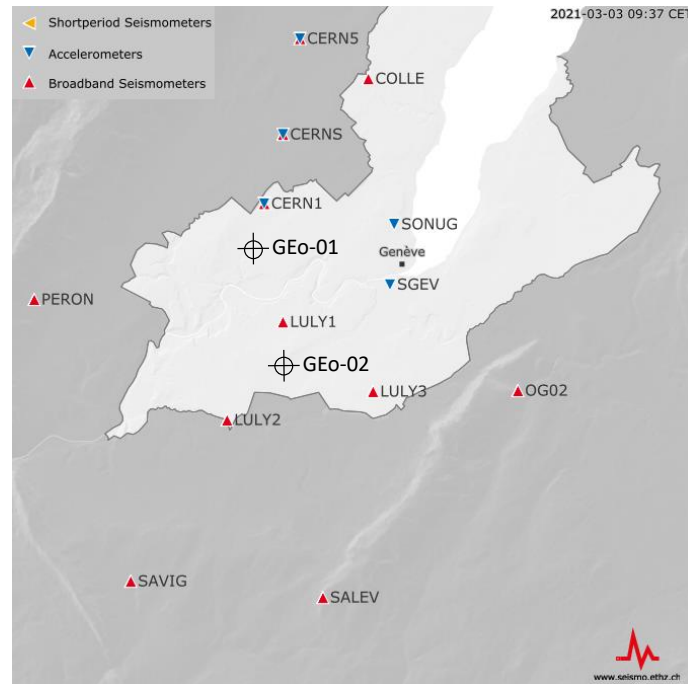


Figure 45. Seismicity monitoring network in the Geneva basin (mod from <http://www.seismo.ethz.ch/>).

2.3.1.6. Potential geochemical reactions occurring within the GEO-01 and GEO-02 wells

The composition of groundwater produced or pumped from GEO-1 and GEO-2 is listed in Table 16. All groundwater samples either refer to the general Ca-HCO_3 or Na-HCO_3 water type. At the wellhead, they are strongly supersaturated with respect to calcite and dolomite. The strong supersaturation is likely inherited from the degassing of CO_2 during sampling. At reservoir conditions, all samples must be at saturation with respect to both dolomite and calcite based on the rather fast reaction kinetics of these carbonate minerals. In case of GEO-1, another characteristic feature is the elevated sulphide concentration of 21.7 mg/L.

Table 16. Chemical composition of groundwater samples produced or pumped from GEO-1 and GEO-2.

Well	Unit	GEO-01	GEO-02	GEO-02
Sampling date		12.12.18	14.07.20	14.07.20
Sampling depth	m	>400 m	880-945	1360-1425
Sampling temperature	°C	32.2	21	20
In-situ reservoir temperature	°C	32.2	38.4	53.4
pH		7.7	8.41	8.22
Oxygen concentration	mg/l	0.1	5.7	1.7
Redox potential	mV	-103	384	395
Sodium (Na ⁺)	mg/l	32	152	52.5
Potassium (K ⁺)	mg/l	2.2	6.92	5.35
Calcium (Ca ²⁺)	mg/l	27	16.0	35
Magnesium (Mg ²⁺)	mg/l	14.0	8.0	14.2
Ammonium (NH ₄ ⁺)	mg/l	0.18	0.6	0.2
Bicarbonate (HCO ₃ ⁻)	mg/l	192	325	179
Chloride (Cl ⁻)	mg/l	10	31.2	15
Sulfate (SO ₄ ²⁻)	mg/l	19	5.1	32.8
Nitrate (NO ₃ ⁻)	mg/l	< 0.2	< 0.1	< 0.1
Sulfide total (HS ⁻ , S ²⁻)	mg/l	21.7	not measured	not measured
Iron (Fe ²⁺)	mg/l	< 0.02	< 0.01	< 0.01
Water type (simplified)		Ca-HCO ₃	Ca-HCO ₃	Na-HCO ₃
Saturation index calcite		0.34	0.57	0.45
Saturation index dolomite		0.81	1.14	1.85
Log(P _{CO2}) at reservoir <i>T</i>		-2.25	-2.00	-1.85

Based on the chemical composition of the collected groundwaters (Table 16), the following risks have been identified for the use of these waters for HT-ATES:

1. Owing to their retrograde solubility (i.e. decreasing solubility with increasing temperature), carbonates such as calcite will likely precipitate when the waters are heated to 90°C during storage cycles. This could impede flow and heat exchange in the surface installations.
2. In case of the water produced from GEO-01, corrosion of technical installations such as pumps, casings, and heat exchangers may occur due to the high sulfide concentration. This could lead to material failure and operational problems.

Figure 46 shows the maximum amount of calcite that could potentially precipitate per day at a hypothetical heat exchanger when heating the three groundwaters from their in situ temperatures to 90°C at a production rate of 50 L/s. This estimation is based on geochemical modelling using PHREEQC and represents a worst-case scenario where the saturation index of calcite is fixed to zero during heating. In other words, kinetic limitations likely playing an important role for the formation of calcite scales were not considered for this estimation. With 38 dm³/day, the calcite scaling potential is greatest for the sample collected from GEO-01 because, compared to GEO-02, the water originates from a shallower depth

where the difference between the in-situ groundwater temperature and 90°C is greater. Figure 46 further demonstrates that the temperature dependence of the calcite solubility is nearly linear and that the slope of the dependence varies with the water composition (e.g., pH, P_{CO_2}).

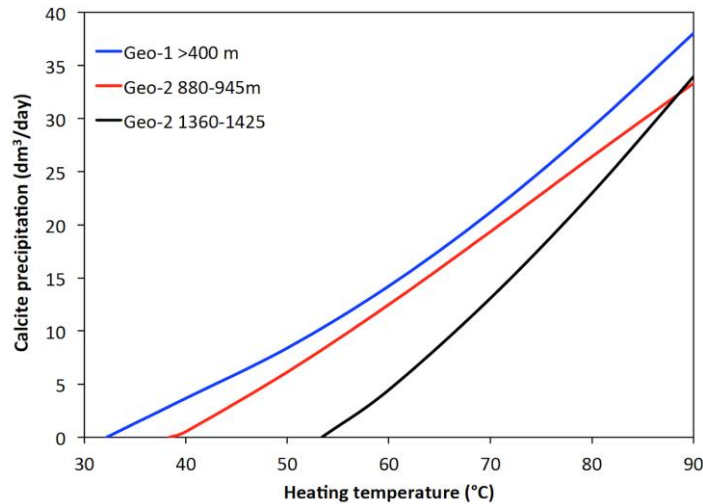


Figure 46. Maximum calcite volumes per day predicted to precipitate when groundwaters accessed by GEO-1 and GEO-2 (Table 16) are produced at 50 L/s and heated to temperatures up to 90 °C.

Figure 47a shows that the water produced from GEO-01 shows a dark color after the well had been closed for more than 3 months during the Covid-19 shutdown in spring 2020. Powder X-ray diffraction demonstrated that the black color is inherited from the precipitation of pyrite likely triggered by the corrosion of the steel casing. The occurrence of corrosion and the precipitation of pyrite within the GEO-1 well was further confirmed by a time-dependent sampling of the produced water (Figure 47b). All dissolved sulfur species (SO_4 , S_2O_3 , H_2S) showed strong variations, indicating that the sulfur system is highly reactive within the GEO-1 well. In particular, the sulfur data suggests that both sulfate reduction and sulfide oxidation are occurring in addition to corrosion of the casing and the subsequent precipitation of pyrite. All these processes are likely mediated by microbes. Their role will be assessed by future microbial analyses.

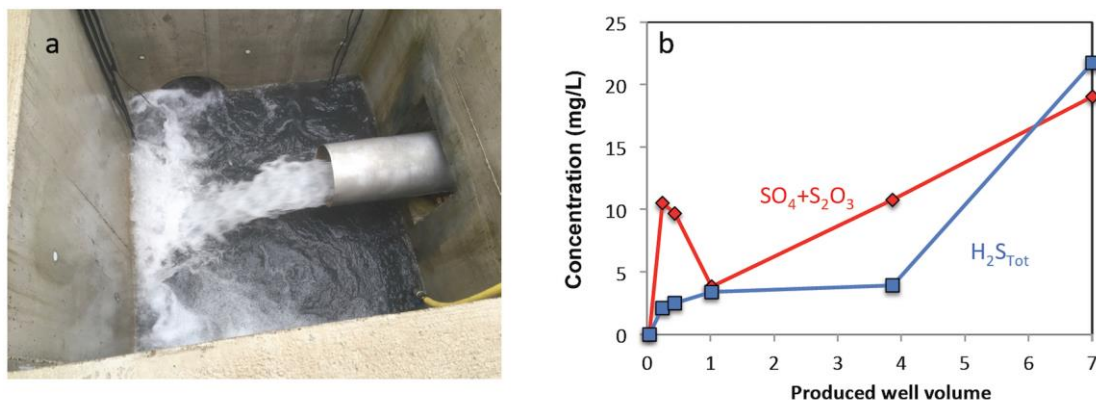


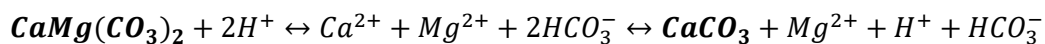
Figure 47. a) Wellhead of GEO-1 producing water after the well had been shut for 3 months during the Covid-19 shutdown in spring 2020. The dark color is inherited from the presence of pyrite in the suspended load. b) Time-dependent concentration of dissolved sulfur species during production after the Covid-19 shutdown.

In addition to minerals precipitating from the reservoir water, mineral reactions will also take place in the reservoir formation during HT-ATES. These reactions were investigated in batch experiments, where fragments of dolomite (81 wt.% dol, 18 wt.% cc, 1 wt.% qtz) from the Calcaire de Tabalcon were reacted with an artificial porewater modelled after the composition of the reservoir water sampled from GEO-02 (Table 16). The experiments were conducted at 20 degrees and 90 °C over two weeks, taking solution samples as a function of time.

The analyses of the sampled solutions show that different elements exhibit different behaviours as a function of time and/or temperature (Figure 48).

These changes in solution composition can be explained by mineral reactions taking place. An increase in concentration suggests mineral dissolution, while a decrease indicates precipitation. In addition, the experimental results were modelled using PHREEQC (equilibrium approach). Together, the following mineral reaction have been identified:

- The increase in Mg is the result of dolomite dissolution. Dolomite is more soluble at lower temperatures, explaining the smaller increase at 90 °C compared to 20 °C.
- The dissolution of dolomite also releases Ca. However, the concentration of Ca is decreasing over the course of the experiments. This is because the Ca released from dolomite dissolution induces calcite precipitation:



- If the reaction runs to completion (i.e. per mol of dolomite dissolved, one mol of calcite is precipitated), the Ca concentration should remain constant. However, as the Ca concentration decreases, it suggests that additional calcite has to form (e.g. due to the release of bicarbonate from dolomite or a change in pH). This will be investigated in additional modelling which is currently ongoing. Calcite is more soluble at lower temperatures, explaining the smaller decrease at 90 °C compared to 20 °C.
- Increase in Si and K suggest that one or several minerals not identified by XRD are present and dissolving. Likely candidates are illites, smectites or mixed-layer I/S. These minerals show a normal solubility, explaining the higher concentrations in the 90 °C experiment compared to the 20 °C one.

PHREEQC simulations only suggest small amounts of minerals dissolving/precipitating (0.7 mmol for dolomite and -1.2 mol for calcite). This suggests that the system is mineral buffered and even in a formation, where dolomite is less abundant, the reactions described above are expected to take place. In pure limestones (such as parts of the Complex Récifal in the upper Formation des Etiollets; 100 wt.% calcite according to XRD) the reactions are even simpler as only calcite is present to dissolve or precipitate.

The replacement of dolomite by calcite slightly increases the porosity of the formation as calcite has a lower molar volume. However, the volumes of minerals dissolving/precipitating are so low that the effect of these mineral reactions on the porosity and permeability of the overall reservoir are assumed negligible. Nevertheless, 3D THC simulations should be performed if a site and reservoir formation have been selected in order to identify if mineral reactions in certain areas (e.g. near the wellbore) could adversely affect the properties of the reservoir over years of HT-ATES operation.

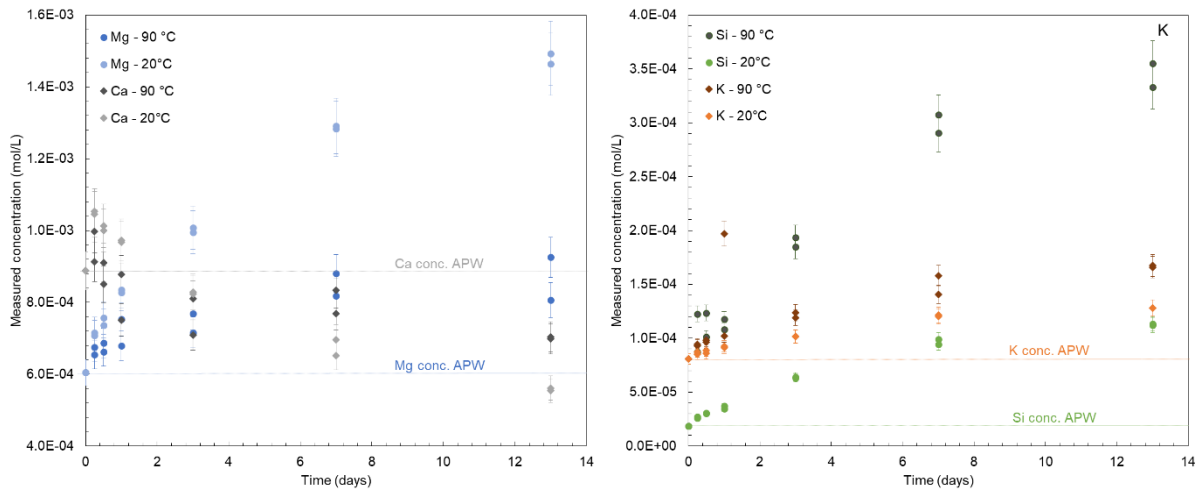


Figure 48. Evolution of solution composition as a function of time during the batch experiments on crushed dolomite from the Calcaires de Tabalcon. Dotted lines represent the initial concentration (= APW concentration) for each ion. Left: Changes in Ca and Mg concentration indicating carbonate reactions. Right: Increase in Si and K indicating silicate reactions. Ions not shown here (Na, Cl, SO₄) show no change over time.

2.3.1.7. CO₂ intensity for the Geneva case study

The CO₂ intensity has been assessed based on HT-ATES performance by combining dynamic reservoir simulations on synthetic models representative of the average Geneva subsurface conditions, and energy system inputs (Daniillidis et al. 2021 submitted) for a 15 year operation.

The operational CO₂ emissions balance is analysed based on current electricity CO₂ intensity data. The avoided CO₂ emissions include the operation of the system and do not consider the installation of the wells and other equipment required for the functioning of the ATES system. The operational CO₂ intensity of the HT-ATES system is given by:

$$HTATES_{CO_2} = \sum_{t=0}^n HTATES_{E_{el}} C_{el} - \sum_{t=0}^n HTATES_{E_{th}} C_{gas}$$

where

- **HTATES_{E_{el}}** is the energy (MWh) required by the HT-ATES system for operation of both pumps and heat pumps,
- **C_{el}** is the CO₂ intensity of the electricity mix,
- **HTATES_{E_{th}}** is the heating energy (MWh) provided by the HT-ATES system and
- **C_{gas}** is the CO₂ intensity of gas heat provided to the DH network that the HT-ATES system is replacing. The latest national Swiss database for CO₂ intensity per source is used as a reference according to (KBOB, 2016)

Table 17. CO₂ intensity values used.

Electricity intensity scenario	CO ₂ intensity
Electricity High (CHP biogas)	0.177 kg CO ₂ eq/kWh
Electricity Mean (CH mix)	0.102 kg CO ₂ eq/kWh
Electricity Low (geothermal CHP)	0.031 kg CO ₂ eq/kWh
Gas heat (provided by DH)	0.3140 kg CO ₂ eq/kWh

The HT-ATES systems that were simulated include a set of 1152 scenarios that were computed combining a complex combination of subsurface and surface constraints.

Parameter	Value	Units
Aquifer thickness	50, 100, 150	m
Aquifer permeability	1×10^{-14} , 5×10^{-14} , 1×10^{-13}	m^2
Aquifer porosity	10, 20	%
Well pattern	Doublet, 5-spot	-
Cut-off temperature	20, 50	$^{\circ}C$
Aquifer depth	500, 1000	m
Aquifer dip	0, 15	$^{\circ}$
Aq. groundwater velocity	0, 2	m/y
Artesian conditions	0, 1	MPa

Results show that with a cut-off temperature of 50 $^{\circ}C$ the HT-ATES is strongly affected by the depth, with values staying below 3% for a 500 m depth aquifer and at least 4% for an aquifer depth of 1000 m (Figure 49). For a cut-off temperature of 20 $^{\circ}C$ the depth difference does not affect the ATES share as drastically, but the amount of avoided CO₂ emissions increases strongly with deeper systems and almost doubles for the systems with a transmissivity of $1.5 \times 10^{-11} m^3$ and artesian conditions (Figure 49). In this case the avoided emissions are in excess of 1 billion kg of CO₂ equivalent when the high profile is used for the electricity grid CO₂ intensity.

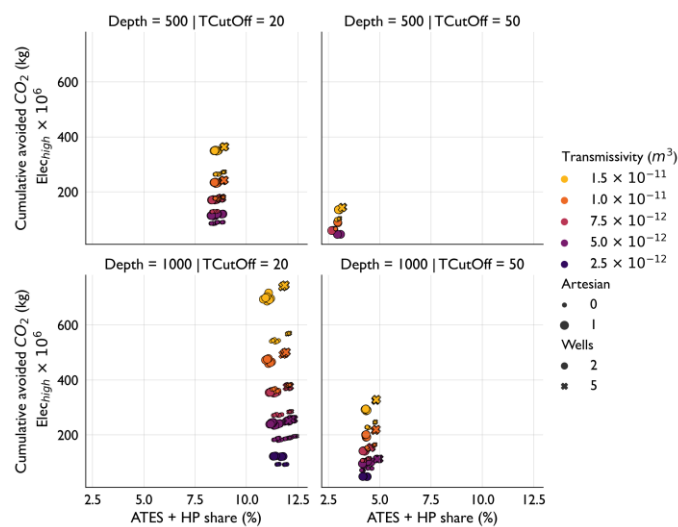


Figure 49. ATES share and cumulative avoided CO₂ emissions for the simulations with an LCOH below 200 CHF/MWh.

An increase of the avoided CO₂ emissions with higher efficiency is evident (Figure 50a). With increasing efficiency, the range of the avoided CO₂ emissions increases. Above an efficiency of circa 50% the range of avoided CO₂ emissions expands substantially (Figure 50a). The aquifer depth, the presence of artesian conditions and the CO₂ intensity of the electricity grid define the final level of avoided CO₂ kg. The cumulative histogram shows an increasing separation between the avoided CO₂ emissions as more CO₂ is avoided that depend on the CO₂ intensity of the electricity grid increases (Figure 50b).

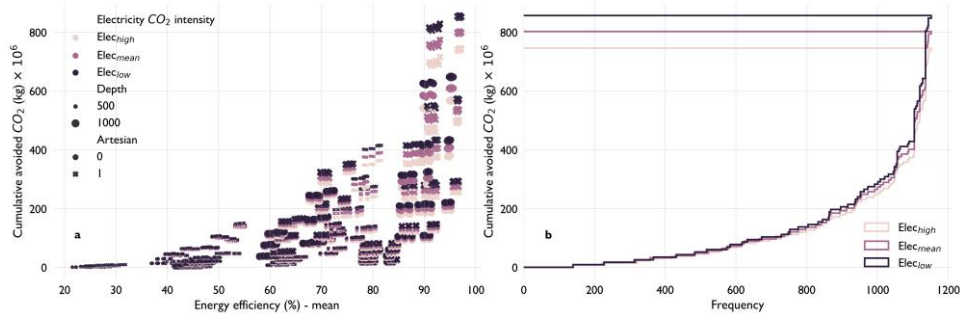


Figure 50. Cumulative avoided CO₂ emissions over 15 years of operation as a function of energy efficiency (a) and cumulative histogram of the avoided CO₂ emissions over 15 years of operation (b).

2.3.1.8. Fast-Track Risk assessment

According to the results of the evaluation of the different effects associated with the drilling activities and production operations a fast-track assessment of the risk linked to the different components is presented in Table 18.

Table 18. Fast-track risk assessment for the Geneva case studies.

GEO-01													
Effect	Phase	Drilling					Operations (predicted)						
		P	A	M	Probability	Consequences	Risk	P	A	M	Probability	Consequences	Risk
Air quality					H	L	M				L	L	L
Noise and vibration					H	L	M				M	L	L
Formation water quality					L	L	L				H	M	H
Formation water temperature											H	L	M
Surface clear water					H	L	M				L	L	L
Soil occupation					H	L	M				H	L	M
Wastes and dangerous substances					H	L	M				M	L	L
Environment					M	L	L				L	L	L
Nature					M	L	L				L	L	L
Soil mechanics											L	L	L
Seismicity					L	H	M				L	H	M
CO2 intensity reduction											H	M	H

GEO-02													
Effect	Phase	Drilling					Operations (predicted)						
		P	A	M	Probability	Consequences	Risk	P	A	M	Probability	Consequences	Risk
Air quality					H	L	M				L	L	L
Noise and vibration					H	L	M				M	L	L
Formation water quality					L	L	L				H	M	H
Formation water temperature											H	L	M
Surface clear water					H	L	M				L	L	L
Soil occupation					H	L	M				H	L	M
Wastes and dangerous substances					H	L	M				M	L	L
Environment					M	L	L				L	L	L
Nature					M	L	L				L	L	L
Soil mechanics											L	L	M
Seismicity					L	H	M				L	H	M
CO2 intensity reduction											H	M	H

2.3.2. Bern case study

The Forsthaus heat-storage project (Geospeicher Forsthaus) intends to store excess heat generated during the summer months by the EWB power plant (Energiezentrale Bern), which combusts municipal waste, wood and natural gas at Forsthaus, Bern. The heat will be stored in a geological reservoir at several hundred metres depth beneath the site. During the winter months the heat will be recovered and fed into the local district-heating network. This report summarizes the results so far of an on-going assessment of geological and geochemical issues that may arise during operation of the Geospeicher, as an aid in planning the installations and operational procedures prior to the start of drilling.

The target heat reservoir is a sequence of water-saturated porous and permeable sandstones and intervening low-permeability claystones that were deposited by ancient meandering rivers as part of the Lower Freshwater Molasse (USM). The summer heat-loading cycle entails extracting formation water from the sandstones through supporting wells, transferring the excess heat to this working fluid via a 90 °C surface heat exchanger, then reinjecting the hot water into the sandstones through a main well. The winter heat-unloading cycle entails pumping the hot formation water to the surface through the main well, recovering part of the heat via the heat exchanger, then reinjecting the cooled water at 50 °C into the reservoir through the supporting wells. Subsurface water volumes and pressures will thus be balanced during both closed-loop, continuous-flow cycles.

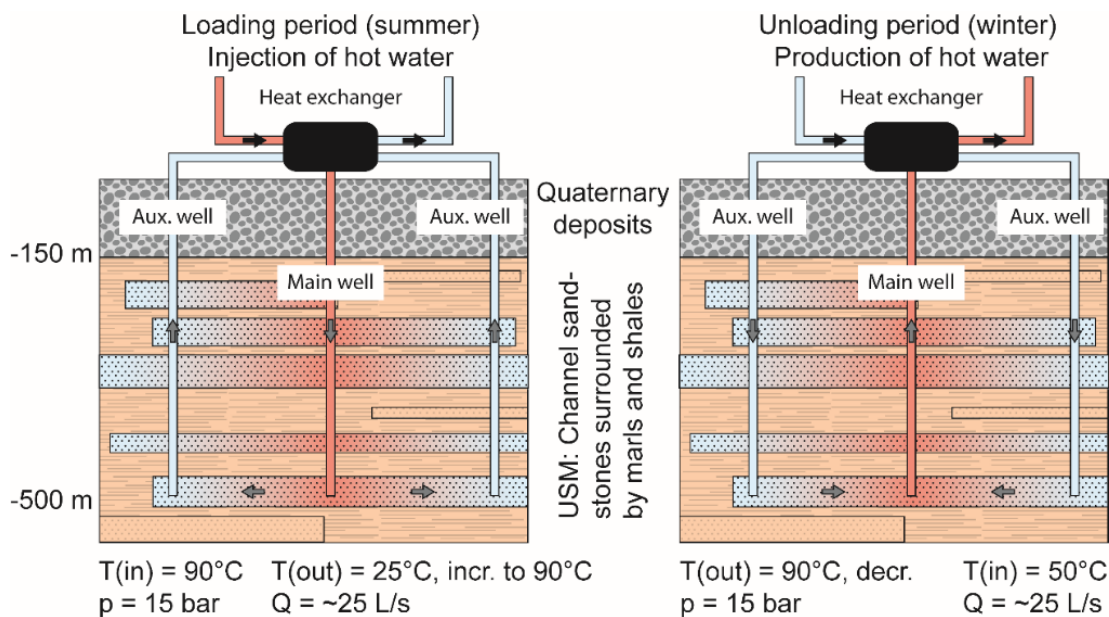


Figure 51. Sketch of the operational design and planned operational parameters of the HT-ATES pilot project Geospeicher Forsthaus.

2.3.2.1. Water-rock interactions during operations

At present, subsurface data are missing for the Bern site, but University of Bern conducted a study to assess the water rock interaction that can occur during ATES operations and the potential of mineral dissolution/precipitation at the reservoir scale and the potential of scaling/corrosion at the surface. Despite being analyses that primarily provide results on the potential performance of the ATES system and associated operational risks, they can also be analyses in terms of effects on water quality perturbations. The detailed results are presented in a report delivered in May 2020 (), which are summarized in this section. In

particular the focus here is directed on three main sources of information: (1) analyses of drill core and formation waters from shallow wells 2 km from the site, which provide material for experiments; (2) laboratory experiments involving heating of the sandstones and formation water to identify the governing water–mineral reactions and to calibrate their rates; (3) 3D numerical simulations of the coupled thermal–hydraulic–chemical (THC) processes during the heat loading and unloading cycles at the reservoir scale, to assess the influence of water–mineral reactions on pore clogging and rock-cement dissolution, and on the thermal evolution and feasibility of the storage concept.

In general, the following risks have been identified and classified as non-critical despite requiring some consideration:

- The results of experiments and simulations suggest that dissolution and precipitation of silicate minerals will occur in the reservoir sandstones (e.g., steady replacement of feldspars by various clays), but that it will have no significant consequences for reservoir porosity and permeability. However, considerable amounts of calcite, which occurs naturally in the sandstones as rock fragments and as cement, are predicted to dissolve and precipitate as a function of the water injection/extraction cycles (owing to their linked variations in fluid temperature and composition). Consequently, the distribution of calcite in the reservoir will become increasingly heterogeneous with time, leading to regions where calcite accumulates and regions where it becomes depleted. Regions of calcite accumulation will become less permeable and may become isolated from the induced injection/extraction flow regime. Regions of calcite depletion will become more permeable and may channel flow and reduce the volume of reservoir rock that is swept by the injected hot water, thereby reducing heat storage efficiency. Regions of calcite depletion may also lose their mechanical integrity and undergo compaction.
- In addition to the above inorganic processes, degradation of naturally occurring organic matter within the reservoir and possibly microbial activity may impact the mineral reactions. Organic compounds may coat mineral surfaces and thus slow down mineral–water reactions or form complexes with ions in solution enhancing mineral solubilities. While this will likely have no adverse effects on the system, it may be difficult to quantify this process in our simulations and hence it may lead us to overestimate reaction products. On the other hand, microbes may enhance corrosion and if they form biofilms, they may lead to clogging, especially if injection temperatures are well below 90 °C. We assume that microbial activity will strongly diminish as the reservoir heats up towards 90 °C.
- Dissolution reactions and mechanical disintegration of mineral and organic particles during repeated water injection and production cycles may mobilise fines and clog pore throats, reducing permeability. This has been neither modelled nor investigated in our experiments but appears likely to occur owing to the observed friability of the sandstones. Its possible occurrence away from the immediate vicinity of the wells and its impact on the flow regime remain unknown.
- Regarding hydrological problems, rise of a buoyant thermal plume to the top of the reservoir is not expected at present, owing to the probable modest thicknesses of individual sandstone layers. However, it is conceivable that discrete, preferential flow paths will develop between the main and supporting wells within one or several sandstone layers, owing to their heterogeneous permeability distributions. Such short-circuits could reduce the volume of reservoir rock swept by the injected hot water and reduce storage capacity.
- The numerical simulations show that the thermal plume and the reaction zone around the main well remains within a 50 m radius from the well. However, the zone of

influence of the entire heat storage reservoir, if defined by the distance to which non-reactive solutes injected or released from the rock can travel in the USM groundwater system, is much larger. There is therefore a possibility that unwanted chemical compounds are transported over large distances.

- Significant carbonate scaling is expected in the surface installations during the heat loading cycle. This could impede flow and heat exchange in the surface installations. Its extent may potentially be mitigated by the natural occurrence of inhibiting ions in solution (Mg, SO₄, organic acids), as suggested by the results of the core and batch experiments.

Source	Effect	Impact
Silicate mineral dissolution/precipitation	Negligible	Negligible
Calcite dissolution/precipitation	Porosity/permeability reduction in sectors of reservoir	Reduction of reservoir performance Reduction of storage potential REDUCTION of the Forsthaus Plant CO ₂ /Air quality footprint mitigation
Degradation of organic matter	O.M. can coat borehole casing enhancing the potential of corrosion/clogging if T<90°C	Reduction of system performances potential REDUCTION of the Forsthaus Plant CO ₂ /Air quality footprint mitigation Possible microbiological contamination of the reservoir
Mobilization of clay particles	Porosity/permeability reduction in sectors of reservoir	Reduction of reservoir performance Reduction of storage potential REDUCTION of the Forsthaus Plant CO ₂ /Air quality footprint mitigation
Thermal buoyancy	Negligible	Negligible
Lateral thermal Contamination	The thermal plume is predicted to remain within a 50 m radius from the well	Negligible
Lateral chemical contamination	Unwanted non- reactive solutes might travel in the groundwater system, over large distances	Contaminants can migrate towards the surface and impact shallow groundwater
Carbonate scaling is expected in the surface installations during the heat loading cycle	Flow and heat exchange in the surface installations can be negatively impacted	Reduction of surface installation performances potential REDUCTION of the Forsthaus Plant CO ₂ /Air quality footprint mitigation

2.3.2.1. Fast-Track Risk assessment

According to the data available, limited to the water geochemistry components, and the results of the water-rock interactions simulations, a fast-track assessment of the risk linked to the different components is presented in Table 19.

Table 19. Fast-track risk assessment for the Bern case studies.

Bern Forsthaus						
Effect	Phase			Operations (predicted)		
	P	A	M	Probability	Consequences	Risk
Air quality						
Noise and vibration						
Formation water quality				H	L	M
Formation water temperature						
Surface clear water						
Soil occupation						
Wastes and dangerous substances						
Environment						
Nature						
Soil mechanics						
Seismicity						
CO2 intensity reduction						

2.4. Case study in Denmark

To assess the environmental effects connected to ATES in Denmark a literature study has been conducted. The existing Danish experience include test sites evaluating temperature increase of injected water from 20/25 °C to 30/35 °C; and another test site evaluating the potential in regards to biodegradation of chlorinated contamination.

2.4.1. ATES test site

2.4.1.1. Effects of temperature increase

Present legislation in Denmark allows for ATES to inject groundwater at temperatures up to an average temperature of 20 °C, and up to 25 °C as peak temperature. At a test site on Funen in Denmark a temperature increase from 20/25 to 30/35 °C has been conducted for an existing ATES (Naturstyrelsen, 2016) at Hjortebjerg Greenhouse to evaluate the effect of the temperature increase on the microorganisms in the groundwater body.

The temperature was increased to 30 °C for 112 days with a maximum up to 35 °C, and water samples were collected before, during and after the temperature increase. The maximum flowrate for the system is 50 m³/hour, but for the test, the flowrate was only up to 20-30 m³/hour.

The aquifer consisted of approximately 25 m of sand located 20-45 m below ground with clayey aquitards above and below the aquifer. The water chemistry showed slightly reduced anaerobic groundwater in the aquifer.

It was estimated that the thermal plume had a radius of 18 meters from the warm well, though this radius does not take into account the natural groundwater flow. The hydraulic flow radius was estimated to 25 m.

It was shown that:

- No apparent change in the geochemical composition in the aquifer was seen.
- A change in the subcultures of microorganisms was seen.
- No indication of increase of pathogens in groundwater was seen, but it was not possible to draw this conclusion for all relevant pathogens since not all were present at the beginning of the test.
- The radius of hydraulic flow is greater than the radius of thermal flow, which may result in further spreading of microorganisms outside the radius of the thermal impact.
- Systems with thermal equilibrium (i.e. alternating injection and production of heat in the same aquifer volume) poses less of a risk to the groundwater than systems used for only cooling where heat is injected and not recovered again.

2.4.1.2. Chlorinated solvents

At a site in Birkerød, Denmark, a test was conducted where the elevated temperature of water from an ATES cooling system was used to further biodegradation of a chlorinated contamination site.

The test shows that it is possible to use ATES for treatment of chlorinated solvents contamination (Climate-Kic, 2018) as the elevated temperature can stimulate biodegradation of chlorinated solvents. To further the process an electron donor was added to lower the redox as well as a specific dechlorinating culture.

2.4.2. HT-ATES

A very preliminary study of the possibility to establish a HT-ATES in chalk reservoirs in a depth of up to 1000 m, and well below fresh groundwater resources, has been performed for the Copenhagen area (EUDUP, 2018, GEUS, 2017).

There is only little available data from the deeper layers in the subsurface which leads to considerable uncertainty of the potential for HT-ATES. This causes an initial barrier to HT-ATES projects in the area. Despite the lack of data, a number of simulations were carried out to examine the potential of the chalk reservoir.

Some of the main conclusions were:

- The chalk is characterized by high porosity but very low matrix permeability, and the potential water production rates are difficult to assess.
- Reservoir simulations indicate that interaction with overlying fresh groundwater zones will be very limited (EUDUP, 2018)
- Cyclical heating and cooling can reduce the mechanical strength of the chalk reservoir rock
- Periodic heating may lead to geochemical reactions in the system (GEUS, 2017) introducing a need for water treatment, which again may have an environmental effect. The technical effect on a reservoir is expected to be very site-specific necessitating local investigations. Water treatment should also be designed according to site specific analyses.

3. Mine Thermal Energy Storage

3.1. General effects MTES

Currently, the German HEATSTORE sub-project is the first pilot site that develops and implements a mine thermal energy storage on the premises of the Fraunhofer IEG site in Bochum. Out of this reason, no comparing data sets exists so far with the respect to the general effects that a MTES system could pose on the environment. Therefore, a generic approach to the effects of UTES systems in Germany is briefly described below with the emphasis mainly on the permission process of such systems.

3.1.1. Drinking water protection

The most important aspect when approving a long-term heat storage facility is compliance with the laws and guidelines for drinking water protection. The provisions of the Water Resources Act (in German: "WHG") in conjunction with the water laws of the respective federal states apply. The WHG regulates all measures concerning the extraction or re-injection, diversion and lowering of groundwater. It also prohibits all measures that could lead to harmful changes in the physical, chemical or biological quality of the water. With regard to the above-mentioned aspects, the various storage concepts must be evaluated differently.

If a possible storage site is located in a drinking water protection zone, a water law permit is only possible in exceptional cases. If the site is located in the extended zone III, i.e. in the outer peripheral zone, an exceptional permit can be granted by the responsible water authority.

3.1.2. Construction and decommissioning

In addition to the above points, which mainly concern the operation of the heat storage, any possible adverse effects on the environment during the construction phase or after a shutdown of the storage site must also be taken into account.

After a possible closure of the storage facility, an orderly decommissioning is often required. This means that for all types of storage systems for which boreholes have been drilled, it must be ensured that the well is backfilled with sealing material. Also, only harmless materials may be introduced into the ground.

3.1.3. Approval process

At present, there is no generally valid approval procedure. Due to the individual conditions of a long-term heat storage facility, it is advisable to contact the responsible water authorities at an early stage and to discuss the necessary application and approval procedure together. If the heat storage facility is located deeper than 100 m below ground level, the approval is the responsibility of the mining authorities of the individual federal states. These then involve the subordinate water authorities in the procedure.

3.1. Case study in Germany

Bochum is located in the center of the Ruhr Coal District and the municipality belongs to the state North-Rhine Westphalia in the western part of Germany. It is characterized by a high-density population and industrial infrastructures. Fraunhofer IEG in Bochum, where the HEATSTORE site is located, hosts a real-world lab which serves as a test site for the exploration and large-scale exploitation of hydrothermal potentials in the Ruhr area. The test

site (Figure 52) represents a 10.000 m² drill site with existing research, observation and production wells.

The shallow subsoil on the Fraunhofer IEG test site is characterized by Upper Carboniferous stratigraphic sequences. It is overlaid by a few meters of glacial loess and weathered Carboniferous rocks. There are only few tectonic faults in the surrounding area. Due to old mining activities some minor local faults are documented. The subsurface is defined as fractured rock aquifer with a low permeability. The sandstone porosity of the matrix is below 5 %. The groundwater flow takes place mainly within the fracture networks. The aquifer consisting of the shallow subsoil is unconfined. Due to impermeable layers of claystones, confined aquifers are observed at greater depths.

The small colliery was accessed within the HEATSTORE project via three vertical 11" boreholes with the Institute's own drilling rig. The mine water piezometric level is steady at 22.9 m below ground level, which documents that all sections of the mine workings are flooded. The cavity created by mining could be confirmed by camera surveys at a depth of 61.5 - 64.3 m below ground level and is thus consistent with the information from the mine images of the 1950s. Initial pumping tests indicated a very high productivity compared to the groundwater observation wells.

The underground lab of ongoing and future projects of the Fraunhofer IEG requires a monitoring system, which is jointly operated by several projects.

The monitoring includes three different main components: hydro-chemical monitoring, monitoring of the hydraulic heads and temperatures and seismic monitoring.

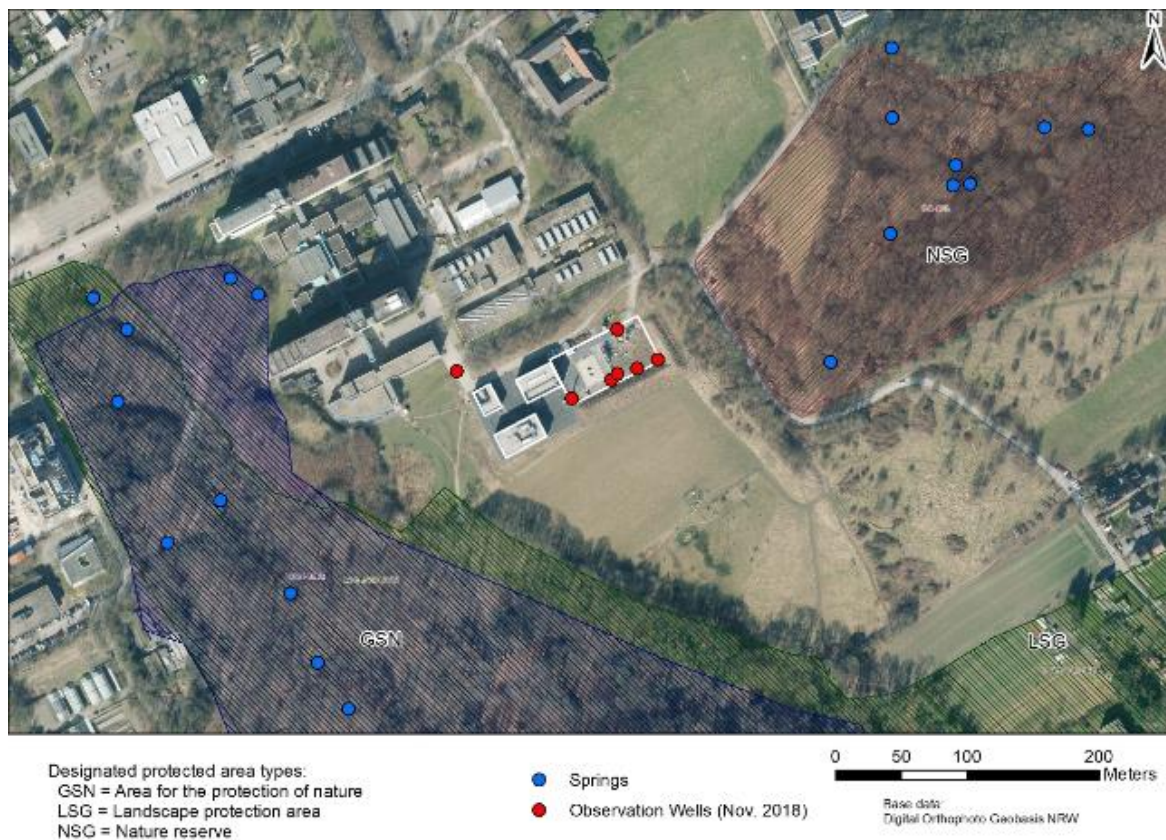


Figure 52. Fraunhofer IEG test site and surrounding area including observation wells and springs.

3.1.1. Groundwater monitoring

Groundwater monitoring includes hydro-chemical monitoring and monitoring of the hydraulic heads and temperatures.

Seven groundwater observation wells (R1 is also used as research well) are operative at Fraunhofer IEG Campus (Figure 53) where the MTES test site is also located. Further observation wells are planned in the near future. The groundwater monitoring wells (Table 21) are located at different depths within fractured sandstone formations. This kind of depth-controlled sampling allows early detection of changes in hydro-chemical parameters, e.g. caused by rising deep waters.



Figure 53. Groundwater monitoring wells at the Fraunhofer IEG site in Bochum

The monitoring includes continuous logging of temperature and pressure (recording has started in four boreholes (O1 Geostar, O2, O3, O4) in 30 minutes intervals since 12/2019. Since the beginning of April 2020, two groundwater observation wells (O3, O4) at the test site and two springs Lottental (LOT) and Königsbusch (KÖBU) in the immediate vicinity have been sampled with two week intervals. Sampling was carried out at irregular intervals before April 2020. During sampling, various parameters are determined in-situ. All data can be provided upon request.

Table 20. Groundwater monitoring wells at the Fraunhofer IEG site in Bochum.

	O1	O2	O3	O4	O5	O1_Geostar	R1
coordinates	51.446534, 7.2745513	51.446480, 7.274425	51.446620 7.274915	51.446816 7.274482	51.446553 7.274697	51.446507 7.272725	51.446338 7.27399
Access restriction	no	No	No	No	No	No	
Power supply	Yes	Yes	Yes	Yes	Yes	Yes	
casing							
Pipe material	PVC	PVC	PVC	PVC	PVC	PVC	
Pipe class	DN 100	DN 100	DN 100	DN 100	DN 100	DN 100	
Wall thickness	5 mm	5 mm	5 mm	7 mm			
Depth	100 m	145 m	130 m	185 m	29 m	120 m	500 m
Flow rate	X	X	X	5 l/min	X		
temperature	Approx. 11°-13°C for obs. wells; approx. 19°C for deep well R1 (bottom)						
Water level	16 m	21 m	12 m	20 m	X	17 m	20 m

Temperature, pH, oxygen content, electrical conductivity and redox potential are measured in-situ during sampling and again in the laboratory with multimeter probes from WTW (Table 21). The hydrogen carbonate and carbon dioxide concentration are determined by titration immediately after sampling in the laboratory. The samples are filtered (0.45 µm) immediately upon arrival at the laboratory and preserved for later analysis of cations and anions. For a fast and effective evaluation of the cations and anions methods were developed.

Parameter	Devices
Hydraulic head	T/P-Logger
Temperature	T/P-Logger
pH	WTW SenTix 41 electrodes
Redox	WTW SenTix ORP
Electrical conductivity	WTW TetraCon 325
Oxygen	WTW CellOx 325
Acid capacity	Titration
Base capacity	Titration
Major anions	Metrohm-ECO IC (Ion Chromatography)
Major cations	Perkin Elmer- Optima 8300 (ICP)
Trace elements (cations)	Perkin Elmer- Optima 8300 (ICP)

Table 21 Measured parameters in wells.

The anions are analyzed with the ECO IC ion chromatograph from Metrohm and include chloride, sulfate, nitrate, fluoride and bromide. The cations are determined with the ICP-OES (Optima 8300) from Perkin Elmer. The content of the major elements Na, Ca, Mg and K as

well as trace elements such as Si, Fe, Mn are determined. The groundwater observation well O1 has been used as reference analysis.

Table 22 provides an overview of all cations and anions measured by the ICP-OES and the IC.

Table 22. List of measured cations and anions by ICP-OES and IC.

Measured	Elements
Cations	Na, K, Mg, Ca, Si, Fe, Mn, Ba, Al, B, Be, Bi, Cd, Co, Cr, Cu, Ga, Li, Ni, Pb, Se, Sr, Te, Tl, Zn
Anions	Cl, SO ₄ , NO ₃ , F, Br

Considering the huge amount of data collected related to the hydro-chemical monitoring activity and with regard to the objectives of this report, results have to be correlated primarily with respect to possible variation registered before, during and after the injection test that was performed in December 2020 with an overall volume of 1.234 m³ and a temperature difference of 35°C. The injected water was circulated directly from the same drift of the colliery. As it can be seen in Figure 54. Temperature and hydraulic head of groundwater monitoring well O2 before, during and after heat injection test, the groundwater temperature resides steady at 10,63 °C. The changes in hydraulic head are correlated with the precipitation rate of the area and time of the year.

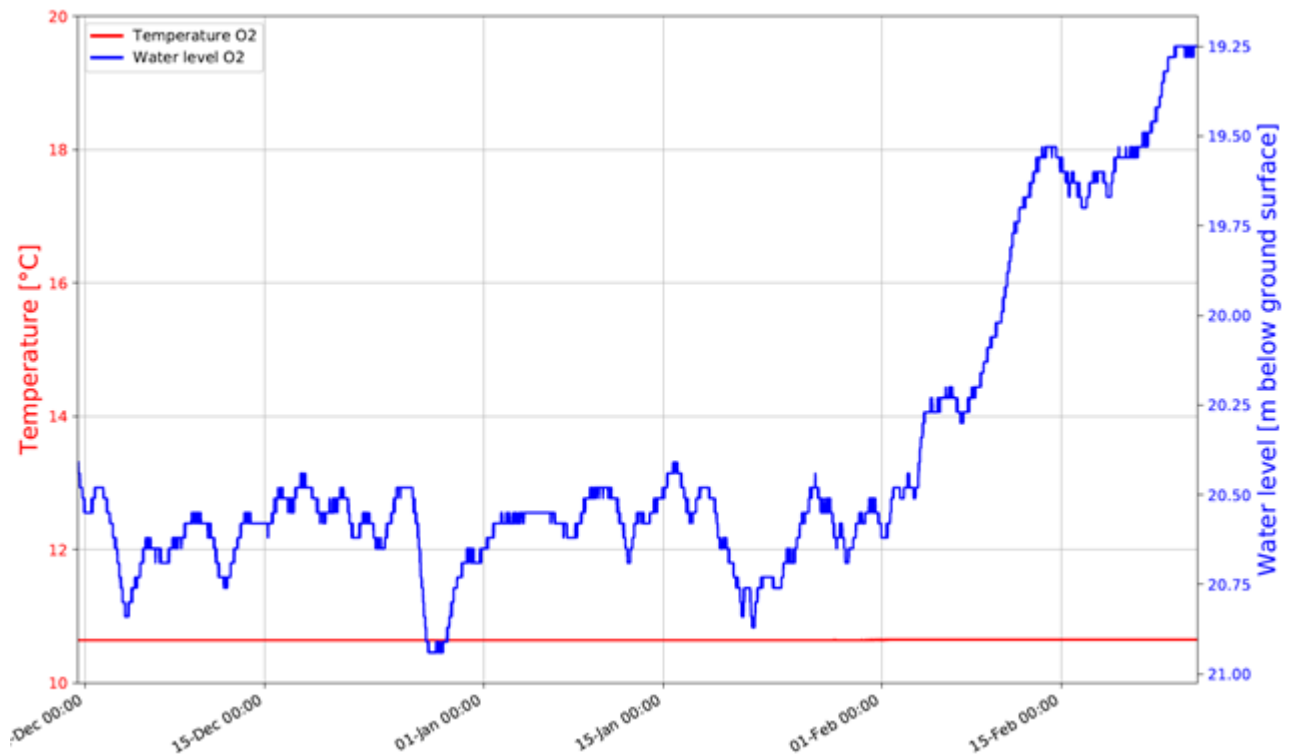


Figure 54. Temperature and hydraulic head of groundwater monitoring well O2 before, during and after heat injection test

Although the observation wells O3 and O4 are in the same sandstone horizon, the groundwater samples differ significantly in some values. The water compositions of the monitored groundwater observation well O3 remains stable during the sampling period. Observation well O4 represents the deepest monitoring well (filter screen between approx.

165 - 185 m) and is characterized by higher Na content and a lower Ca and Mg contents indicating a deep groundwater reservoir. Minor elements and trace elements remain constant in their values. Cl⁻ does not show a stable value and needs further investigation. K content is similar in both wells.

Measurements of groundwater samples from the O3 and O4 observation wells show that there are no major changes in the respective concentrations of cation and anion values between April 2020 and March 2021. The pH remained slightly basic and respectively constant in each well (respectively O3=7 and O4= 8.1-8.6) as well as oxygen content, redox potential and electrical conductivity.

The surface waters at the locations Königsbusch (KÖBU) and Lottental (LOT) show partly strong fluctuations in their cation and anion contents. The values from the site Königsbusch do not show very large fluctuations. The location is not easily accessible, therefore less anthropogenic influences are to be assumed here. The measuring station Lottental, on the other hand, is located on a highly frequented pedestrian path. Here, strong fluctuations in Na, Cl and SO₄ can be observed. Along with the aforementioned influences on the surface water, the parameters pH (respectively at KÖBU=7.4-8.2 and LOT=7-8), oxygen content, redox potential and electrical conductivity also vary. The CO₂ concentrations are below 0.2 mmol/L at all sites.

The variation shown by the surface water (spring water) Lottental is possibly due to surface runoff by rain events. The surface water (spring water) Königsbusch shows relatively stable values and much higher value of SO₄ with respect to the other waters. An explanation for this can be found in the different drainage of the two valleys: The Lottental-valley is equipped with drainage basins to collect surface runoff, whereas the Königsbusch-valley is a protected area ("Naturschutzgebiet") with minor human influences.

Moreover, after the wells MP1, MO1 and MI1 were successfully drilled into the small colliery a full water analysis was performed for each well by an external laboratory (WESSLING). The waters are Fe-rich with pH-values of 6.5, lower than the unaffected groundwater. After each pump test the water was clear and free of turbidity. The total mineralization is about 500 mg/l (calculated from conductivities). No PCB, PAH or hydrocarbons were found.

It can be concluded that the deeper groundwater (above 90 m and deeper) shows a more consistent groundwater composition, whereas the spring monitoring (Lottental and Königsbusch Valley) are influenced by surface runoff. This must be considered for the analysis of the groundwater monitoring data. A variation in the composition of surface waters can be of natural origin.

Seasonal changes are expected for both groundwater monitoring sites and surface waters. The groundwater level drops and rises due to seasonal effects. In summer, there is a possibility that the surface springs will dry up. The amount of fill is lowest here. In winter, the fill will increase again.

Despite the abovementioned differences among the water compositions of the four monitored wells and the fluctuations over time, no correlation is observed with respect to the injection test. Also pH values remain unaffected and can be considered as a further indicator of no direct connection between the two water bodies. Potential mixing processes could be better investigated with isotopic analyses which are planned in the next future.

3.1.1.1. Hydro-Geochemical modelling

In order to perform hydro-geochemical modeling the following organoleptic as well as physicochemical parameters were determined on site: electrical conductivity: 765 µS/cm; pH: 6.5; temperature at the outlet: 11.5 °C; redox potential: -56 mV; oxygen content: 0.58

mg/l (probably a contamination due to sampling). The odor of iron was detected as well as traces of hydrogen sulfide with accounts for reducing conditions. The analysis data suggest the presence of a shallow, iron-rich water-reservoir, with a genesis similar to groundwater (Table 23).

Table 23. Water sample analysis of well MP1 of the deepest part of the colliery shortly after drilling activities;*Analysis from 30.11.2020.

MP1 Sampling 08.09.2020	
Temp (°C)	11,5
EC (µS/cm at 25°C)	765
Redox (mV)	-56
pH	6,5
Ions (mg/l)	
Cl	31
S	29
Alkalinity	430,17
F	0,22
Fe (total)	6,4
Mn (total)	1
Ca	84
K	8,4
Mg	33
Na	21
Si*	9,35
Ba*	0,187
Al*	0
B*	0,807
Li*	0,082
Sr*	0,418
Br*	0,278

The first mine water analyses collected from the colliery (Table 23) was modeled to evaluate a future geothermal heat storage operation using the hydrogeochemical modeling software PHREEQC 3. Due to the freshwater to brackish water characteristics, it was modeled with the PHREEQC standard database "PHREEQC.dat". The criterion for accurate modeling is a complete water analysis, which consists of the temperature, redox, acidity as pH, the dissolved main constituents and secondary constituents (anions and cations).

The calculation of a saturation index (SI) indicates whether a mineral phase in the solution is supersaturated at the appropriate pressure and temperature and tends to precipitate, or whether the solubility is undersaturated and the mineral remains in solution and is dissolved

from the rocks respectively. Mineral phases are in equilibrium with the thermodynamic conditions at SI 0.0. Positive values, in particular values above 1 indicate a supersaturation and possibly a growth of crystals.

In general, the mineral solubilities increase with rising temperature (e.g. $\text{Fe}(\text{OH})_3$), which is beneficial for the operation of the plant (Figure 55). However, the slight decrease in the solubility of carbonates, especially calcite and dolomite, is noteworthy. Siderite is not expected to form crystals even at a slight supersaturation, as the supersaturation is not considered to be high. The mineral phase $\text{Fe}(\text{OH})_3$ known as amorphous ferrihydrite typically forms rapidly in the presence of oxygen and then precipitates as iron ochre (“iron clogging”). Since the iron content of 6.4 mg/l is relatively high for mine waters based on experience, the dissolved iron content is estimated to be a potential hazard for the designed plant. Assuming sufficient oxygen and sufficient mixing (due to pumping activities), 12.25 mg/l of iron ochre could precipitate in the form of reddish particles and coating formation, if sufficient countermeasures during the storage operation are not foreseen.

The same is valid for the relatively high manganese content of 1 mg/l. The manganese is also forming oxides in contact with oxygen. The recommended course of action is to avoid the introduction of oxygen into the system, which can be technically implemented by introducing an inert gas (e.g. argon or nitrogen) into the system during pressure changes.

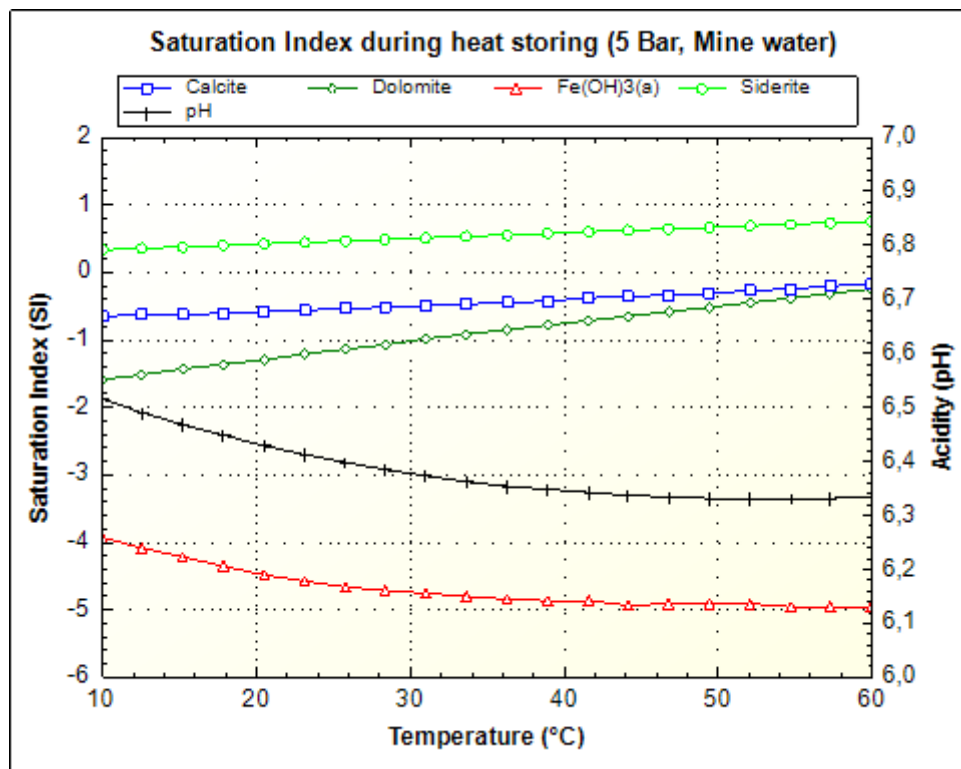


Figure 55. Preliminary results of PHREEQC modelling of the first in-situ water sample of the well MP1 (sampling: 08.09.2020).

3.1.2. Seismic monitoring

In order to monitor the seismic response of various activities at the well site at the Bochum campus of the Fraunhofer IEG, a small scale seismic network has been installed (Figure 56) as a cooperation of the University of Applied Sciences Bochum and the Fraunhofer IEG.

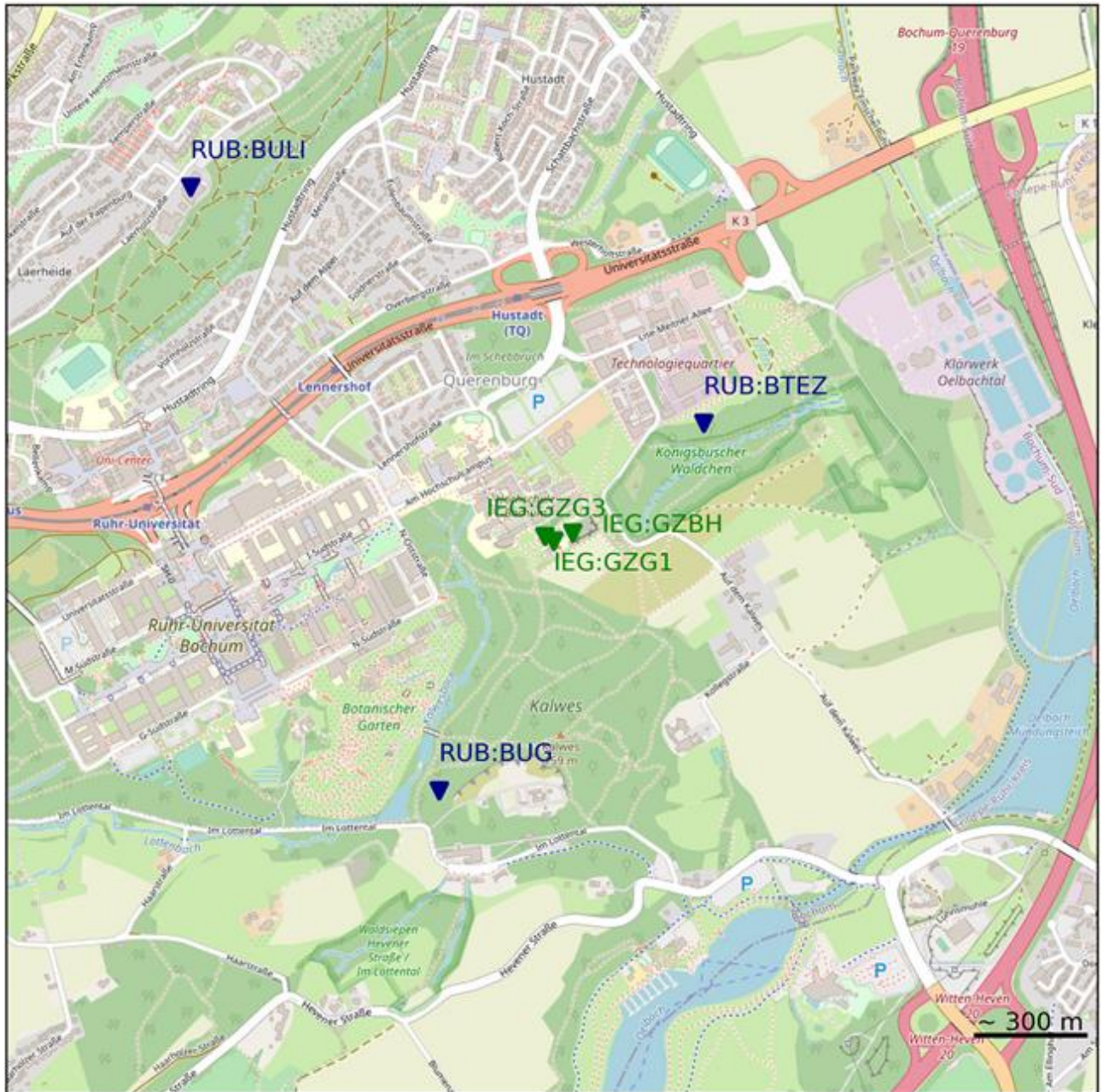


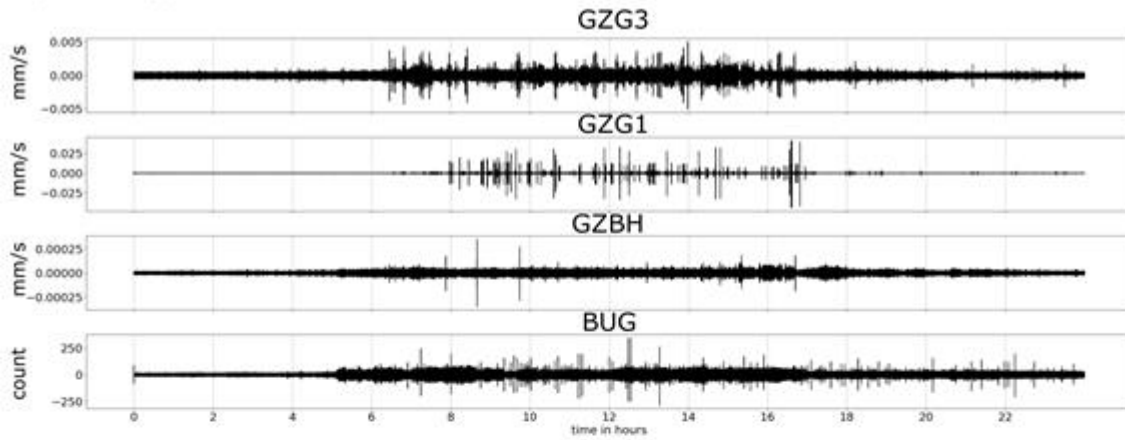
Figure 56. Map of the South of Bochum showing seismic stations of the regional seismic network in the area operated by the Ruhr-University Bochum (blue markers) and seismic stations operated by the Fraunhofer IEG (green markers).

This small-scale network complements the larger regional seismic network operated by the Ruhr-University Bochum (<http://www.gmg.ruhr-uni-bochum.de/geophysik/seisobs/index.html.de>). The small-scale network consists of station GZG3 which is equipped with a three-component broadband seismometer (Trillium Compact PH 20s) installed on a granite pillar in one of the office buildings of the IEG. GZG3 is recording continuously since 2017. Furthermore, station GZG1 is situated in the geotechnical laboratory of the IEG and equipped with the same sensor as GZG3. GZG1 is operational since September 2020. Since GZG3 and GZG1 are strongly influenced by the

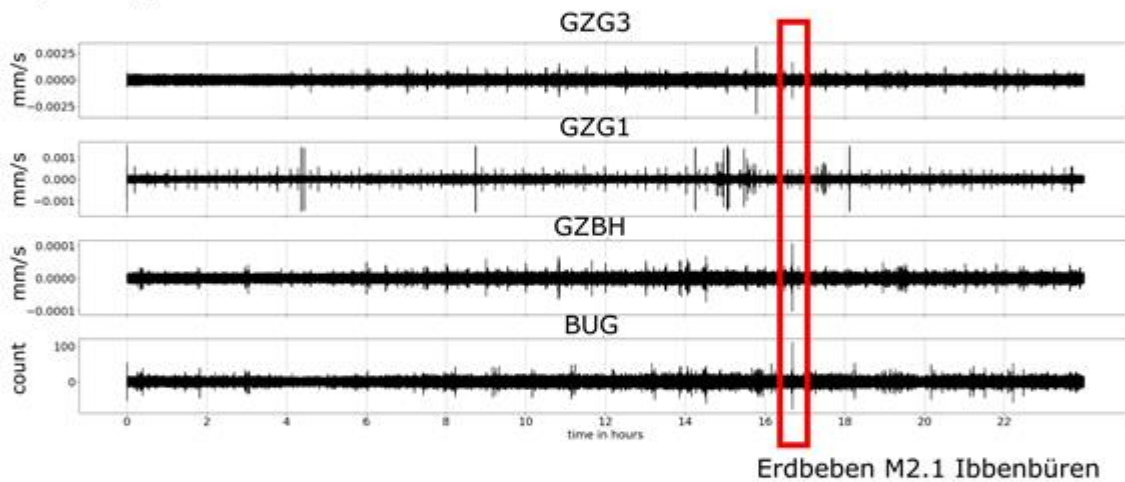
daily activities at the institute, a borehole seismometer has been installed in a shallow water well (station GZBH, so-called sensor of type 'Peter Mallin') and is continuously recording since September 2020. The borehole seismometer exhibits significantly lower amplitudes than the surface stations. All three stations are equipped with GPS time synchronization and data is automatically sent to local servers. This set-up allows to detect any potentially occurring micro-seismicity beneath the IEG campus.

During the first preliminary heat injection test in December 2020, the continuous seismic data has been monitored to identify any seismic response. Seismograms were analysed in multiple frequency bands. Figures display the frequency band from 4.9 Hz to 9Hz. This frequency band exhibits the highest amplitudes from anthropogenic noise sources and also displays signals from seismic events that are close to the stations. Among others, the maximum amplitudes, the power spectral density over time and the horizontal-to-vertical spectral ratio over time have been observed. The latter two did not show any changes correlated to the injection experiment. The amplitudes of the east component during three full days are shown in Figure 57. The east component has the highest amplitudes from all three recorded components and is associated with shear energy. On the 03.12.2020 (Figure 2a) it is clearly visible when daily work at the campus started and ended. Increased amplitudes around midday are due to doors opening and closing, cars going by, people walking by and various machinery. The borehole station GZBH and the RUB station BUG are noticeably quieter but still show increased amplitudes during the day. In comparison, on Sunday 13.12.2020 the amplitudes are overall decreased. However, around 17:18 there was a seismic event in Ibbenbüren with a magnitude of 2.1 (as reported by the RUB seismological observatory). This event is clearly visible as a large peak on 3 of the 4 stations and has larger amplitudes than the cultural noise on the 03.12.2020 for stations GZBH and BUG. On Monday, 07.12.2020, there was a seismic event in Hamm with a magnitude of 1.2 (as reported by RUB seismological observatory). This event is much closer than the Ibbenbüren one but is also significantly weaker. Due to the closer vicinity, it is clearly visible on all stations and has amplitudes significantly larger than the cultural noise of that workday. Therefore, we assume that a small seismic event very close to the seismic stations would be clearly visible in the data. A more sophisticated approach to detect events using triggering algorithms has been attempted but is not possible due to the high cultural noise. We do not see any signals related to the injection experiment and therefore conclude that the experiment did not cause any seismic response or it was too small to be detected.

a) Thursday, 03.12.2020



b) Sunday, 13.12.2020



c) Monday, 07.12.2020

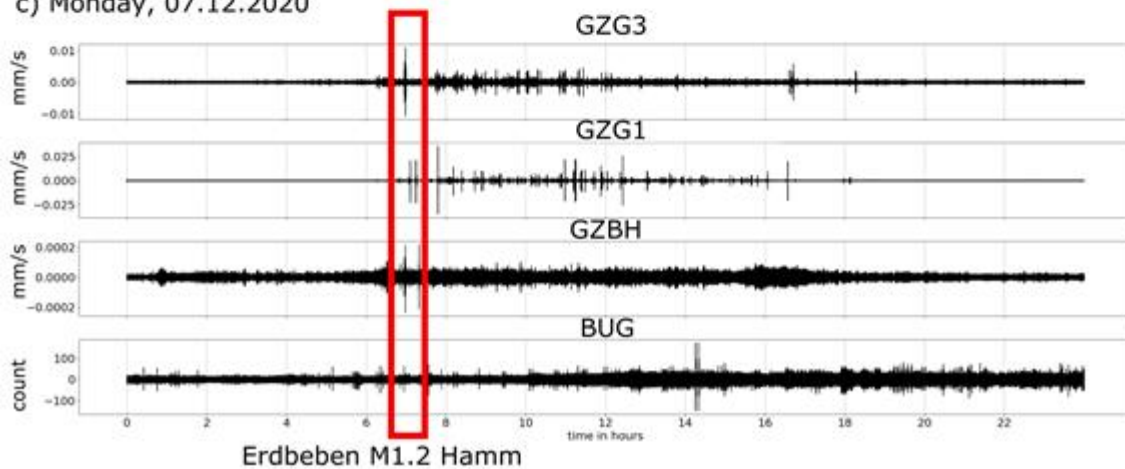


Figure 57. East component of seismic traces for the three station at the IEG campus and the BUG station of the regional seismic network. Two seismic events are marked with magnitudes reported by the RUB seismological observatory.

3.1.3. Geomechanical monitoring

A geomechanical heave and subsidence prediction model was developed in conjunction with the help of the RWTH Aachen. Due to unforeseen circumstances the results of this work have not been published yet, so that no direct reference can be utilized here. However, the prediction model did not reveal any hazardous ground deformation within the foreseen temperature range of the pilot operation of the MTES.

3.1.3.1. Mineberry

The geomechanical monitoring of plugged and abandoned mine shafts requires methods which monitor the stability of infilled material in the shaft. For this application several direct and indirect methods are available. A direct method would place a sensor directly on top of the infilled material of the shaft (Figure 58). For the shaft of the former IEG colliery an indirect method was chosen, because the top of the former shaft cannot be exactly located. Therefore a small concrete column will be installed at the surface above the former shaft. The concrete column is equipped with two one-axis inclinometers in an angle of 90°. The inclinometers now enable to monitor any changes in x,y,z direction due to a potential collapse of the shaft filling. The monitoring values are transmitted via the Sigfox network into a secured and access protected web-GUI for further analysis.



Figure 58. Monitoring-System "Mineberry" - TH Georg Agricola (thga.de).

3.1.3.2. Photogrammetry

Photogrammetry is a recognized method for determining the terrain surface. Here, photographs are taken with special measuring cameras over the area to be surveyed. The data is then converted into a 3D point cloud, from which digital elevation models (triangulation) can be derived. Aircraft or, in recent years, increasingly Unmanned Aerial Vehicles are used as sensor carriers. The latter offer the advantage that the images can be taken from a very low altitude at a high sampling rate. The low recording distance also increases the accuracy of the terrain survey (Spreckels et al. 2016). The IEG area was first surveyed in March 2021 (Figure 59) with a 1 cm sampling rate (840 exposures). Once data from the second campaign are available in June 2021, ground subsidence can be detected by comparing elevation models. A third and fourth measuring campaign is scheduled for autumn and winter of 2021.

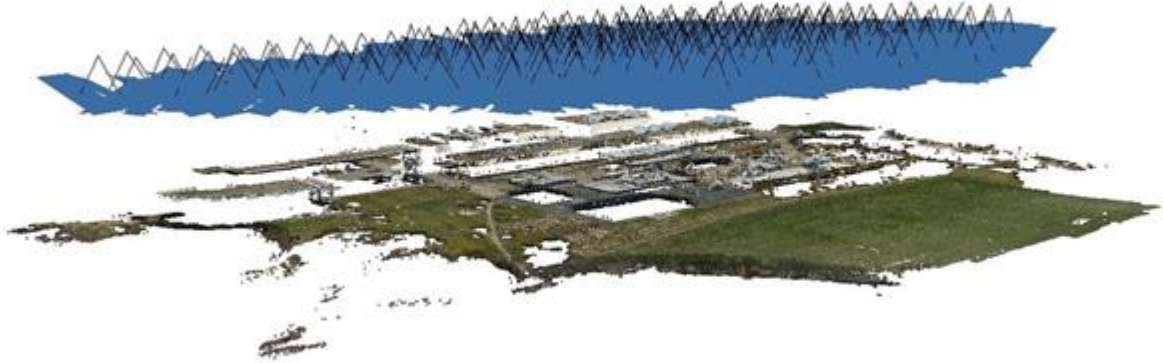


Figure 59. IEG elevation model in March 2021.

3.1.4. Carbon intensity

In order to provide a quantitative analysis of CO₂ reduction factors, the data of the first heat injection test from December 2020 was utilized. Specific CO₂ emission factors have been kindly provided by the municipal energy supplier of Bochum (Table 24), which were updated specifically for the region in November 2020.

Table 24. CO₂ emission factors for Bochum, Germany.

CO ₂ emission factor	g/kWh
District heating	185
Heating oil	315
Electricity	422

The measured amount of pump energy that was utilized for the hydraulic circulation of the mine water during the injection test for nine days was 429,3 kWh. The injected power of 50,22 MWh was calculated with the following formula (Daniilidis et al. 2021):

$$P = Q\rho_f c_f \Delta T$$

To extract the injected heat from the colliery the same amount of pump energy is assumed. Due to the lack of existing data for a MTES, three storage efficiencies were proposed (30, 50 and 70 %) to calculate CO₂ reduction factors. The results are summarized in Table 25. Here it should be highlighted that the district heating provides better CO₂ emission factors, if the storage efficiency is assumed to be only 30 %.

Table 25. MTES CO₂ reduction potential.

	District heating (t/kWh)	CO ₂ saving (%)	heating oil (t/kWh)	CO ₂ saving (%)	natural gas (t/kWh)	CO ₂ saving (%)
η (30%)	0,279	-23,08	0,475	30,98	0,38	3,95
η (50%)	0,465	28,21	0,791	118,30	0,63	73,25
η (70%)	0,650	79,49	1,107	205,62	0,88	142,56

3.1.5. Microbiological monitoring

After the completion of the three MTES wells (MP1, MO1 and MI1) into the abandoned IEG colliery, a full mine water analysis was conducted for each well by the WESSLING laboratory. This also included a full microbiological investigation of the mine water samples (Table 26).

It can be stated that only for the mine water sample from the shallowest MI1 well, which was taken from a depth of 26,67 m bgl, a certain colony count is observed at temperatures of 20°C and 36°C. The deeper wells (MO1 and MP1) reveal no specific microbiological activity.

Table 26: Microbiological investigation of mine water samples

Parameter	Unit	MO1	MP1	MI1
Coliform germs	KBE/100 ml	5	10	>80
Escherichia coli	KBE/100 ml	0	0	0
Enterococci	KBE/100 ml	0	0	0
Colony count at 20°C	KBE/ml	65	62	>1.000
Colony count at 36°C	KBE/ml	54	37	>1.000
Pseudomonas aeruginosa	KBE/100 ml	0	0	0
Clostridium perfringens	KBE/100 ml	1	0	4

This is in accordance with the fact that microbiological activities drastically decrease at depth below 20 m, which is resembled by a decreasing abundance and diversity, due to anaerobic conditions. Anaerobic aquifers are generally free of fauna.

3.1.6. Fast-track risk assessment

Based on the drilling operations performed during June and September 2020 and the first heat injection test in December 2020, a MTES risk assessment was developed in Table 27.

Table 27. MTES risk assessment.

Bochum												
Effect \ Phase	Drilling						Operations (predicted)					
	P	A	M	Probability	Consequences	Risk	P	A	M	Probability	Consequences	Risk
Air quality				L	L	L				L	L	L
Noise and vibration				H	L	M				L	L	L
Formation water quality				L	H	M				H	H	M
Surface clear water				L	H	M				L	H	M
Soil occupation				L	L	L				H	L	L
Wastes and dangerous substances				L	L	L				M	L	L
Soil mechanics				L	L	L				L	L	L
Seismicity				L	L	L				L	M	L
CO2 intensity reduction										H	M	H

4. Borehole Thermal Energy Storage

4.1. General effects BTES

In the application of BTES systems a volume of soil/rock is heated during charging and cooled during discharging by circulating a fluid in plastic u-tubes installed in a large number of closely spaced so-called closed loop boreholes or Borehole Heat Exchangers (BHE) and completed with a sealing grout, (Figure 60). The distance between the boreholes is typically in the range of 2-5 m and BTES is typically limited to boreholes of approx. 20-200 m depth. The thermal losses depend on the thermal and hydraulic properties of the subsurface (heat losses by conduction and density driven flow), the shape of the storage volume (defined by the lay-out of the boreholes) regional groundwater flow (heat losses by advection) and heat losses to the surface.

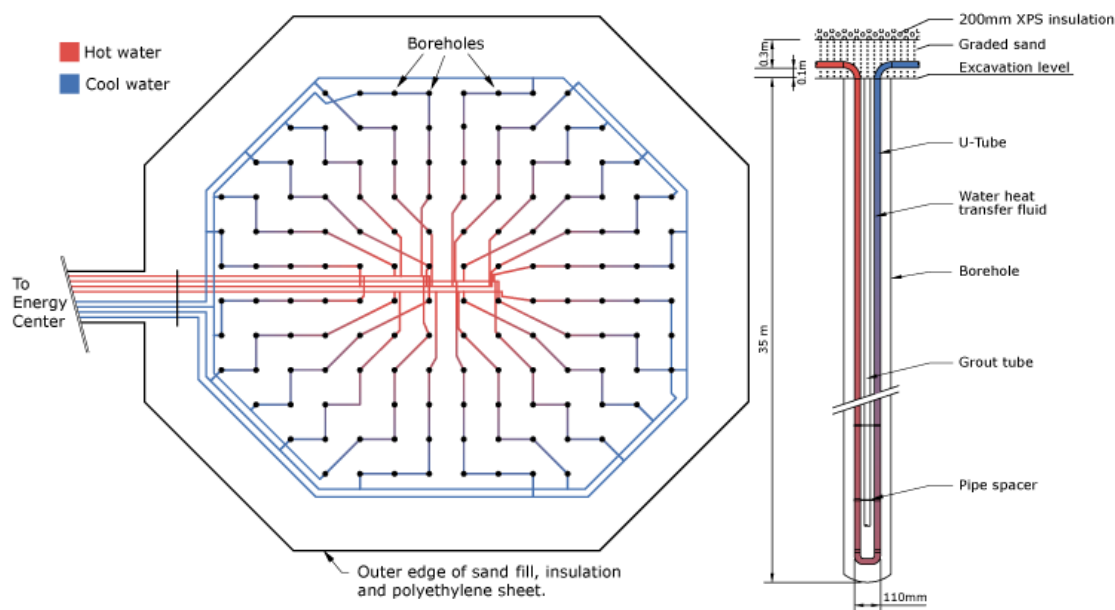


Figure 60. Layout of a borehole thermal energy storage and cross-section of a single borehole and u-tube (from Sibbit et al. 2015).

The most important potential environmental effects of Borehole Thermal Energy storage are temperature effects in the subsurface and seepage along boreholes as well as leakage from the u-tubes posing a risk for introducing contaminants in the groundwater.

4.1.1. Thermal effect

Operation of a BTES system both for heating and/or cooling and for heat storage will cause a temperature effect in the vicinity of the system. Heat extraction will cause cooling of the surrounding soil/rock and ground source cooling systems as well as heat storage will cause heating of the surrounding soil/rock.

4.1.1.1. Extracting heat (BHE)

Modelling of cooling around BHE's constructed solely for heat production indicates that the temperature effect from the borehole decreases quickly with distance. The study shows that

the expected temperature decrease 1 m from the BHE (GeoEnergi, 2011) was 3 °C and 1 °C 5 m from the BHE. Referring to a literature review, the study concludes that while an effect on the biological activity is likely at these temperature changes, the effect already a short distance from the borehole is limited. The same study examines the geochemical processes in soil affected by a temperature decrease. With a focus on calcite solubility, the study finds that the effect is also limited.

4.1.1.2. Storing heat

Another study examining heat flow and efficiency for BTES in typical Danish soil types, where the surrounding formation is heated has been carried out (GeoEnergi, 2011). The soil types include clay, sand and gravel, as well as chalk and granite. The study finds that the heat plume from the storage depends on the thermal diffusivity of the storage medium. Modelling of the temperature changes in the BTES systems with high temperature storage followed by temperature discharge shows that the surrounding area is only slightly affected and only within a limited distance from the BTES if there is no groundwater flow. If the BTES is in contact with a groundwater aquifer a heat plume will develop in the direction of the flow (Poulsen, 2019).

Monitoring data from an active BTES test site at Brædstrup, Denmark shows a temperature increase of approx. 5 °C when 10 meters from the storage (Sørensen, 2018).

4.1.2. Seepage along insufficiently sealed BTES boreholes

In most countries the environmental regulation prohibits surface water intrusion through a borehole and interconnection of aquifers caused by drilling operations. The regulation differs and vary between countries, regions and provinces, but very often sealing the boreholes with grout is mandatory in order to protect groundwater resources.

Seepage along insufficiently sealed boreholes can be a pathway for surface contamination and may cause mixing of groundwater from different aquifers with different geochemical properties (GeoEnergi, 2011). Changes in inorganic geochemistry will e.g. be seen in case of oxygen reaching anaerobic groundwater aquifers causing precipitation and changes in the chemical equilibrium in the groundwater.

4.1.3. Leakage of brine from BTES boreholes to groundwater

For BHE's for heating and cooling, ethanol, ethylene and propylene glycol mixed with water are commonly used as heat carrier fluids and sometimes corrosion inhibitors and other additives are also used in the BHE brines. For BTES systems that work well above the freezing point and in BTES systems used for storage of heat only, typically pure water is used.

If a leak occurs from a BHE, brine and additives will be released to the surrounding soil and potentially the groundwater. The risk to the surrounding environment depends on the type and amount of brine and additives in the leak as well as transport and degradation in the soil. Biodegradation will be most effective in the unsaturated zone where oxygen is present. If pure water is used in a BTES system, there will be no environmental effect of the water leak itself.

It is expected that biodegradation of e.g. defrosting additives in BHE brine will occur a short distance from the leak. Specific types of anticorrosion additives may be used in some brines but should be avoided. A study in Denmark did not find any analyses of groundwater samples for anticorrosives and since there can be several other sources for these in groundwater the presence would not necessarily indicate leakage from a BHE system and

the study draws no conclusion for the degradation in soil of these substances. Furthermore, the heat pump industry in Denmark claims to be looking to avoid the use of anticorrosives.

The risk of pollution also depends on where the leak occurs. If a leak occurs above the groundwater table, the effect of the leak mainly depends on the sedimentology of the layers and the thickness of the unsaturated zone. If the leak occurs in a groundwater aquifer, the brine will spread with the groundwater flow.

The risk associated with a nearby drinking water supply in case of a BHE leak depends on the factors listed in Table 28.

Table 28. Important factors for the risk for drinking water associated with a leak.

Leak	Drinking water
Amount of brine	Thickness of unsaturated zone
Dissolution in water	Thickness of reduced clays above the aquifer
Volatility	Infiltration
Sorption	Flowrates
Degradability	Horizontal distance to drinking water wells
Toxicity properties	Extraction volume

In general, with most brines and additives used in Denmark, the risk to drinking water boreholes more than 50 m from a small leak is considered minimal. This distance depends very much on the amount of water extracted and the flowrates in the aquifers where extraction occurs etc. as well as measures taken after the leak to minimize the amount of pollutant in the soil. To account for the large variability of the geology and the different requirements of the drinking water supply in Denmark, it is suggested to establish a restriction zone of 300 meters where BHE/BTES cannot be established around active wells used for drinking water supply (Miljøministeriet, 2008).

In an existing BTES in Denmark, water is used in the borehole system (Schmidt, 2019). The temperature is kept above freezing so no defrosting additives are added, and a potential leak is therefore considered not to constitute an environmental risk.

4.2. Case study in France

In France, BTES implementation falls under the regulation “Arrêté du 25 juin 2015 relatif aux prescriptions générales applicables aux activités géothermiques de minime importance”.

The BTESmart project contains glycolated water (30% MEG), because circulating fluid temperature can go below 0°C. Annual monitoring of the circulating loop is required with a follow-up on the following parameters: pressure, heat pump working hours, input and outlet temperatures. Proper sealing of the circulating fluid network should be ensured, and action plan implemented in case of leak. To avoid the risk of leak, “Norme NF X 10_970” define the protocol of tests to be performed when the borehole drilling and the circulating loop are completed.

The boreholes are connected to the manifold in parallel, hence, in case of a leaking borehole, this specific borehole can be disconnected while the other are kept in production.

The thermal heating of the surroundings is not compulsory and is currently not performed. The drilling of monitoring borehole is contemplated to assess the heating of the surroundings of the boreholes.

4.3. Case study in Denmark

In Denmark there is one existing BTES, which is up and running. The storage system is connected to a district heating network, where it is used for storing excess heat from a solar thermal plant.

An interview with the district heating company operating the existing BTES has been conducted to clarify present and potential negative environmental impacts from the system, as seen when it is in use.

In general, the district heating company consider the risks of a negative environmental impact to the surrounding areas small.

The environmental pressures connected to BTES in Denmark are identified through a literature study as well as an interview with the district heating company with an active BTES.

The main pressures consist of:

- Thermal heating of the surrounding soil layers
- Thermal heating of groundwater
- Risk of leaks

To identify in which way the pressures from the BTES affect the state of the environment a series of monitoring programs have been set up.

4.3.1. Brædstrup BTES

The borehole thermal energy storage placed in Brædstrup is built as a pilot storage and has a soil storage volume of 19.000 m³. The storage is constructed with 48 boreholes placed 3 m apart and drilled to a depth of 45 m, which is 5 m above expected groundwater level to prevent heating of the groundwater (Sørensen, 2018).

4.3.1.1. Thermal heating of the surroundings

Temperature monitoring of the BTES and the surrounding layers is facilitated by installing 100 temperature sensors in five dedicated boreholes in order to monitor the heat loss and to ensure that groundwater heating does not exceed 20 °C (PlanEnergi, 2019), as defined in the regulation. The temperature monitoring boreholes are drilled to a depth of 59 meters to monitor the underlying groundwater as well as the surrounding soil layers.

The five boreholes monitoring the vertical temperature distribution are placed within and outside of the BTES. Four sensor strings, with each 20 temperature sensors are placed within the storage volume and one was placed outside, 11 m downstream from the southernmost borehole in the storage volume (Figure 61) (Schmidt, 2018).

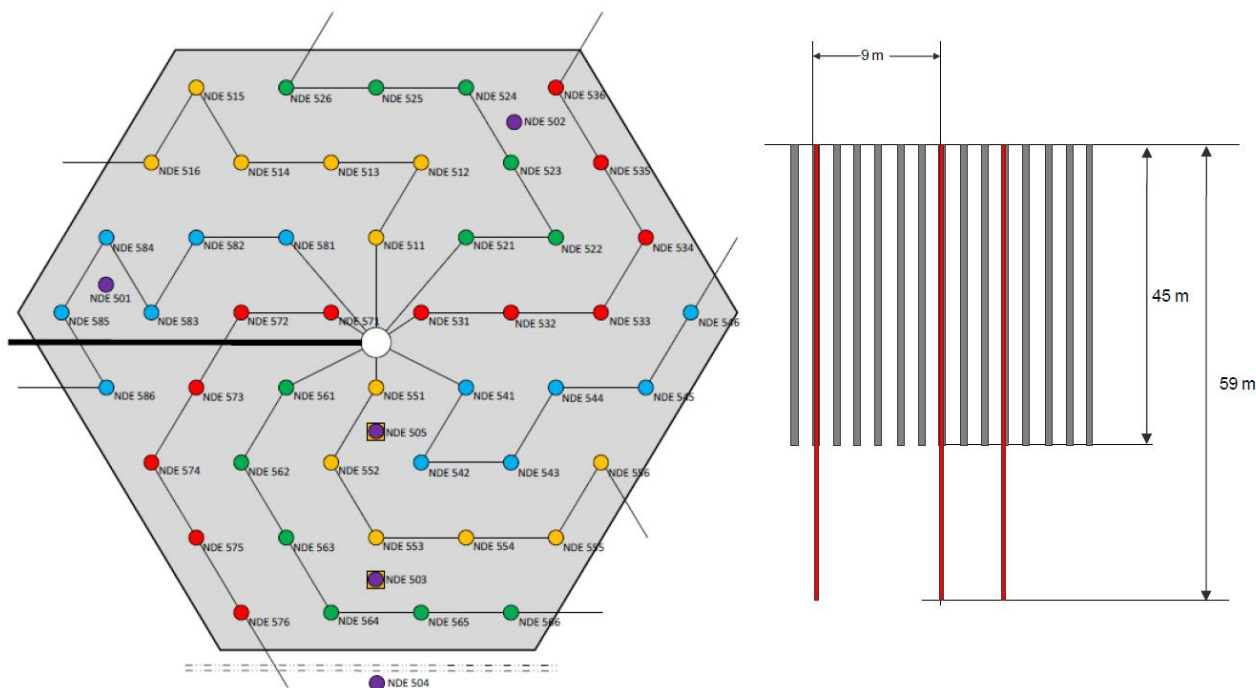


Figure 61. Position of borehole heat exchangers and temperature sensors in the Brædstrup BTES. Left: Top view, NDE 501 to NDE 505: Temperature sensors. NDE 504 is located 11 m south of the storage. Right side: Red lines: Temperature sensors, Gray lines: Borehole heat exchangers. (PlanEnergi, 2019).

Hot water is circulated from the center and out to create a horizontal storage stratification with the hottest part in the center and colder towards the edge of the storage. The storage has reached a maximum temperature of 50 °C, and there is little to no vertical temperature stratification. A lower temperature is seen close to the top and bottom of the storage though, because of heat transfer to the surrounding volume. An insulating lid has been installed to minimize the heat loss to the surface.

Temperature data from the center of the storage during operation can be seen in Figure 62, showing a maximum temperature of approximately 50 °C in Autumn and the lowest temperatures in Spring. Temperature changes down to approximately 15 m below the bottom of the storage including the top of the groundwater aquifer are shown.

It was found that the soil immediately beneath the storage volume followed the temperature variations within the storage, but at a lower temperature and with increasing time delay (PlanEnergi, 2019).

Temperature data from a borehole placed 11 m downstream from the storage are shown in Figure 63. The figure shows that the temperature in the depth interval of the BTES has increased by approx. 5 °C. Nevertheless, the significantly lower temperature compared to the central part of the storage indicates that the thermal heating of the surrounding soil layers is limited already a short distance (11 m) away from the BTES.

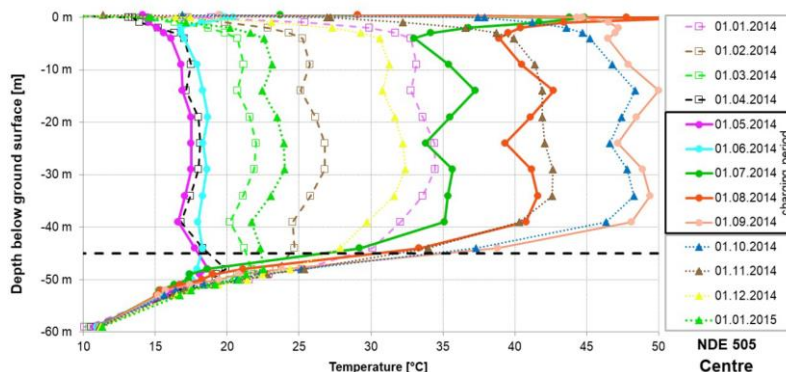


Figure 62. Vertical temperature in borehole NDE 505 in the centre of the BTES at Brødstrup. (PlanEnergi, 2019).

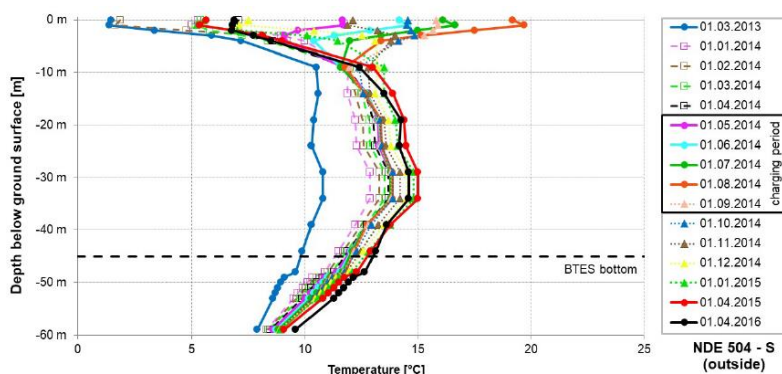


Figure 63. Vertical temperatures in borehole NDE 504 placed 11 m south of the BTES. The slight decrease in temperature between April 2015 and April 2016 corresponds to a decrease in temperature within the BTES (PlanEnergi, 2019).

4.3.2. Thermal heating of groundwater.

The boreholes in Brødstrup were drilled to 45 meters below ground level, corresponding to 5 meters above groundwater level in the area. It is possible to heat up a borehole storage to 90 °C, but due to limited solar thermal excess heat, the storage in Brødstrup is heated to a maximum of 50 °C only.

Figure 63 shows that in the center of the storage the temperature drops to required levels when reaching the groundwater aquifer five meters below the bottom of the BTES. Figure 63 shows that 11 meters from the BTES the temperature in the groundwater aquifer has dropped further indicating the effect on the aquifer is limited.

4.3.3. Risk of leaks

Since pure water is used as heat carrier fluid in the Brødstrup BTES system, the environmental effect to the surrounding formation in case of a leak is very limited. Nevertheless, the borehole u-tubes were tested for leaks during the construction phase by pressurized water, before being connected. And, to ensure that a potential leak is discovered during operation of the BTES, the system also includes a pressure drop alarm, as well as measures to ensure a potential leak will remain small (Kallesøe, 2019).

4.3.3.1. CO₂ intensity

As an integrated part of the application process for the BTES at Brædstrup an estimate of the change in the CO₂ intensity has been made.

The estimate is made with comparison to a “business as usual” scenario where the existing plant continues operation without any changes (PlanEnergi, 2010). The existing plant was at the time of the application using natural gas for heat production.

For the project the calculations were made by assuming a continuation of the existing plant supplemented by 8.000-10.000 m² solar collectors, 8.000 m³ BTES, 5.000 m³ accumulation tank, a heat pump with an effect of 1,2 MW and transmission lines.

The calculations have been made according to guidelines from the Danish Energy Agency (Energistyrelsen 2005, 2010). The calculations include CO₂ emission from electricity produced from coal and the result is shown in Table 29 and

Table 30 below. Over a 20-year period, the CO₂ emissions will be reduced with 9.600 tons.

Table 29. Changes in emissions as a result of the pilot project at Brædstrup.

Emissions	Unit	Reference	Project	Project minus reference	Change
CO ₂	Ton/year	3.434	2.975	-459	-13%
CH ₄	Kg/year	39.459	38.661	-798	-2%
N ₂ O	Kg/year	90	82	-9	-10%
CO ₂ equiv.	Ton/year	4.290	3.812	-478	-11%
SO ₂	Kg/year	-1.966	-1.933	33	-2%
NO _x	Kg/year	10.348	9.858	-490	-5%

Table 30. Changes in emission over a 20-year period as a result of the pilot project at Brædstrup.

CO ₂ equiv.	9.600 tons
SO ₂	-0,7 tons
NO _x	9,8 tons

4.3.3.2. Fast-track Risk assessment

A fast-track risk assessment is carried out for the Brædstrup BTES system (Table 31).

Table 31. Fast-track risk assessment for the Brædstrup pilot BTES system where possible environmental effects are evaluated according to type, probability, consequences and risk.

Brædstrup						
Effect	Phase			Operations (predicted)		
	P	A	M	Probability	Consequences	Risk
Air quality				L	L	L
Noise and vibration				L	L	L
Formation water quality				L	M	L
Formation water temperature				L	M	L
Surface clear water				L	L	L
Soil occupation				L	L	L
Wastes and dangerous substances				L	L	L
Environment				L	L	L
Nature				L	L	L
Soil mechanics				L	L	L
Seismicity				L	L	L
CO2 intensity reduction				H	M	H

5. Pit Thermal Energy Storage

5.1. General effects PTES

The principle of PTES is simple and works by storing hot water in very large excavated basins with an insulated lid. Sides and bottom are typically covered by a polymer-liner, but can also be made of concrete (Figure 64). Temperatures up to approx. 90°C can be stored and PTES offers the same flexibility to e.g. district heating energy systems as BTES.



Figure 64. Picture of Dronninglund Pit Storage under construction. Dronninglund District heating; 37,573 m² of solar collectors and a 62,000 m³ water pit heat storage (PlanEnergi).

The most important potential environmental effects of Pit Thermal Energy storage are:

- Thermal changes causing
 - heating of the surrounding geological formation and groundwater
 - changes in water chemistry
 - changes in microbiology
- Effects of water abstraction for filling the PTES
- Effects of leakage from the pit

To assess the potential effects of establishing a PTES e.g. in Denmark, the local authorities evaluate for each site whether an individual environmental impact assessment (Rambøll, 2013) should be made since the potential environmental effects are linked to the local conditions such as geology, groundwater flow, microbiology, protected areas etc.

Extra focus is given to areas with specific interest in regard to drinking water supply, protected areas or areas with nearby known pollution.

5.1.1. Thermal effects

Operation of a PTES system will cause heating of the surrounding soil and groundwater if present. To evaluate the effect of a PTES on groundwater temperatures, thermal changes around and beneath the PTES have to be assessed specifically in regard to present and future drinking water supply in the area. The effect depends on the geological formation surrounding the PTES and the thermal conductivity as well as the separation to the groundwater aquifer. The evaluation will typically focus on ensuring that the groundwater in the area will not be affected by an increase in temperature or microbiological activity making it unfit for drinking water supply.

To evaluate changes in water chemistry, local water samples are usually tested for solubility of chalk and other minerals such as iron hydroxides at the expected temperature changes. If the temperature around the PTES is kept below 25 °C the risk of precipitation of minerals is generally considered to be little, though this is very much dependent on local conditions.

Changes to the microbiology in the soil and groundwater are also generally considered to be small if the temperature is kept below 25 °C (Rambøll, 2013). For areas with an expected higher temperature an evaluation of the effect on groundwater aquifers and present/future drinking water supply must be made.

5.1.2. Water supply for the PTES

A large amount of water is needed to fill a PTES. Although the groundwater abstraction will be temporary, the possible effect on groundwater level and hence on groundwater dependent/protected nature areas and surface waters must be evaluated. It must also be ensured that there will be no adverse effect on nearby drinking water supplies and other factors depending on the local environment.

The water for the PTES needs to be demineralized which can be done by reverse osmosis membrane filtering. The process will leave an amount of residual water in the form of a concentrated retentate. The residual water will have an increased chloride content and it will be necessary to assess if re-infiltration will pose a risk for the groundwater quality e.g. in terms of chloride-content.

Before filling into the PTES, NaOH is added to the demineralized water to bring the pH to 9,8 in order to avoid biological activity and corrosion. Thus, except for the high pH, the pit water can be regarded as very clean and the pH can easily be lowered by adding HCl and re-infiltrated should this be necessary (Rambøll, 2013).

5.1.3. Leaks

In case of leaks to a groundwater aquifer the following parameters must be assessed:

- pH
- Impurities in NaOH, which is added to the PTES
- Temperature

To prevent corrosion of pipes and other metals and biological activity in the storage NaOH is added to the water, raising pH to 9,8 as mentioned above.

In case of a leak from the storage, the effect on the surrounding environment depends entirely on the amount of water leaked, the water quality, the composition of the geological formation and the separation to the groundwater aquifer.

Changes to the pH in the soil can lead to changes of sorption of metals in the soil resulting in dissolution or precipitation. Cations such as for instance chromium, lead or nickel may have increased sorption whereas some anions such as phosphate, silicate and chromate may have reduced sorption (Rambøll, 2013). The degree to which the soil and the groundwater are capable of neutralizing the higher pH in case of a leak will be site specific.

Impurities in the added NaOH such as trace elements are assumed to be very low in concentrations and not to constitute a significant risk to groundwater (Rambøll, 2013).

Continuous monitoring of water level in the PTES should take place to identify possible leaks.

The construction of the PTES has to follow a specific set of geotechnical norms, as given in Eurocode 7 DS/EN 19974 – DK NA-2013, ensuring e.g. wall stability (Rambøll, 2013).

5.2. Case study in Denmark

In Denmark there are several PTES systems. The storage systems are connected to district heating networks, where they are used for storing excess heat from solar thermal plants.

Interviews with district heating companies with existing PTES systems has been conducted to assess present and potential negative environmental impacts from the systems, as seen when they are in use.

In general, the district heating companies consider the risks of a negative environmental impact to the surrounding areas small.

The environmental effect connected to PTES in Denmark are identified through a literature study as well as the interviews with district heating companies with an active PTES mentioned above.

The main environmental pressures from PTES consist of:

- Thermal heating of the surrounding soil layers
- Thermal heating of groundwater
- Risk of leaks
- For PTES the construction area of the storage can be large
- Drainage of rainwater from the PTES lid can be challenging

To identify in which way the pressures from the PTES affect the state of the environment a series of monitoring programs have been set up.

The PTES systems in Denmark monitor a variety of component (Sørensen, 2018; PlanEnergi, 2019; Schmidt, 2019). Examples from the PTES constructed at Marstal are shown below (PlanEnergi, 2019).

5.2.1. Monitoring of the PTES at Marstal

For monitoring temperature changes in and around the PTES in Marstal, a total of 85 temperature sensors have been installed inside the pit and in 5 boreholes (Figure 65) outside the pit to monitor the long-term temperature changes in the soil around the PTES (PlanEnergi, 2019).

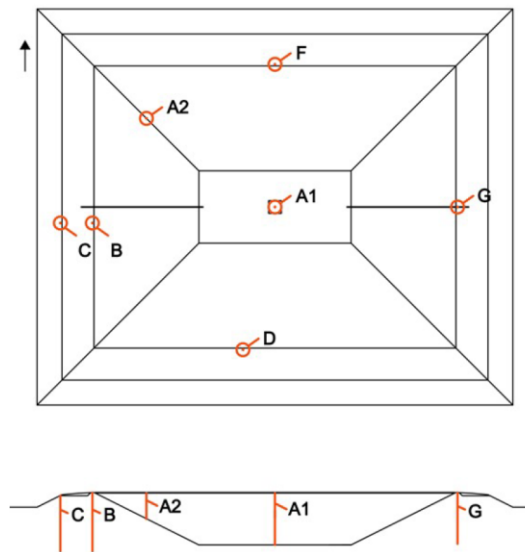


Figure 65. Position of temperature sensors inside and outside the PTES in Marstal (PlanEnergi, 2019).

Data are collected from several sensors at various depths. The temperature measurements recorded at 18 m below ground level corresponds to two meters below the bottom of the PTES. Temperature data from borehole B and C can be seen in Figure 66 and Figure 67. In both borehole B and C, seasonal changes can be seen in the shallower temperature sensors overlaying the temperature changes caused by the PTES (PlanEnergi, 2019). The temperature sensors from approximately 10 meters below ground level are less affected by seasonal fluctuations. In borehole B, placed at the edge of the PTES (Figure 66), a temperature increase at 10 m of depth was seen from approximately 12 °C to 25 degrees C from 2013 to 2017 (Figure 67). The temperature monitoring from two meters below the bottom of the PTES (18 meters below ground level) shows an increase in temperature from approximately 10 °C to 18 °C during the four-year period.

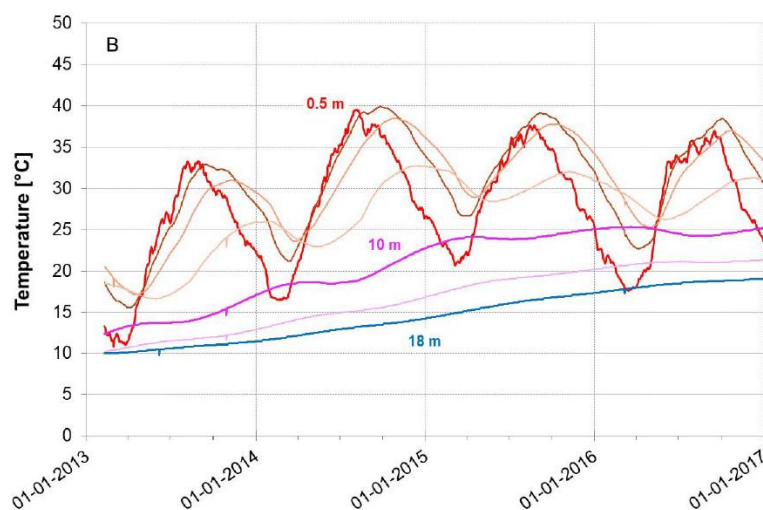


Figure 66 Vertical temperature increase next to the PTES (Borehole B). Depth intervals [m]: 0,5, 1,5, 3, 6, 10, 14 and 18 (PlanEnergi, 2019).

Ten meters further away from the PTES, in borehole C, temperature measurements showed an increase at 10 m of depth from approximately 12 °C to 16 °C during the four-year time span, see Figure 67.

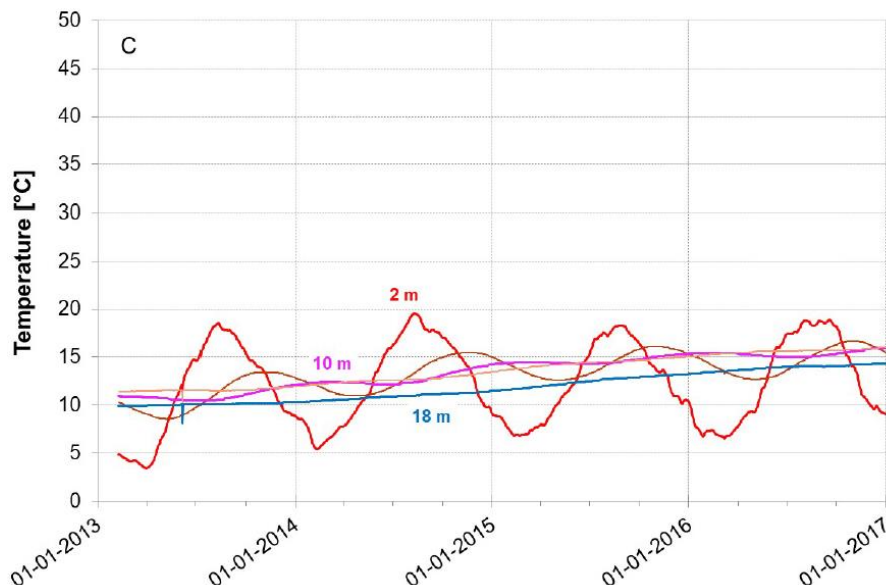


Figure 67. Vertical temperature increase in Borehole C, 10 m further away from the PTES and Borehole B shown in Figure 66. Depth intervals [m]: 2, 6, 10, 14 and 18 (PlanEnergi, 2019).

The water levels of the PTES are monitored continuously to identify if there are leaks in the storage. The liner is checked once a year by a diver to locate leaks, though this can only be done if the water temperature is below 40 °C.

A leak at the PTES at the town of Marstal was found during the construction phase, and a diver was sent to repair the hole in the lining. The leak resulted in the loss of approximately 35 m³/day of water from the storage. As the lining can only be repaired when the water temperature in the storage is low enough for a diver to enter the PTES, it is important to evaluate if the water in the PTES constitutes a risk to the environment in case of a leak while the temperature in the PTES is high.

Water chemistry is monitored yearly (pH, oxygen and salts) to prevent corrosion of the installations. It has proven necessary to raise pH to 9,8 to prevent corrosion of the technical installations in the PTES. The changes to the water chemistry are not considered a great risk to the surrounding environment by the district heating companies in case of leaks.

A daily inspection is carried out to ensure that insulation, water level and top liner are as they should be.

Several of the district heating companies interviewed commented that a general concern met when presenting plans for a PTES was fear of pit walls collapsing. Each site has been individually assessed by geotechnical engineers who have calculated construction dimensions for the PTES to ensure a stable pit structure. In the case of a breach to the walls the amount of water loss from the PTES was also regarded as small since most of the PTES is below terrain. The consensus among the district heating companies was that this risk would be rather small because the construction is considered structurally stable.

5.2.1.1. CO₂ intensity

As an integrated part of the application process for a PTES, an estimate of the changes in CO₂ intensity has been made.

The estimate is made with a comparison to a “business as usual” scenario where the existing plant continues operation without any changes.

Below are given 2 examples for changes in CO₂ intensity as a result of a PTES in Denmark.

The first example is from the PTES at Marstal where the reference scenario is based on the use of biooil and solar which is considered CO₂ neutral (Marstal Fjernvarme, 2010).

The second example is from a PTES at Dronninglund, where the reference scenario is based on gas engines and bio-oil boilers as well as a gas boiler used as a reserve (PlanEnergi, 2010).

The calculations have been made according to guidelines from the Danish Energy Agency (Energistyrelsen, 2005; Energistyrelsen, 2010).

Marstal PTES

The reference scenario used for the calculation of CO₂ intensity at Marstal PTES consist of 18.300 m² sun collectors, 18,3 MW bio-oil boilers, 10.340 m³ PTES, 3.500 m³ sand storage and a 2.100 m³ steel storage tank. The reference scenario is considered CO₂ neutral.

The project includes in addition to the reference scenario production from further 15.000 m² sun collectors, 4 MW woodchip boiler, 1½ MW CO₂ driven heat pump and 75.000 m³ PTES. The results are shown in Table 32 below.

Table 32. Changes in emissions as a result of the PTES project at Marstal.

Emissions	Unit	Reference	Project	Project minus reference
CO ₂	Ton/year	0	-1.478.227	-1.478.227
CH ₄	Kg/year	109	1.561	1.452
N ₂ O	Kg/year	145	183	37
CO ₂ equiv.	Ton/year	1	21	310
SO ₂	Kg/year	73	540	467
NO _x	Kg/year	4.714	2.952	-1.763

Dronninglund PTES

The reference scenario used for the calculations of CO₂ intensity at Dronninglund PTES consist of 4 gas engines (5,7 MW heat and 3,48 MW electricity), 2 bio-oil boilers (4 MW and 8 MW) and a gas boiler used as a reserve (8 MW).

The project includes in addition to the reference scenario further production from 35.000 m² solar collectors, 60.000 m³ PTES and a heat pump (3 MW). The results are shown in Table 33 and Table 34 below. Over a 20 year period, the CO₂ emissions will be reduced with 25.000 tons.

Table 33. Changes in emissions as a result of the PTES project at Dronninglund.

Emissions	Unit	Reference	Project	Project minus reference	Change
CO ₂	Ton/year	2.525	1.623	-902	-36%
CH ₄	Kg/year	57.268	41.564	-15.704	-27%
N ₂ O	Kg/year	158	71	-87	-55%
CO ₂ equiv.	Ton/year	3.776	2.517	-1.259	-33%
SO ₂	Kg/year	-481	-697	-216	-45%
NO _x	Kg/year	15.257	10.182	-5.075	-33%

Table 34. Changes in emission over a 20-year period as a result of the PTES at Dronninglund.

CO ₂ equiv.	25.000 tons
SO ₂	4,3 tons
NO _x	100 tons

5.2.1.2. Fast-track Risk assessment

A fast-track risk assessment is carried out for PTES at Marstal, (Table 35)

Table 35 Fast-track risk assessment for Marstal PTES where possible environmental effects are evaluated according to type, probability, consequences and risk.

Marstal							
Effect	Phase	Operations (predicted)					
		P	A	M	Probability	Consequences	Risk
Air quality					L	L	L
Noise and vibration					L	L	L
Formation water quality					L/M	M	M
Surface clear water					L	L	L
Soil occupation					L	L	L
Wastes and dangerous substances					L	L	L
Environment					L	L	L
Nature					L	L	L
Soil mechanics					L	L	L
Seismicity					L	L	L
CO ₂ intensity reduction					H	M	H

6. Assessment framework

This section aims to provide an overarching perspective on the environmental impacts assessed for UTES technologies, both generic and specific for several case studies. And not only reflecting on the environmental themes or topics that are relevant for UTES, but also on how the environmental performance of UTES projects has been assessed. This will provide the input to arrive at a conceptual assessment framework, or at least general guidance to assessing environmental impacts and risks for UTES projects.

6.1. General observations

When reviewing the environmental impacts described in section 2-5 for several UTES projects or for technologies in general some general observations are rather standing out.

6.1.1. Structure and framework of assessment of environmental performance and risks differs per country

The environmental performance and assessment of it varies per country and per project. The countries under study have different frameworks and regulations in place for assessing the environmental impacts and risks for UTES projects. This leads to different reporting on the possible and expected environmental impacts.

6.1.2. Every UTES project site is unique; environmental impacts are site-specific

On top of point 1, the surface and subsurface conditions for every project makes every project rather unique. This means that temperature, geological setting and aquifer composition, depth, well configuration, system design, system operation, efficiency etc. are rather project specific. As a consequence the environmental impacts are project specific as well. In that sense a UTES storage project is much different than assessing for example the environmental impacts of a modular Li-Ion battery system.

6.1.3. Environmental themes and topics are not unique

Clearly, environmental impacts are site-specific, but this does not mean that the environmental themes and topics that are assessed in an environmental assessment or environmental impacts assessment are unique and one-of-a-kind. It is possible to highlight key environmental themes across UTES technologies. The table below provides an overview of typical environmental themes that are addressed when assessing the environmental impacts and risks for UTES technologies. They typically are in line with themes that are part of an Environmental Impact Assessment, although UTES projects do not necessarily require a full Environmental Impact assessment. As observed in this report this varies per country what level of assessment is required.

The European Commission report describes it as “The environmental impact assessment must identify, describe and assess the direct and indirect effects of a project on a number of environmental factors (population and human health, biodiversity, land, soil, water, air, climate, landscape, material assets and cultural heritage), as well as the interaction between these various elements.”¹

¹ 35 years of EU Environmental Impact Assessment. Luxembourg: Publications Office of the European Union, 2021.

https://ec.europa.eu/environment/eia/pdf/EIA_Directive_35_years.pdf

Environmental themes that are common in the environmental assessments of UTES technologies and projects are presented in the Table 36.

Table 36. Environmental themes commonly assessed for UTES technologies and projects.

Environmental theme
Soil & Water Hydrothermal
Soil & Water Geochemical
Soil & Water Microbiological populations
Soil & Water Geohydrological
Soil & Water Geomechanical
Soil & Water General
Energy & Climate
Noise & vibrations
Air quality
Nature: Flora & Fauna
Cultural heritage, Landscape and archaeology
Visual disturbance
Resource, waste and byproducts (circularity)
External safety
Socio-economic environment

Next to the typical environmental themes as suggested above for UTES technologies the environmental themes focus on subsurface impacts. Therefore we have broken 'Soil and Water' themes into subthemes that highlight the typical environmental processes and impacts that are induced by UTES technologies: hydrothermal, geochemical, microbiology, geohydrology, geomechanical and general impacts.

In general the UTES projects reviewed in this report share environmental impacts reported on:

- **Thermal effects** of injecting and producing heat from the subsurface has an effect on physical properties, chemistry and microbiology in the subsurface that in turn could affect performance of the UTES system or pose a potential risk for subsurface and surface ecology
- **Groundwater and drinking water quality** are under scrutiny in many UTES projects. The process by which the UTES technology may affect for example groundwater flow, level, mixing and composition differs per technology and location. For PTES it is for example the water abstraction and possible leakages that are of high importance. For BTES it is possible **leakage and seepage** as a result of insufficiently sealed boreholes. For ATES it is possible mixing of aquifer water (within or between different aquifers) with contamination or salinization as a result. Or possible impacts as a result of hydrothermal effects (causing geochemical and microbiological equilibria to be disturbed) or reservoir water conditioning to prevent carbonate deposition affecting groundwater quality. For MTES it is mainly the drilling and operations resulting in re-injection, diversion and lowering of groundwater levels. Which in turn affect changes in physical, chemical or biological quality of the water. All in all most UTES projects entail groundwater quality monitoring.

- The third environmental impact that is commonly reported on are **soil mechanic effects**. This includes possible seismicity, and heave and subsidence as a result of drilling and/or operations of the UTES. For the MTES and Geneva ATES case study clearly seismicity was of high interest, while this is or relative less concern when the UTES is targeted in unconsolidated strata. For UTES in general thermal settlement and swelling resulting in subsidence or heave may for example result in damage to buildings and infrastructure.

A very detailed list of environmental topics assessed in UTES projects is presented in the appendix. This may help possible future projects with a reference list or checklist for structural assessment of environmental performance. A snapshot is provided in Table 37 where it is shown that the environmental topics are classified per environmental theme to ease the assessment and look up.

Table 37. Environmental topics classified by environmental theme.

Environmental criterion/topic	Environmental theme
Dust / particulate matter emissions	Air quality
NOx emissions	Air quality
Land use for location	Cultural heritage, Landscape and archaeology
CO2 emission balance (and savings)	Energy & Climate
Energy efficiency / storage efficiency	Energy & Climate
Seasonal performance factor electricity consumption for system operation	Energy & Climate
Individual risk	External safety
Societal risk	External safety
Noise disturbance	Noise & vibrations
Noise disturbance during drilling of (test) wells	Noise & vibrations
Waste generation quantity	Resource, waste and byproducts (circularity)
Subsurface space requirement	Socio-economic environment
Traffic movements for materials	Socio-economic environment
Waste water disposal from well drilling	Soil & Water General
Calcite precipitation	Soil & Water Geochemical
Etc	Etc

It is very important to discern between environmental impacts and risks

When reviewing sections 2-5 it becomes very clear that the environmental assessments of UTES projects concerns both environmental impacts with a certain occurrence and with a (very) uncertain occurrence. A good example is the abstraction of groundwater. This results into observable effects on for examples the groundwater table. This is a effect with a certain occurrence. Then there are also environmental risks that may not occur or have a uncertain occurrence. The failure of a well or pit with leakage/seepage as a result is a good example for this scenario. In such a case the environmental consequences are also not certain to occur. For these environmental risks with a certain probability and impact it is wise to execute a risk assessment. The table below shows how the risks are assessed for the HT-

ATES project at ECW in the Netherlands². The probability is assessed between Low and High and the consequences or impacts are assessed between Low and High. This results in a risk rating as shown in Table 38.

To make the distinction between certain and uncertain environmental effects allow for better comparison and overall assessment of the environmental impacts associated to a UTES project or technology.

Table 38. Risk/opportunity matrix used in this study.

Risk rating				Opportunity rating			
Consequence \ Probability	Low	Medium	High	Consequence \ Probability	Low	Medium	High
	Low	L	L		M	Low	L
Medium	L	M	H	Medium	L	M	H
High	M	H	H	High	M	H	H

6.1.4. System components

Following the risk assessment framework proposed for the ECW HT-ATES site the following system components can be discerned (Table 39).

Table 39. System component definition.

General	Risks and environmental impacts that are relevant for all (or multiple) of the system components
Surface Facilities	These include compressors, piping, instrumentation, process facilities
Well	This includes the X-mas tree, wellhead, well (completion and cemented casings), sand-face completion
Subsurface (reservoir and overburden)	The target storage reservoir, the caprock and overburden

6.1.5. Clarity is need on the impacts and risk for the different project phases

When reviewing the assessed environmental impacts across the project phases it stands out that most environmental impacts are assessed for the Execute (i.e. drilling and building phase) and the Operate phase. Less attention typically is given to the pre-execute phase, albeit that projects provide baseline environmental measurements for this phase to allow for assessing impacts later on (Table 40). And also little attention is given to the decommissioning and post-abandonment phase. For heat store projects these phases maybe of relevance as the soil has still heat in place that slowly dissipates into the surrounding environment. For the reviewer of environmental assessments from competent authority or stakeholder perspective it could be of high interest to understand in which project phase a certain environmental impact or risks occurs (and how long that phase takes).

² Van Unen et al. HEATSTORE risk assessment approach for HT-ATES applied to demonstration case Middenmeer, The Netherlands. 2020
https://www.heatstore.eu/documents/TNO%20report%202020%20R10192_HEATSTORE_Fi nal_2020.03.18.pdf

Table 40. Phases of an UTES project.

1. Pre-execute	All work done prior to the start of the execution phase; including analysis and design
2. Execute	The Execution phase; in this phase the facility is built (or updated) for energy storage
3. Operate	The operational phase; the actual phase where energy is stored and produced
4. Decommission	The Decommissioning phase; this includes the abandonment of wells, removal of the surface facilities and clearing the site for future use
5. Post-abandonment	The post decommissioning phase; these include risks that could come to light by monitoring of the abandoned site
6. All phases	All of the above defined project phases (to prevent having them in all phases)

6.1.6. Data and assessment quality of the environmental impacts assessed is not always clear

For the review of environmental assessments it could also be of high relevance to understand the quality of the assessment and uncertainty of certain (qualitative and quantitative) statements. We propose to make a distinction between estimated, modelled and measured/observed impacts. For UTES projects often subsurface models are used to model the performance of the system and possible impacts in the subsurface. These modelled results need to be validated with actual measurements. Monitoring requirements for UTES project are therefore an important part of the environmental assessment (Table 41).

Table 41. Conceptual assessment model.

Data & Assessment
Estimated
Modelled
Measured/monitored

All in all, the elements (environmental themes, topics, project phases, probability, data quality) discussed above allow for a more structured assessment of the environment impacts and risks of UTES projects.

There is one critical aspect missing, however. This is the way cause-effect causality in environmental assessments is dealt with. When reviewing the results of environmental assessments, it becomes clear that very often (implicitly) a cause-effect chain is described for environmental effects. To give an example:

For BTES systems typically the following environmental impacts are assessed: The operation of the BTES results in heat injection and extraction. This has the effect of heating/cooling of the surrounding rock/soil. As a consequence, this might alter biological activity and geochemical processes in the surrounding rock/soil.

A conceptual model that might be of use here the DPSIR framework. This has been developed and used by the European Environmental Agency as a conceptual model to describe the relationships between the environment and society in a simplified manner. "According to the DPSIR framework there is a chain of causal links starting with 'driving

forces' (economic sectors, human activities) through 'pressures' (emissions, waste) to 'states' (physical, chemical and biological) and 'impacts' on ecosystems, human health and functions, eventually leading to political 'responses' (prioritization, target setting, indicators)."

³ An example for the application of the DPSIR framework to air quality is provided in Figure 68.

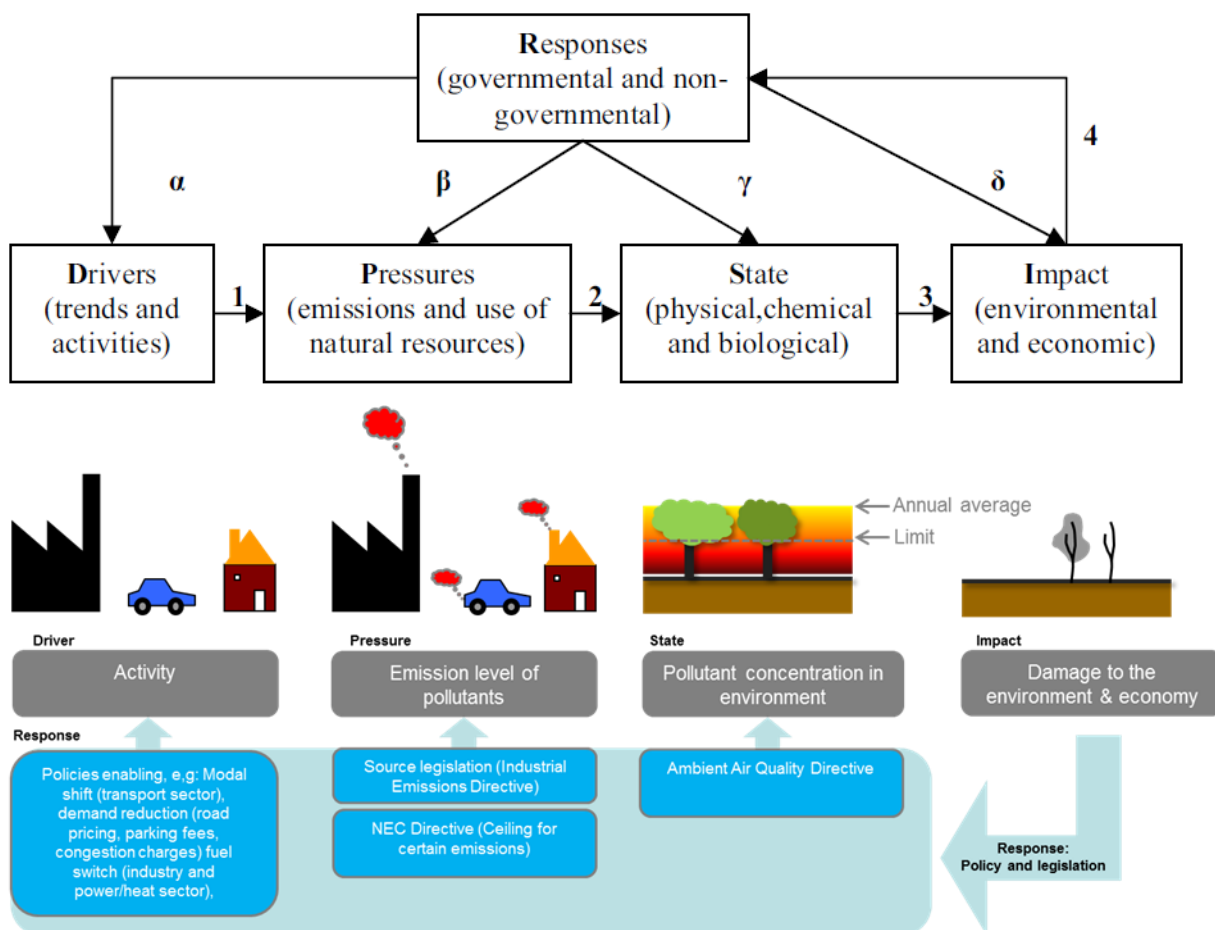


Figure 68. Schematic (above) and Simple representation of the cause effect chain of air quality using the DPSIR framework (below) (source: TNO).

When applied to UTES this would allow to structurally assess/identify environmental 'Drivers' (operating the UTES) that via 'Pressure' (heat injection into the subsurface) on the environment have an effect on the 'State' of the environment (effect on heat balance, groundwater chemistry etc). that can be translated then to 'Impacts' (changed biological diversity and activity). Then the 'Responses' are basically the mitigation and remediation efforts for environmental impacts (that limit or steer the Drivers and other elements). Responses are also typically policies and legislation that provide the environmental boundary conditions for UTES projects (Table 42).

³ Kristensen, 2004 <http://wwz.ifremer.fr/dce/content/download/69291/913220/file/DPSIR.pdf>

Table 42. Elements of the DPSIR framework.

DPSIR	Description
Driver	Trends and activities
Pressure	Emissions and use of natural resources
State	Physical, chemical and biological
Impact	Environmental and economic
Response	Societal: governmental and nongovernmental

Integration of the elements of the observations (environmental themes, topics, project phases, probability, data quality etc) in with a simplified version of the DPSIR model would allow to structurally assess the environmental impacts and risks of UTES projects. It also will provide reviewers of an environmental assessment with a clear overview of which environmental impacts and risk are assessed for the UTES project. The HEATSTORE project and this report has already provided for an long list of environmental topics (see appendix) that are typically assessed for UTES projects. This long list could be used as a checklist or starting point for future environmental assessments of UTES projects.

Finally the framework could be used to summarize the most important environmental effects of UTES projects. In Table 45 the general environmental effects from PTES are summarized using the conceptual framework.

Table 43. Conceptual assessment framework for assessing and reporting environmental impacts and risks for UTES projects.

Environmental theme	System component	Environmental topic	PSI			Phase			Probability & Risk		Responses			
			Pressure	State	Impact	Pre-execute	Execute	Operate	Decommission	Post-abandonment	Certain occurrence	Uncertain occurrence	Risk rating	Mitigation
select from list	select from list	select from list or create new									select from list	select from list	fill in	fill in
Soil & Water Hydrothermal	General	Dust / particulate matter emissions	x	x	x	x	x	x	x	x	Low	Low	free text	free text
Soil & Water Geochemical	Surface Facilities	NOx emissions	-	-	-	-	-	-	-	-	Medium	Medium		
Soil & Water Microbiological populations	Well	Land use for location									High	High		
Soil & Water Geohydrological	Subsurface (reservoir and overburden)	CO2 emission balance (and savings)												
Soil & Water Geomechanical		Energy efficiency / storage efficiency												
Soil & Water General		Seasonal performance factor electricity consumption for system operation												
Energy & Climate		Individual risk												
Noise & vibrations		Societal risk												
Air quality		Noise disturbance												
Nature: Flora & Fauna		Noise disturbance during drilling of (test) wells												
Cultural heritage, Landscape and archaeology		Waste generation quantity												
Visual disturbance		Subsurface space requirement												
Resource, waste and byproducts (circularity)		Traffic movements for materials												
External safety		Waste water disposal from well drilling												
Socio-economical environment		Calcite precipitation												
		Carbon Mobilization - Dissolved Organic Carbon												
		Enhanced weathering of aquifer sediments												
		Fresh/ brackish/ salt water interface changes												
		Leakage from the pit storage												
		etc												

Table 44. Example of applying the assessment framework on a hypothetical ATEs project.

Environmental theme	System component	Environmental topic	PSI	Phase							Probability & Risk	Responses	Mitigation	Monitoring		
				Pressure State Impact	Pre-execute	Execute Operate	Decommission	Post-abandonment	Certain occurrence	Uncertain occurrence					Risk rating	
Soil & Water General	General	baseline monitoring	x	x	x											baseline monitoring for reference
Soil & Water General	General	Waste water disposal from well drilling	x			x				x						collection and treatment or monitored disposal
Soil & Water Hydrothermal	Subsurface (reservoir and overburden)	heating of groundwater near well	x			x				x						well insulation
	Subsurface (reservoir and overburden)	heating of overburden	x			x	x	x		x						DTS cables
	Subsurface (reservoir and overburden)	heating of reservoir	x			x	x	x		x						DTS cables
Soil & Water Geomechanical	Subsurface (reservoir and overburden)	Subsidence	x			x	x	x			x	Low				
	Subsurface (reservoir and overburden)	Uplift	x			x	x	x	x			Low				
Soil & Water Geochemical	Subsurface (reservoir and overburden)	Ph of reservoir water as result of CO2 or HCl dosing to prevent calcite precipitation	x							x						Ph monitoring
	Subsurface (reservoir and overburden)	Mixing of water with different quality	x	x		x	x			x						Chloride monitoring
	Subsurface (reservoir and overburden)	mobilisation of trace elements	x			x					x	Low				Boron and Arsenic monitoring
	Subsurface (reservoir and overburden)	Calcite precipitation	x			x				x						CO2 or HCl dosing
Soil & Water Microbiological populations	Subsurface (reservoir and overburden)	negatively affect microbiological populations in target reservoir		x							x	Low				DNA sequencing
	Subsurface (reservoir and overburden)	negatively affect microbiological populations in overburden		x							x	Low				DNA sequencing
Noise	Surface Facilities	Noise disturbance during drilling of (test) wells		x	x	x				x						
Visual disturbance	Surface Facilities	Visual hindrance of drilling rig		x	x					x						
Socio-economical environment	General	traffic movements for materials	x			x	x	x		x						
	Surface Facilities	electricity consumption for system operation	x							x						
Energy & Climate	Surface Facilities	energy efficiency	x				x			x						
	Surface Facilities	CO2 emission balance	x							x						
	Surface Facilities	NOx and particulate matter emissions during drilling and operation	x				x	x		x						

Table 45. General PTES environmental effects represented with the conceptual framework.

Environmental theme	System component	Environmental topic	PSI			Phase				
			Pressure State	Impact		Pre-execute	Execute	Operate	Decommission	Post-abandonment
PTES-Thermal effects										
Soil & Water Geohydrological	Subsurface (reservoir and overburden)	Water abstraction for filling the PTES	x				x	x		
Soil & Water Geohydrological	Subsurface (reservoir and overburden)	Groundwater level changes		x			x	x		
Soil & Water General	Subsurface (reservoir and overburden)	impact on drinking water supply, protected areas or areas with nearby known pollution			x		x	x		
PTES - water abstraction for Pit filling										
Soil & Water Hydrothermal	Subsurface (reservoir and overburden)	Heat injection and extraction	x					x		
Soil & Water Hydrothermal	Subsurface (reservoir and overburden)	heating of groundwater near well/reservoir		x				x		
Soil & Water Hydrothermal	Subsurface (reservoir and overburden)	heating of overburden		x				x		
Soil & Water Hydrothermal	Subsurface (reservoir and overburden)	heating of reservoir		x				x		
Soil & Water Geochemical	Subsurface (reservoir and overburden)	Mixing of water with different quality		x				x		
Soil & Water Geochemical	Subsurface (reservoir and overburden)	mobilisation of trace elements		x				x		
Soil & Water General	Subsurface (reservoir and overburden)	impact on drinking water supply, protected areas or areas with nearby known pollution			x			x		
PTES - Leakage from the Pit										
Soil & Water General	Subsurface (reservoir and overburden)	Leakage from the pit	x				x	x		
Soil & Water Hydrothermal	Subsurface (reservoir and overburden)	temperature effect		x			x	x		
Soil & Water Geochemical	Subsurface (reservoir and overburden)	pH effect, NaOH impurities on geochemical state		x			x	x		
Soil & Water Geochemical	Subsurface (reservoir and overburden)	combined effect on geochemical equilibrium (precipitation or dissolution or minerals, mobilisation of trace elements)		x			x	x		
Soil & Water General	Subsurface (reservoir and overburden)	impact on drinking water supply, protected areas or areas with nearby known pollution			x		x	x		

6.2. Appendix Environmental criterion/topic

Environmental criterion/topic	Theme
Dust / particulate matter emissions	Air quality
NOx emissions	Air quality
Land use for location	Cultural heritage, Landscape and archaeology
CO2 emission balance (and savings)	Energy & Climate
Energy efficiency / storage efficiency	Energy & Climate
Seasonal performance factor electricity consumption for system operation	Energy & Climate
Individual risk	External safety
Societal risk	External safety
Noise disturbance	Noise & vibrations
Noise disturbance during drilling of (test) wells	Noise & vibrations
Waste generation quantity	Resource, waste and byproducts (circularity)
Subsurface space requirement	Socio-economic environment
Traffic movements for materials	Socio-economic environment
Waste water disposal from well drilling	Soil & Water General
Calcite precipitation	Soil & Water Geochemical
Carbon Mobilization - Dissolved Organic Carbon	Soil & Water Geochemical
Enhanced weathering of aquifer sediments	Soil & Water Geochemical
Fresh/ brackish/ salt water interface changes	Soil & Water Geochemical
Leakage from the pit storage	Soil & Water Geochemical
Leakage of brine and additives from BTES boreholes to groundwater and soil	Soil & Water Geochemical
Mixing of water with different quality	Soil & Water Geochemical
Mobilisation of trace elements	Soil & Water Geochemical
Ph of reservoir water as result of CO2 or HCl dosing to prevent calcite deposition	Soil & Water Geochemical
Seepage along insufficiently sealed boreholes/wells can be a pathway for surface contamination and may cause mixing of groundwater from different aquifers with different geochemical properties	Soil & Water Geochemical
Soil contamination	Soil & Water Geochemical
Spread of already existing groundwater contamination	Soil & Water Geochemical
Surface water intrusion through a borehole and interconnection of aquifers caused by drilling operations	Soil & Water Geochemical
(fresh) Water balance	Soil & Water Geohydrological
Effects of water abstraction for filling the PTES	Soil & Water Geohydrological
Groundwater level changes	Soil & Water Geohydrological
Hydraulic head changes	Soil & Water Geohydrological
Reservoir pressure	Soil & Water Geohydrological
The radius of hydraulic flow in relation to the radius of thermal flow	Soil & Water Geohydrological
Withdrawal of reservoir water	Soil & Water Geohydrological
Seismicity	Soil & Water Geomechanical
Soil movement (subsidence/uplift/settlement)	Soil & Water Geomechanical
Cyclical heating and cooling effect on mechanical strength of the reservoir rock	Soil & Water Hydrothermal
Heat balance for heat injected and produced	Soil & Water Hydrothermal
Heating of groundwater near well	Soil & Water Hydrothermal
Heating of overburden	Soil & Water Hydrothermal
Heating of reservoir	Soil & Water Hydrothermal
Heating of shallow subsurface near well	Soil & Water Hydrothermal

Environmental criterion/topic	Theme
Microbiological & pathogens populations in target reservoir (pathogens include viruses, bacteria, fungi, protozoa, or other parasites)	Soil & Water Microbiological populations
Microbiological populations in overburden (incl pathogens)	Soil & Water Microbiological populations
Visual hindrance of drilling rig	Visual disturbance

7. Conclusion

The presented study reports the results of a study aimed at identifying the effects of the implementation of UTES systems. The overall approach was to highlight the effects rather than quantify the impacts also emphasising the potential positive effects such as the reduction of the CO2 intensity for each site. The results are based on the outcomes from the different activities carried out in WP2 (subsurface modelling), WP4 (Implementation of the UTES systems at the study sites) WP5 (Monitoring of the study sites). The challenges of the study are mostly related to the heterogeneity of the data available across the different phases of each UTES project due to the different level of maturity and advancement at each site. Additionally, the type of data collected might vary from site to site due technical requirements (e.g. for drilling operations), and country-specific regulatory framework constraints.

We identified a set of potential common effects that would eventually allowed to compare the performances among UTES types. Effects for both the subsurface and surface compartments have been identified, and then we looked if such effects were Predicted, Assessed and Mitigated. Then we focussed on a fast-track risk assessment based on the correlation between probability and consequences of each effect to occur. For ATES and MTES systems, we separated between drilling activities and production operations. Where data for production operations were lacking, we based our outcomes on the results of modelling predictions (e.g. Thermo-hydraulic, hydro-mechanical, thermo-hydro-chemical models).

The results are summarised in Table 46. It is quite important to highlight that HT-ATES system are the ones which show stronger effects compared to the other systems. If for drilling operations, the effects are limited in time and not permanent, for operations the effects on the subsurface component during operations are definitely more important than for other UTES systems in particular on the reservoir component (eater quality and temperature).

Table 46. Summary of the fast-track risk assessment performed at the different UTES study sites.

Effect \ Risk	HT-ATES							MTES		BTES	PTES
	Koppert_Cress	NIIO	GEO-01	GEO-02		Bern	Bochum		Brædstrup	Marstal	
	Operations	Operations	Drilling	Operations	Drilling	Operations	Operations	Drilling	Operations	Operations	
Air quality	L	L	M	L	M	L		L	L	L	L
Noise and vibration	L	L	M	L	M	L		M	L	L	L
Formation water quality	M	M	L	H	L	H	M	M	M	L	M
Formation water temperature	M	M		M		M				L	
Surface clear water	L	L	M	L	M	L		M	M	L	L
Soil occupation	L	M	M	M	M	M		L	L	L	L
Wastes and dangerous substances	L	L	M	L	M	L		L	L	L	L
Environment	L	L	L	L	L	L				L	L
Nature	L	L	L	L	L	L				L	L
Soil mechanics	L	L		L		M		L	L	L	L
Seismicity	L	L	M	M	M	M		L	L	L	L
CO2 intensity redyction	H			H		H			H	H	H

8. References

- Alt-Epping, P., Mindel, J., et al. (2020). HEATSTORE D2.3: Benchmarking and improving models of subsurface heat storage dynamics.
- Bakema, G., Pittens, B., Buik, N., Drijver, B. (2019). HEATSTORE - Design considerations for high temperature storage in Dutch aquifers. IF Technology, Arnhem, the Netherlands.
- Birdsell, D. T., Adams, B. M., & Saar, M. O. (2021). Minimum transmissivity and optimal well spacing and flow rate for high-temperature aquifer thermal energy storage. Equation 4. *Applied Energy*, 289, 116658.
- Bloemendal, M., Beernink, S., Hartog, N., & Van Meurs, B. (2019). Transforming ATES to HT-ATES. Insights from Dutch pilot project. Paper presented at the European Geothermal Congress EGC, Den Haag.
- Bloemendal, M., et al. (2020). Open bodemenergie met verhoogde opslag temperatuur Nieuwegein, KWR 2020.156.
- Bonte, M. (2013). Impacts of shallow geothermal energy on groundwater quality. geo sciences. Amsterdam, Vrije Universiteit Amsterdam. PhD Thesis.
- Bonte, M., 2014. Impacts of Shallow Geothermal Energy on Groundwater Quality. Water Intell. Online 13. <https://doi.org/10.2166/9781780406824>
- Bonte, M., Stuyfzand, P.J., Hulsmann, A., van Beelen, P., 2011. Underground thermal energy storage: Environmental risks and policy developments in the Netherlands and European Union. *Ecol. Soc.* 16. <https://doi.org/10.5751/ES-03762-160122>
- Brons, H.J. (1992). Biogeochemical aspects of aquifer thermal energy storage. 127 p. LUW, Wageningen.
- Climate-Kic, 2018: D1d E-USE(aq). Technical performance & monitoring report. Danish pilot.
- Daniilidis, A. et. al., 2021: Interference between geothermal doublets across a fault under subsurface uncertainty; implications for field development and regulation
- DARTS, Delft Advanced Research Terra Simulator (DARTS), (2021). <https://darts.citg.tudelft.nl/>.
- Deltares (2010). Effecten van warmte- en koudeopslag (WKO) op fysisch chemische omstandigheden en micro-organismen in grondwater.
- Dooren, T.C.G.W. van, Beernink, S.T.W., Timmers, P.H.A., Bloemendal, J.M. (2019), Prestaties en effecten van ondergrondse warmteopslag. Een verkenning voor het P2X project, KWR
- Dooren, T.C.G.W., van, Beernink, S.T.W., Timmers, P.H.A., Bloemendal, J.M., 2019. Prestaties en effecten van ondergrondse warmteopslag.
- Driesner, T. (ed.) 2021 (in prep.): Final Report on tools and workflows for simulating subsurface dynamics of different types of High Temperature Underground Thermal Energy Storage. GEO THERMICA – ERA NET Cofund Geothermal, unpublished report in preparation for Month 35 of HEATSTORE.
- EIA (2021). 35 years of EU Environmental Impact Assessment. Luxembourg: Publications Office of the European Union. https://ec.europa.eu/environment/eia/pdf/EIA_Directive_35_years.pdf
- Eissa, E. A. and A. Kazi. (1988). Relation Between Static and Dynamic Young's Moduli of Rocks. *Int. J. Rock Mech. Min. Sci & Geomech. Abstr.* Vol 25, No. 6, pp 479-482.
- Energistyrelsen (2005). Vejledning i samfundsøkonomiske analyser på energiområdet
- Energistyrelsen (2010). Forudsætninger for samfundsøkonomiske analyser på energiområdet
- EUDP (2018). Final report. Termisk lagring (HTES). Journalnummer 64016-0014.
- Ferguson, G., Woodbury, A.D., 2006. Observed thermal pollution and post-development simulations of low-temperature geothermal systems in Winnipeg, Canada. *Hydrogeol. J.* 14, 1206–1215. <https://doi.org/10.1007/s10040-006-0047-y>

- GeoEnergi (2011). D21 miljøpåvirkning ved jordvarmeboringer. EUDP 10-II. Journal nummer 64011-0003.
- GEUS (2017). Examining the possibilities of establishing thermal storage in the chalk/limestone aquifer in the greater Copenhagen area. Phase 1 of project HTES, High Temperature Energy Storage
- Hartog, N., Drijver, B., Dinkla, I. and Bonte, M. (2013) Field assessment of the impacts of Aquifer Thermal Energy Storage (ATES) systems on chemical and microbial groundwater composition. European Geothermal Congress 2013, Italy.
- Huber, M.L., Perkins, R.A., Laesecke, A., Friend, D.G., Sengers, J. V., Assael, M.J., Metaxa, I.N., Vogel, E., Mareš, R., Miyagawa, K. (2009) New international formulation for the viscosity of H₂O, J. Phys. Chem. Ref. Data. 38 101–125. <https://doi.org/10.1063/1.3088050>.
- J.J.G. Romera, Python library for IAPWS standard calculation of water and steam properties, (2020). <https://doi.org/10.5281/ZENODO.3734292>.
- Kallesøe, A.J. & Vangkilde-Pedersen, T. (eds). 2019: Underground Thermal Energy Storage (UTES) – state-of-the-art, example cases and lessons learned. HEATSTORE project report, GEOTHERMICA – ERA NET Cofund Geothermal. 130 pp + appendices.
- KBOB, 2016. Ökobilanzdaten im Baubereich 2009/1:2016.
- Koumrouyan, M. (2019). Geomechanical Characterization of Geothermal Exploration Borehole: Implication for the GEO-01 Well, in Geneva. Master Thesis, University of Neuchatel.
- Koumrouyan, M., Sohrabi, R., Valley, B. (2019). Geomechanical characterisation of geothermal exploration borehole for Aquifer thermal energy storage (ATES) development in Geneva, Switzerland. Proceedings European Geothermal Congress 2019. Den Haag, The Netherlands.
- KWR (2013). Grondwaterbescherming en hoge- temperatuur opslagsystemen. Nieuwegein.
- KWR, (2011). Microbiologische risico's van een Hoge Temperatuuropslag GeoMEC Vierpolders (Brielle). Nieuwegein.
- Khait, M., Voskov, D., (2018). Operator-based linearization for efficient modeling of geothermal processes, Geothermics. 74 (2018) 7–18. <https://doi.org/10.1016/j.geothermics.2018.01.012>.
- Marstal Fjernvarme, 2010: Sunstore 4 projekt. Projektforslag.
- Meer met Bodemenergie (2012). Rapport 2: Literatuuronderzoek - Overzicht van kennis en onderzoeksvragen rondom bodemenergie.
- Miljøministeriet, 2008: Jordvarmeanlæg. Teknologier og risiko for jord- og grundvandsforurening. Cowi.
- Miljøministeriet, 2008: Jordvarmeanlæg. Teknologier og risiko for jord- og grundvandsforurening. Cowi.
- Mindel, J., Driesner, Th. 2020. HEATSTORE: Preliminary Design of a High Temperature Aquifer Thermal Energy Storage (HT-ATES) System in Geneva Based on TH Simulations. Proceedings World Geothermal Congress 2020, Reykjavik.
- MMB, 2012, Aquifer Thermal Energy Storage in the Netherlands, results of the research programme
- MMB, 2012. Aquifer Thermal Energy Storage in the Netherlands, results of the research programme 000–001.
- MMB, 2012. Aquifer Thermal Energy Storage in the Netherlands, results of the research programme 000–001.
- MMB, 2012. Aquifer Thermal Energy Storage in the Netherlands, results of the research programme 000–001.
- [Monitoring-System "Mineberry" - TH Georg Agricola \(thga.de\)](#)

- Naturstyrelsen, 2016: Mikrobiologisk risikovurdering af øgede temperaturer i grundvandet ved ATEs (Aquifer Thermal Energy Storage).
- OnCyt (2020). Microbial monitoring (non-published presentation). www.oncyt.com.
- PlanEnergi (2010). Projektforslag for etablering af pilotprojekt med borehulslager i Brædstrup
- PlanEnergi, (2010). Dronninglund Fjernvarme. Projektforslag for solvarmeanlæg, damvarmelager og varmepumpe
- PlanEnergi, (2019). Best practice for implementation and operation of large scale borehole and pit heat thermal storage. Based on Danish experiences. EUDP
- Poulsen, S. E (2019). Varmelagring i den øvre del af den danske undergrund. Beregningsundersøgelser af lukkede og åbne jordvarmeanlæg. Via University College.
- Rambøll, (2013) VVM redegørelse og miljørapport ved solvarmeanlæg ved Vojens. Haderslev Kommune.
- Schmidt, T. (2019) Brædstrup district heating. Monitoring data evaluation for the years 2014-2017. Solites, on behalf of PlanEnergi. Supported by EUDP project no 64014-0121
- SERVICES INDUSTRIELS DE GENEVE (2017). Forage de prospection géologique GGeo-01 - Notice d'impact sur l'environnement accompagnant la demande d'autorisation de construire. Unpublished report
- SERVICES INDUSTRIELS DE GENEVE (2018). Forage de prospection géologique GGeo-02 - Notice d'impact sur l'environnement accompagnant la demande d'autorisation de construire. Unpublished report
- Sharqawy, M. H., et al. (2012). "Thermophysical properties of seawater: a review of existing correlations and data." *Desalination and Water Treatment* 16(1-3): 354-380.
- Sibbitt B. & McClenahan D. (2015) Seasonal Borehole Thermal Energy Storage – Guidelines for design & construction, IEA-Solar Heating & Cooling TECH SHEET 45.B.3.1, page 1-15, April 2015.
- Soerensen, P. A. and Schmidt, T. Design and construction of large scale heat storage for district heating in Denmark. 14th International Conference on Energy Storage
- Spreckels, V.; Schlienkamp, A.; Greiwe, A.; Eberhardt, L., (2016). Eignung von ALS, Aero- und AUS-Photogrammetrie zur Früherkennung und Erfassung von Tagesbrüchen
- Voss, C. I. (1984). A finite-element simulation model for saturated unsaturated, fluid-density-dependent groundwater flow with energy transport or chemically reactive single-species solute transport. Reston, Va, USGS.
- Vreede, G.v.d., Groot, M.I., 2010. Ketenemissies hernieuwbare elektriciteit CE Delft, Delft.
- Wang, H. F. (2000). Theory of Linear Poroelasticity with Applications to Geomechanics and Hydrogeology. Princeton University Press. Princeton, NJ.
- Wang, Y, Voskov, D., Khait, M., Bruhn, D. (2020). An efficient numerical simulator for geothermal simulation: A benchmark study, *Appl. Energy*. 264 114693. <https://doi.org/10.1016/j.apenergy.2020.114693>.
- Willemsen, N. (2016). Rapportage bodemenergiesystemen in Nederland. Arnhem, RVO / IF technology.